

# Spectroscopic characteristics of the cyanomethyl anion and its deuterated derivatives

Liton Majumdar<sup>1</sup>, Ankan Das<sup>1</sup>, Sandip K. Chakrabarti<sup>2,1</sup>

<sup>1</sup> Indian Centre for Space Physics, Chalantika 43, Garia Station Rd., Kolkata, 700084, India  
e-mail: ankan@csp.res.in, liton@csp.res.in

<sup>2</sup> S. N. Bose National Centre for Basic Sciences, Salt Lake, Kolkata 700098, India  
e-mail: chakraba@bose.res.in

Received ; accepted

## ABSTRACT

**Context.** It has long been suggested that  $\text{CH}_2\text{CN}^-$  (cyanomethyl anion) might be a carrier of one of the many poorly characterized diffuse interstellar bands. In this paper, our aim is to study various forms (ionic, neutral & deuterated isotopomer) of  $\text{CH}_2\text{CN}$  (cyanomethyl radical) in the interstellar medium.

**Aims.** Aim of this paper is to predict spectroscopic characteristics of various forms of  $\text{CH}_2\text{CN}$  and its deuterated derivatives. Moreover, we would like to model the interstellar chemistry for making predictions for the column densities of such species around dark cloud conditions.

**Methods.** We have performed detailed quantum chemical simulations to present the spectral properties (infrared, electronic & rotational) of various forms of the cyanomethyl radical. Moller-Plesset perturbation theory along with the triple-zeta correlation-consistent basis set is used to obtain different spectroscopic constants of  $\text{CH}_2\text{CN}^-$ ,  $\text{CHDCN}^-$  and  $\text{CD}_2\text{CN}^-$  in the gas phase which are essential to predict rotational spectra of these species. Depending on the total number of electrons, there exist several allowed spin states for various forms of the cyanomethyl radical. We performed quantum chemical calculation to find out energetically the most stable spin states for these species. We have computed IR and electronic absorption spectra for different forms of  $\text{CH}_2\text{CN}$ . Moreover, we have also implemented a large gas-grain chemical network to predict the column densities of various forms of the cyanomethyl radical and its related species.

In order to mimic physical conditions around a dense cloud region, the variation of the visual extinction parameters are considered with respect to the hydrogen number density of the simulated cloud.

**Results.** Our quantum chemical calculation reveals that the singlet spin state is the most stable form of cyanomethyl anion and its deuterated forms. For the confirmation of the detection of the cyanomethyl anion and its two deuterated forms, namely,  $\text{CHDCN}^-$  and  $\text{CD}_2\text{CN}^-$ , we present the rotational spectral information of these species in the Appendix. Our chemical model predicts that the deuterated forms of cyanomethyl radicals (specially the anions) are also reasonably abundant around the dense region of the molecular cloud.

**Key words.** Interstellar Medium, Astrochemistry, Molecular cloud, Star formation

## 1. Introduction

Over the past years, several works have been carried out to investigate the formation of complex molecules in and around cold interstellar clouds (Hasegawa and Herbst 1993; Hasegawa, Herbst and Leung 1992; Majumdar et al. 2012, Majumdar et al. 2013, Das et al. 2013a). Till date, more than 170 molecules have been observed in Interstellar Mediums (ISMs) or circumstellar shells. It is now well known that in order to model the formation of complex molecules in ISMs, the interstellar grain chemistry has to be an integral part of the chemical evolutionary path (Stantcheva, Shematovich and Herbst 2002, Chakrabarti et al. 2006a,b; Das et al. 2008b, Das, Acharyya & Chakrabarti, 2010; Das & Chakrabarti, 2011; Cuppen & Herbst, 2007; Cuppen et al. 2009).

One of the stumbling blocks in spectroscopy in astronomical context is the lack of adequate knowledge of the origin of unidentified diffuse interstellar bands (DIBs). These DIBs are basically a series of absorption lines that are observed toward just about every star in our galaxy that has interstellar material in front of it. Herbig (1995) and Sarre (2006) reviewed the very long-standing problem of the diffuse interstellar bands. They pointed out that some organic molecules could be the possible candidates for more than 300 DIBs in the ISM. According to Sarre (2000), some (possibly many) of the DIBs are due to electronic transitions between the ground and the dipole bound states of negatively charged polar molecules or small polar grains. Sarre (2000) also first pointed out that  $\text{CH}_2\text{CN}^-$  might be a carrier of the DIBs. A follow up study by Cordiner & Sarre (2007) explored the possibility of  $\text{CH}_2\text{CN}^-$  as a possible carrier of the narrow DIB at  $8037 \pm 0.15 \text{ \AA}$ .

The cyanomethyl radical ( $\text{CH}_2\text{CN}$ ) is the simplest cyanide derivative of the methyl radical ( $\text{CH}_3$ ). Due to the presence of a cyano group in the molecule, a dipole moment is generated which makes it possible to search for the  $\text{CH}_2\text{CN}$  radical by electric-dipole allowed microwave transitions. According to Herbst (2001), an appreciable amount of  $\text{CH}_3$  radical is expected in the diffuse and dense molecular clouds. The first detection of  $\text{CH}_2\text{CN}$  was reported by Irvine et al. (1988), in two of the best characterized molecular clouds, namely, TMC-1 and Sgr B2. Their work was based on the observations performed using the decommissioned 14m antenna at the Five College Radio Astronomy Observatory, the 43m antenna at NRAO's Green Bank facility, the 20m antenna at Onsala Space Observatory, and the 45m antenna at Nobeyama Radio Observatory. A few years ago, the observed spectra was verified experimentally in the laboratory by Ozeki et al. (2004), using a Fourier-transform microwave spectrometer in combination with a pulsed-discharge nozzle. The first detection of  $\text{CH}_2\text{CN}$  in IRC +10216 was reported by Agundez et al. (2008).

Lykke et al. (1987) employed the auto-detachment spectroscopy technique to study the dynamics of  $\text{CH}_2\text{CN}^-$  and one of its deuterated isotopomers, namely,  $\text{CD}_2\text{CN}^-$ . In their work,

dynamics of the auto-detachment process was studied and various mechanisms for detachment were described. Cordiner & Sarre (2007) used the rotational constants obtained by Lykke et al. (1987) to compute the absorption spectrum arising from the  $^1B_1 - \tilde{X}^1 A'$  transition of  $\text{CH}_2\text{CN}^-$  for  $\text{CH}_2\text{CN}^-$  in equilibrium with CMB at 2.74K. According to their calculation, if  $\text{CH}_2\text{CN}^-$  is present in the ISM with an ortho to para abundance ratio of 3:1,  $^1B_1 - \tilde{X}^1 A'$  transitions having  $K''_a = 1$  would produce strong spectral features at  $8024.8\text{\AA}$  and  $8049.6\text{\AA}$ . However, these features are absent in the interstellar spectra. Hence, according to them though  $\lambda 8037$  DIB and transition of  $\text{CH}_2\text{CN}^-$  is consistent, this could not be treated as granted. Further study regarding the  $\text{CH}_2\text{CN}^-$  is essential for making such strong assignments. Fortenberry & Crawford (2011a) carried out quantum chemical calculations for the prediction of new dipole-bound singlet states for anions of interstellar interest. Fortenberry, Crawford & Lee (2013) used quartic force fields and second order vibrational perturbation theory to calculate the appropriate spectroscopic constants and fundamental vibrational frequencies for  $\tilde{X}^1 A'$   $\text{CH}_2\text{CN}^-$  to facilitate its confirmed detection.

According to Park and Woon, (2006), ions embedded in icy grain mantles are thought to account for various observed infrared spectroscopic features, particularly in certain young stellar objects like W33A. Observations of different interstellar molecules ( $\text{CH}_3\text{OH}$ ,  $\text{HCOOH}$ ,  $\text{NH}_3$ ,  $\text{H}_2\text{O}$ ,  $\text{CO}$ ,  $\text{CO}_2$ ,  $\text{CH}_4$ ,  $\text{H}_2\text{CO}$ ,  $\text{OCS}$  etc.) by Gibb et al. (2000), anions ( $\text{OCN}^-$ ,  $\text{HCOO}^-$ ) by Soifer et al. (1979) and Schutte et al. (1997, 1999), cations ( $\text{HCO}^+$ ,  $\text{NH}_4^+$ ) by Schutte & Greenberg (1997), Demyk et al. (1998), Hudson et al. (2001), Novozamsky et al. (2001) motivated us to consider the spectroscopy of different forms (neutral, cationic, anionic) of  $\text{CH}_2\text{CN}$  embedded in icy grain mantles. According to Park and Woon, (2006), quantum chemical approach along with a continuum model is well suited for modeling the spectroscopic properties of molecules and ions embedded within amorphous ice matrices. Inspired by these studies, we performed a detail spectroscopy as well as astrochemical modeling of different forms of  $\text{CH}_2\text{CN}$ . We expect that our study would throw lights on the possibility of finding other forms of  $\text{CH}_2\text{CN}$  in and around ISMs.

The plan of this paper is the following. In Section 2, method and computational details for the purpose of spectroscopy of  $\text{CH}_2\text{CN}$  and its related molecules are discussed. Different computational results are presented in Section 3. In Section 4, we draw our conclusion. In Appendix A, we discuss the chemical modeling and results. Moreover, in the Appendix B, we have included four Tables for presenting different vibrational (Table B1) and rotational transitions (Table B2, B3 & B4).

## 2. Methods and Computational Details

### 2.1. Quantum chemical simulation & spectroscopy

Recent work by Huang & Lee (2008) suggests that the quantum chemical computational tools could be very useful to obtain rotational constants often within an accuracy of 20 MHz (especially

for the B-type and C-type constants). Vibrational frequencies accurate to  $5\text{ cm}^{-1}$  or better could be obtained from the quantum chemical calculations (Huang & Lee 2008, 2009, 2011; Huang et al. 2011; Inostroza et al. 2011; Fortenberry & Crawford 2011a, 2011b, 2011c; Fortenberry et al. 2012a, 2012b; Fortenberry, Crawford & Lee, 2013). Motivated by these works, we perform a detailed quantum chemical simulation to report various spectral aspects of different forms of  $\text{CH}_2\text{CN}$  molecule in the vibrational (harmonic), electronic and rotational mode.

All the computations on neutral  $\text{CH}_2\text{CN}$  are performed by using spin-unrestricted (UHF) wave functions, while computations of the closed-shell anions used spin-restricted (RHF) wave functions. First, the geometries of the neutral and ionic forms of  $\text{CH}_2\text{CN}$  are optimized at Becke three-parameter Exchange and Lee, Yang and Parr correlation functional (B3LYP) with 6-311++G as the basis set. B3LYP is the most popular DFT model. This method is termed as a hybrid method, because it uses corrections for both gradient and exchange correlations. Becke Three Parameter Hybrid Functional forms were devised by Becke in (1993) along with the non-local correlation provided by LYP (Lee, Yang & Parr 1988). Dipole moments of all of these species are computed by using the same level of theory. For the computation of dipole moments, we have considered the center of mass to be our standard origin in the Gaussian 09W program (Frisch et al. 2009). Gas phase vibrational frequencies of these species are obtained from the minimum energy structure at the same level of theory. Our computed vibrational frequencies are harmonic in nature since the Gaussian 09W program computes these frequencies based on the harmonic oscillator approximation. In order to find out the harmonic vibrational frequencies of these species in the ice phase, we have also optimized these geometries in B3LYP/6-311++G level using the SCRF method. The SCRF method in Gaussian 09W program is used to perform calculations in presence of a solvent by placing the solute in a cavity within a solvent reaction field. The Polarizable Continuum Model (PCM) using the integral equation formalism variant (IEFPCM) is the default SCRF method. This method creates the solute cavity via a set of overlapping spheres. It was initially devised by Tomasi and co-workers and Pascual-Ahuir and co-workers (Tomasi et al. 2002; Tomasi, Mennucci & Cammi 2005; Tomasi, Mennucci & Cancès 1999, Pascual-Ahuir, Silla & Tun 1994). The electronic absorption spectra of these species are also obtained using the higher order method (EOM-CCSD) with the basis set aug-cc-pVDZ. This method use coupled cluster for the description of excited states using the equation of motion approach. Depending on the total number of electrons of a species, we vary the spin multiplicities to locate the most reasonable spin state. In order to get more accurate information about the rotational spectral parameters (rotational & distortional constants), we have used MP2/aug-cc-pVTZ level of theory in the symmetrically as well as asymmetrically reduced Hamiltonian. Rotational motion of a molecule in Gaussian 09W program commonly starts from the rigid rotor model which assumes that the molecule is rigid. For our calculation, we have to know the structure of the molecule and from that we could get the moment of inertia which could then utilized to obtain the eigen values. Generally, this requires a very good estimation of the structure and optimization of a molecule. In an earlier paper (Das et al. 2013), we carried out a similar type of calculation for

HCOCN, where we implemented MP2/aug-cc-pVTZ level of theory and showed that this level of theory produced results which were in good agreement with the experiment. For the computation of vibrationally averaged structures, the corrections for the interactions between rotation and vibration are important. We have computed these vibrational-rotational coupling by Gaussian 09W program. Further corrections for vibrational averaging and anharmonic corrections to the vibration are also implemented by using Gaussian 09W program. These rotational and distortional constants are required to predict the spectrum of a particular species. Herb Pickett's SPCAT program (Pickett, 1991) was designed in such a way that one would get the spectral information by putting the rotational and distortional constants and other relevant parameters according to the prescribed format. In our calculations, rotational and distortional constants are computed from the Gaussian 09W program. These values are then inserted into the SPCAT program to obtain the spectral information of  $\text{CH}_2\text{CN}^-$ ,  $\text{CHDCN}^-$  and  $\text{CD}_2\text{CN}^-$ .

### 3. Results and Discussion

#### 3.1. Chemical parameters

The way the energy of a molecular system varies with small changes in its structure is specified by its potential energy surface. In this work, the geometry optimization of different forms of  $\text{CH}_2\text{CN}$  (neutral, ionic and its isotopomers) has been performed to locate the minima on the potential energy surface, thereby predicting the equilibrium structure of these molecules. At the minima, the first derivative of the energy (i.e., the energy gradient) is zero and thus the forces are also zero. It is customary to know energetically the most stable form of  $\text{CH}_2\text{CN}$  that can exist in and around the ISM. In Table 1, we provide the relative energies of the different spin states of the gas/ice phase  $\text{CH}_2\text{CN}$ ,  $\text{CH}_2\text{CN}^+$  and  $\text{CH}_2\text{CN}^-$  in eV unit and their dipole moments in Debye unit. Dipole moments of all the species are computed by considering the center of mass as our standard origin. For the neutral  $\text{CH}_2\text{CN}$ , the total number of electrons are 21. Because it is an odd number, the allowed spin states are doublet, quartet, sextet etc. By performing the geometry optimization and energy calculation at B3LYP/6-311++G level of theory, we found that the doublet spin state of neutral  $\text{CH}_2\text{CN}$  is most stable. Relative energies of the quartet and sextet spin states of  $\text{CH}_2\text{CN}$  with respect to its minimum energy spin state (doublet) are found to be 4.08 eV and 8.16 eV respectively. The mono-cationic form of  $\text{CH}_2\text{CN}$  ( $\text{CH}_2\text{CN}^+$ ) is an even electron system which corresponds to the fact that it has the singlet, triplet, quintet etc. as the allowed spin states. Among these allowed spin states, the singlet spin state is found to be the most stable spin state for  $\text{CH}_2\text{CN}^+$ . Relative energies of the triplet and quintet spin states of  $\text{CH}_2\text{CN}^+$  with respect to its minimum energy spin state (singlet) are found to be 1.94 eV and 5.47 eV respectively. The cyanomethyl anion also has an even electron system having singlet, triplet, quintet etc. as the allowed spin states. The singlet spin state of  $\text{CH}_2\text{CN}^-$  is found to be most stable spin state. Relative energies of the triplet and quintet spin states of  $\text{CH}_2\text{CN}^-$  with respect to its minimum energy spin state (triplet) are found to be 2.06 eV and 6.35 eV respectively. In

**Table 1.** Relative energies (eV) of different forms of CH<sub>2</sub>CN (neutral, cationic & anionic) in the gas phase and the ice phase along with their dipole moments.

Species	Spin State	Relative energy in gas phase (in eV)	Dipole moments in gas phase (in Debye)	Relative energy in ice phase (in eV)	Dipole moments in gas phase (in Debye)
CH <sub>2</sub> CN	doublet	0	3.5974	0	4.6355
	quartet	4.08	2.4705	4.15	3.3207
	sextet	8.16	1.5430	8.28	1.8471
CH <sub>2</sub> CN <sup>+</sup>	singlet	0	5.305	0	6.606
	triplet	1.94	3.802	2.08	4.474
	quintet	5.47	3.653	5.63	4.213
CH <sub>2</sub> CN <sup>-</sup>	singlet	0	1.212	0	2.469
	triplet	2.06	6.712	3.17	3.183
	quintet	6.35	6.5460	6.52	2.8671

Table 1, the relative energies of different spin states of neutral CH<sub>2</sub>CN, CH<sub>2</sub>CN<sup>+</sup> and CH<sub>2</sub>CN<sup>-</sup> are shown along with their respective dipole moments.

These molecules could also be trapped into the interstellar ice. So it is also necessary to identify the most stable configuration of the various forms of CH<sub>2</sub>CN in the interstellar grain. For this purpose, we have considered the self-consistent reaction field method which considers the solvent (ice) as a continuum of uniform dielectric constant and the solute (different forms of CH<sub>2</sub>CN) is placed into a cavity within the solvent. In the ice phase, it has been found that the doublet CH<sub>2</sub>CN (dipole moment= 4.6355 Debye), singlet CH<sub>2</sub>CN<sup>+</sup> (dipole moment= 6.606 Debye) and singlet CH<sub>2</sub>CN<sup>-</sup> (dipole moment= 2.469 Debye) are the most stable configurations in the ice phase. Among the deuterated forms, doublet CD<sub>2</sub>CN, singlet CD<sub>2</sub>CN<sup>+</sup>, singlet CD<sub>2</sub>CN<sup>-</sup>, doublet CHDCN, singlet CHDCN<sup>+</sup>, singlet CHDCN<sup>-</sup>, are the most stable configurations in the ice phase.

### 3.2. Astronomical spectroscopy

#### 3.2.1. Vibrational spectroscopy

In order to study the spectral properties (vibrational) for various forms of CH<sub>2</sub>CN, we need to compute the infrared peak positions with their absorbance in the gas phase and in other astrophysical environments. As discussed in Sec 3.1, depending on the total electron content of the system, the spin multiplicity varies. In the present work, we have considered that the neutral, mono-cationic and mono-anionic forms of CH<sub>2</sub>CN are possible in the ISM. For each of this state, we considered three different spin states.

In Table B1, we present vibrational frequencies (harmonic) of CH<sub>2</sub>CN with its different charge and spin states for the gas phase and the ice phase. Observational evidences suggest that ice could be mixed in nature. Major contributor of interstellar ice is H<sub>2</sub>O but carbon monoxide and methanol are also contributing significantly (Keane et al. 2001; Das & Chakrabarti, 2011). Since H<sub>2</sub>O is the major constituent (> 70%) of the interstellar ice, we are considering only the water ice for our simulation purpose. For the pure water ice, Gaussian 09W uses a dielectric con-

stant of  $\sim 78.5$  by default. We note that the most intense peak as well as other peaks for almost all forms of  $\text{CH}_2\text{CN}$  in the gas phase are shifted in the ice phase (Table B1). Isotopic effects on the spectral shifts is caused by differences in vibrational modes (harmonic) due to different isotopic masses. In our chemical model, we have consider two types of isotopomer of  $\text{CH}_2\text{CN}$ , namely,  $\text{CHDCN}$  and  $\text{CD}_2\text{CN}$ . They have different infrared spectra because the substitution of isotope changes the reduced mass of the corresponding molecule. In this case also, we find that the most intense mode as well as the other modes of  $\text{CHDCN}$  and  $\text{CD}_2\text{CN}$  in the gas phase are shifted in the ice phase. Infrared peak positions of  $\text{CHDCN}$  and  $\text{CD}_2\text{CN}$  with their absorbance in the gas phase as well as in other astrophysical environments are shown in Table B1. High value of the absorbance in Table B1 implies most probable transitions. According to Person & Kubulat (1990), one of the most challenging problems in the study of infrared spectroscopy is to understand the intensity of absorption by the different fundamental modes of vibration in the infrared spectrum of a molecule. Magnitudes of the integrated molar absorption coefficients are calculated by the following relation;

$$A = \frac{1}{100Cl} \int \ln(I_0/I)dv. \quad (1)$$

Depending on the mode of vibration and the molecule involved, the value of the absorption coefficients could vary from  $0 - 10^4$  km/mol. Here,  $C$  is the concentration in  $\text{mol}^{-1}$ ,  $l$  is the path length in cm,  $I_0$  is the intensity of the light incident,  $I$  is the intensity of light transmitted and  $v$  is the wavenumber in  $\text{cm}^{-1}$ . The factor of 100 converts the values to km/mol, with the resulting convenient range of possible values. The integration is taken over the entire absorption band. From our relative energy calculation, it is clear that the singlet state of  $\text{CH}_2\text{CN}^-$ ,  $\text{CHDCN}^-$  and  $\text{CD}_2\text{CN}^-$  is the most stable spin state. From Table B1 it is evident that in case of gas phase  $\text{CH}_2\text{CN}^-$  (singlet), transition at  $2056.73 \text{ cm}^{-1}$  is the strongest one. In the ice phase, strongest transition for  $\text{CH}_2\text{CN}^-$  (singlet) comes out to be at  $2016.35 \text{ cm}^{-1}$ . Transitions at  $2053.96 \text{ cm}^{-1}$  and  $2013.34 \text{ cm}^{-1}$  are the most probable for  $\text{CHDCN}^-$  (singlet) in the gas phase and ice phase respectively. In case of  $\text{CD}_2\text{CN}^-$  (singlet), transition at  $2050.23 \text{ cm}^{-1}$  and  $2009.48 \text{ cm}^{-1}$  are the most probable in gas phase and ice phase respectively. In order to have some idea about the accuracy of our computed harmonic vibrational frequencies, we compare our result for the singlet state of  $\text{CH}_2\text{CN}^-$  with that of the Fortenberry, Crawford & Lee (2013) in Table B1. Our results appear to be reasonable.

In Fig. 1, we have shown how the isotopic substitution ( $\text{CD}_2\text{CN}$ ) as well as spin multiplicity plays a part in the vibrational (harmonic) progressions of  $\text{CH}_2\text{CN}$  in the gas (denoted by G in Fig. 1), ice (denoted by I in Fig. 1). ‘Y axis’ of Fig. 1 represent the absorbance (in km/mol) and ‘X axis’ represent the wavenumber in ( $\text{cm}^{-1}$ ).

### 3.2.2. Rotational spectroscopy

In Table 2, we have summarized our calculated rotational and distortional constants along with other spectroscopic constants for only stable spin state of  $\text{CH}_2\text{CN}^-$ ,  $\text{CHDCN}^-$  and  $\text{CD}_2\text{CN}^-$ . To

have an estimation about the accuracy of our model, we compare our results with those from other existing theoretical and experimental work. Fortenberry, Crawford & Lee (2013) reported theoretically computed rotational and distortional constants along with other spectroscopic constants of  $\text{CH}_2\text{CN}^-$  using CCSD(T)/aug-cc-pVQZ level of theory. For the computation of anharmonic frequencies, analytic second derivative of energies at displaced geometries are required. But the CCSD(T) method in the Gaussian 09W program only implements energies, so analytic second derivative of energies are not available at this level of theory. So it is not possible to compute the rotational and distortional constants at CCSD(T)/aug-cc-pVQZ level of theory as used by Fortenberry, Crawford & Lee (2013) using the Gaussian 09W program. In our calculation, we have computed the rotational and distortional constants at MP2/aug-cc-pVTZ level of theory. In Table 2, we have also compared our results with the experimental results of Lykke et al. (1987) who carried out auto-detachment spectroscopy technique to study the dynamics of  $\text{CH}_2\text{CN}^-$  and one of its deuterated isotopomer ( $\text{CD}_2\text{CN}^-$ ). They also reported the rotational and distortional constants of  $\text{CH}_2\text{CN}^-$  and  $\text{CD}_2\text{CN}^-$ . From Table 2, it is clear that our results are in close agreement with the theoretical and experimental work. This leads us to believe that our computed parameters for the deuterated isotopomers of  $\text{CH}_2\text{CN}^-$  could be useful for the further astronomical investigation of these molecules.

In order to summarize the results of our computation on rotational spectroscopy, we prepare our spectral information for  $\text{CH}_2\text{CN}^-$ ,  $\text{CHDCN}^-$ ,  $\text{CD}_2\text{CN}^-$ . In Tables B2, B3 & B4, the computed rotational transitions for the gas phase  $\text{CH}_2\text{CN}^-$ ,  $\text{CHDCN}^-$  and  $\text{CD}_2\text{CN}^-$  are respectively shown. Tables B2 and B4 contain the data for  $\text{CH}_2\text{CN}^-$  and  $\text{CD}_2\text{CN}^-$  respectively. These Tables are prepared with the experimental constants (Lykke et al. 1987) given in Table 2. Here, errors on the computed line frequencies are related to the errors on the constants given in Table 2. Lykke et al., (1987) reported the rotational and distortional constants for  $\text{CH}_2\text{CN}^-$  and  $\text{CD}_2\text{CN}^-$  by fitting the observed experimental transitions with the Watson S-reduced Hamiltonian using a least square routine. Our reported spectroscopic constants are in symmterially reduced Hamiltonian and they can be computed in Gaussian 09W program by considering anharmonic vibration-rotation coupling via perturbation theory. By following Lykke et al., (1987), in Table 2, we also have tabulated the values of  $1\sigma$  in the unit of MHz in the parentheses of the corresponding experimental constants. The quantity  $\sigma$  corresponds to the standard deviation of the fit to the entire band. Armed with these values, we have prepared Table B2 and B4 to report the rotational transitions of  $\text{CH}_2\text{CN}^-$  and  $\text{CD}_2\text{CN}^-$  respectively. Expected errors on any line frequencies are clearly mentioned in the captions of Table B2 and B4. In case of Table B2, for the line frequencies  $19\text{GHz} - 319\text{GHz}$ , there could be errors in between  $\pm 1 - 20\text{MHz}$  ( $d\nu/\nu = 6.16 \times 10^{-5}$  for any line frequency). Similarly for Table B4, for the transitions in between  $18\text{GHz} - 314\text{GHz}$ , there could be errors in between  $\pm 0.6 - 12\text{MHz}$  ( $d\nu/\nu = 3.77 \times 10^{-5}$ ). Since, till now, there are no experimental constants reported for the  $\text{CHDCN}^-$ , in Table B3, we have given the information regarding the rotational transitions for  $\text{CHDCN}^-$  by using our calculated rotational and distortional constants (Table 2). Table B2, B3 and B4 are prepared by selecting only those tran-

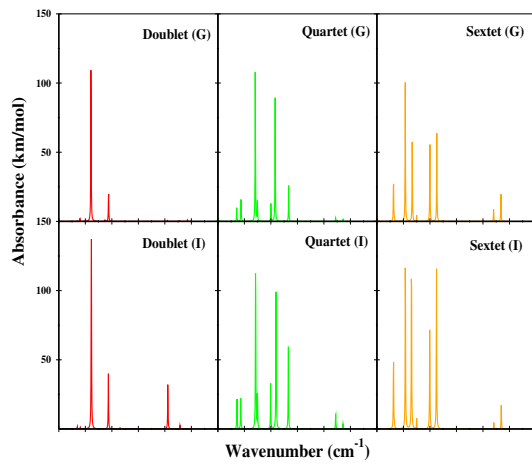


**Fig. 1.** Infrared spectrum of different forms of CD<sub>2</sub>CN in gas phase, ice phase and mixed ice.

sitions which have intensities beyond 10<sup>-7</sup> nm<sup>2</sup> MHz (base 10 logarithm of the intensities are tabulated). It is noticed that we are having several different entries of greatly differing intensities for the same line frequency. Since strongest component suffice, here (in Table B2, B3 & B4), only the component having largest intensity for the same line frequency is tabulated.

### 3.2.3. Electronic spectroscopy

CH<sub>2</sub>CN<sup>-</sup> only has one excited state (a second singlet state) in the gas phase. This has been shown experimentally (Lykke et al., 1987) and theoretically (Fortenberry & Crawford 2011a). Additionally, as for the triplet and quintet states of CH<sub>2</sub>CN<sup>-</sup> are above the lowest energy (doublet) state of CH<sub>2</sub>CN radical and thus the electron will be removed from the anion before it excites into these high spin states. Hence, those states cannot exist and this is why we have not considered the higher spin states of the different forms of CH<sub>2</sub>CN. In Fig. 2, we show the electronic absorption spectra of CH<sub>2</sub>CN, CH<sub>2</sub>CN<sup>+</sup> and CH<sub>2</sub>CN<sup>-</sup> for their most stable spin configuration. As per discussion in Section 3.1, doublet CH<sub>2</sub>CN, singlet CH<sub>2</sub>CN<sup>+</sup> and singlet CH<sub>2</sub>CN<sup>-</sup> are the most stable spin states of these species. Intense peaks in Fig. 2 are assigned due to various electronic transitions shown in Table 3. It is clear that, depending on the composition of the interstellar grain mantle, peak positions in the ice phase are shifted. Different electronic absorption spectral parameters for CH<sub>2</sub>CN, CH<sub>2</sub>CN<sup>+</sup>, CH<sub>2</sub>CN<sup>-</sup> in the gas phase as well as in the ice phase are given in Table 3.

## 4. Conclusions

There are some indications in the literature that CH<sub>2</sub>CN<sup>-</sup> might be the carrier of one of the many poorly characterized diffuse interstellar bands. In this paper, we investigated different ways to manifest cyanomethyl radicals in the ISM. The highlights are:

**Table 2.** Different spectroscopical constants of  $\text{CH}_2\text{CN}^-$ ,  $\text{CHDCN}^-$ ,  $\text{CD}_2\text{CN}^-$  in gas phase at MP2/aug-cc-pVTZ level of theory.

Species	Constants	Theoretical values in MHz by Fortenberry, Crawford & Lee (2013) at CCSD(T)/aug-cc-pVQZ level of theory	Experimental values in MHz (Lykke et al. (1987)	Our calculated values in MHz
$\text{CH}_2\text{CN}^-$	$A_0$	233945.4	278636.4( $\pm 4.197095$ )	298584.615
	$B_0$	10823.22	10145.79( $\pm 0.599585$ )	10069.925
	$C_0$	10386.01	9805.043( $\pm 0.629564$ )	9687.183
	$A_e$	230904.9	-	287675.631
	$B_e$	10849.79	-	10086.765
	$C_e$	10445.37	-	9745.074
	$\tau'_{aaaa}$	-100.708	-	-87.6704
	$\tau'_{bbbb}$	-0.020	-	-0.0155
	$\tau'_{cccc}$	-0.017	-	-0.013
	$\tau'_{aabb}$	-1.812	-	-1.540
	$\tau'_{aacc}$	0.043	-	-0.01594
	$\tau'_{bbcc}$	-0.018	-	-0.01436
	$D_J$	0.005	0.0049465( $\pm 0.00029979$ )	0.0035
	$D_{JK}$	0.434	0.3888308( $\pm 0.00449689$ )	0.3823
	$D_K$	24.739	30.06319( $\pm 0.06295642$ )	21.531
	$d_1$	0.000	-0.0002698( $\pm 0.00005396$ )	-0.0001297
	$d_2$	0.000	-0.000175678( $\pm 0.00002308$ )	-0.000032387
$\text{CHDCN}^-$	$A_0$	-	-	203788.893
	$B_0$	-	-	9432.261
	$C_0$	-	-	8960.774
	$A_e$	-	-	197655.384
	$B_e$	-	-	9454.839
	$C_e$	-	-	9023.214
	$\tau'_{aaaa}$	-	-	-52.524
	$\tau'_{bbbb}$	-	-	-0.0144
	$\tau'_{cccc}$	-	-	-0.0115
	$\tau'_{aabb}$	-	-	-1.268
	$\tau'_{aacc}$	-	-	0.0469
	$\tau'_{bbcc}$	-	-	-0.0128
	$D_J$	-	-	0.0031
	$D_{JK}$	-	-	0.2994
	$D_K$	-	-	12.828
	$d_1$	-	-	-0.0001804
	$d_2$	-	-	-0.00005339
$\text{CD}_2\text{CN}^-$	$A_0$	-	140757.7( $\pm 4.496888$ )	147451.465
	$B_0$	-	9004.927( $\pm 0.329772$ )	8916.168
	$C_0$	-	8487.186( $\pm 0.329772$ )	8353.217
	$A_e$	-	-	143948.398
	$B_e$	-	-	8939.687
	$C_e$	-	-	8416.965
	$\tau'_{aaaa}$	-	-	-21.951
	$\tau'_{bbbb}$	-	-	-0.0127
	$\tau'_{cccc}$	-	-	-0.00967
	$\tau'_{aabb}$	-	-	-1.0326
	$\tau'_{aacc}$	-	-	0.01407
	$\tau'_{bbcc}$	-	-	-0.01096
	$D_J$	-	0.003165808( $\pm 0.00013191$ )	0.0026
	$D_{JK}$	-	0.2320094( $\pm 0.00233838$ )	0.2498
	$D_K$	-	7.10808( $\pm 0.13190870$ )	5.235
	$d_1$	-	-0.0000288( $\pm 0.00004797$ )	-0.0001928
	$d_2$	-	-0.00008094( $\pm 0.00001229$ )	-0.000070902

The numbers in the parentheses represents the errors (in MHZ) of the fit to the entire band obtained by Lykke et al. (1987).

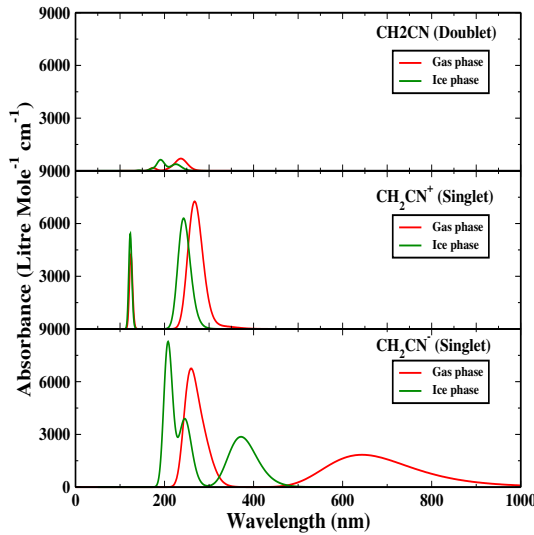


**Fig. 2.** Electronic absorption spectra of  $\text{CH}_2\text{CN}$  (doublet),  $\text{CH}_2\text{CN}^+$  (singlet) and  $\text{CH}_2\text{CN}^-$  (singlet) in gas phase and in ice phase.

**Table 3.** Electronic transitions of the most stable spin state of  $\text{CH}_2\text{CN}$ ,  $\text{CH}_2\text{CN}^+$  and  $\text{CH}_2\text{CN}^-$  at EOM-CCSD/aug-cc-pVDZ level of theory in gas phase and water ice phase

Name & spin state	Wavelength (gas phase) (in nm)	Absorbance	Oscillator strength	Transitions	Wave length ( $\text{H}_2\text{O}$ ice) (in nm)	Absorbance	Oscillator strength	Transitions
<b>Doublet <math>\text{CH}_2\text{CN}</math></b>	237.47	696.35	0.0167	$2-\text{A}'' \rightarrow 2-\text{A}'$	225.57	379.59	0.0093	$2-\text{B}1 \rightarrow 2-\text{A}1$
	174.07	170.09	0.0042	$2-\text{A}'' \rightarrow 2-\text{A}'$	190.29	625.57	0.0133	$2-\text{B}1 \rightarrow 2-\text{B}1$
					142.68	28.28	0.0007	$2-\text{B}1 \rightarrow 2-\text{B}2$
<b>Singlet <math>\text{CH}_2\text{CN}^+</math></b>	267.63	7762.40	0.1793	$1-\text{A}' \rightarrow 1-\text{A}'$	242.6	6291.27	0.1538	$1-\text{A}' \rightarrow 1-\text{A}'$
	124.44	4250.86	0.1055	$1-\text{A}' \rightarrow 1-\text{A}'$	122.95	5423.60	0.1346	$1-\text{A}' \rightarrow 1-\text{A}'$
<b>Singlet <math>\text{CH}_2\text{CN}^-</math></b>	643.5	1838.62	0.0454	$1-\text{A}' \rightarrow 1-\text{A}''$	371.74	2862.63	0.0707	$1-\text{A}' \rightarrow 1-\text{A}''$
	257.03	6743.34	0.1528	$1-\text{A}' \rightarrow 1-\text{A}'$	245.92	3892.09	0.0951	$1-\text{A}' \rightarrow 1-\text{A}'$
					207.81	8252.17	0.20411	$1-\text{A}' \rightarrow 1-\text{A}'$

- We performed quantum chemical calculations to find out energetically the most stable spin configuration for various forms of  $\text{CH}_2\text{CN}$ .
- By introducing a large deuterated network into our chemical model, we have explored the existence of different isotopologues of  $\text{CH}_2\text{CN}$ ,  $\text{CH}_2\text{CN}^+$  and  $\text{CH}_2\text{CN}^-$  (provided in the Appendix). Our chemical modeling shows that different isotopomers of various forms of  $\text{CH}_2\text{CN}$  could efficiently be formed in the ISM. Column densities of various isotopomers of cyanomethyl anions are reasonably higher and could be observed with the present instrumental facility, like, ALMA, JVLA etc..
- We explored the vibrational (harmonic), rotational and electronic spectral properties of different forms of  $\text{CH}_2\text{CN}$  in different astrophysical environments. Our result could be used as a guideline for observing various forms of  $\text{CH}_2\text{CN}$  around ISM. In the Appendix, we have pre-

sented the rotational transitions of  $\text{CH}_2\text{CN}^-$ ,  $\text{CHDCN}^-$  and  $\text{CD}_2\text{CN}^-$  which could be useful for observational identifications.

## Acknowledgments

LM is grateful to DST for partial financial support through a project (Grant No. SR/S2/HEP-40/2008) and AD wants to thank the ISRO respond project (Grant No. ISRO/RES/2/372/11-12). The authors would like to thank the anonymous referee and Prof. Malcolm Walmsley whose valuable suggestions have helped to improve this paper significantly.

## References

- Agundez, M., Fonfria, J. P., Cernicharo, J., Pardo, J. R., & Guelin, M. 2008, A&A, 479, 493  
 Allen, M., Robinson, G. W., 1977., ApJ, 212, 396  
 Albertsson, T., Semenov, D. A., Vasyunin, A. I., Henning T., Herbst, E., 2013, APJS, 207, 27  
 Arzoumanian, D., Andr , P., Didelon, P., et al. 2011, A&A, 529, L6+  
 Becke A. D., 1993, J. Chem. Phys., 98, 5648  
 Chakrabarti, S., Chakrabarti, S.K., 2000a. A&A 354, L6  
 Chakrabarti, S. K., Chakrabarti, S., 2000b. Ind. J. Phys 74B, 97  
 Chakrabarti, S.K., Das, A., Acharyya, K.,Chakrabarti, S., 2006, A&A, 457, 167  
 Chakrabarti, S.K., Das, A., Acharyya, K.,Chakrabarti, S., 2006, BASI, 34, 299  
 Churchwell, E. 1980, ApJ, 240, 811  
 Clouthier, D. J., Moule, D.C., 1987, J. Am. Chem. Soc. 109, 6259  
 Cordiner, M. A., & Sarre, P. J. 2007, A&A, 472, 537  
 Cuppen, H. M., Herbst, E., 2007, APJ, 668, 294  
 Cuppen, H. M., Van Dishoeck E., F., Herbst, E., Tielens, A. G. G. M., 2009, A&A, 508, 275  
 Cummins, S. E., Line, R. A., Thaddeus, P., 1986, APJS, 60, 819  
 Das, A. Majumdar, L., Chakrabarti, S. K., & Chakrabarti S., 2013a, New Astronomy, 23, 118  
 Das, A. Majumdar, L., Chakrabarti, S. K., Saha, R., Chakrabarti S., 2013b, MNRAS, 433, 3152  
 Das, A., Acharyya, K., Chakrabarti, S. & Chakrabarti, S. K., 2008b, A&A, 486, 209  
 Das, A., Acharyya, K. & Chakrabarti, S. K., 2010, MNRAS 409, 789  
 Das, A., Chakrabarti, S. K., Acharyya K. & Chakrabarti, S., 2008a, NEWA, 13, 457  
 Das, A. & Chakrabarti, S. K., 2011, MNRAS, 418, 545  
 Demyk, K., Dartois, E., dHendecourt, L., Jourdain de Muizon, M., Heras, A. M., Breitfellner, M. 1998,  
     A&A, 339, 553  
 Fortenberry, R. C. Crawford, T. D., Lee, J., T., 2013, ApJ, 762, 121  
 Fortenberry, R. C., Huang, X., Francisco, J. S., Crawford, T. D., Lee, T. J., 2012a, JPCA, 116, 9582  
 Fortenberry, R. C., Huang, X., Francisco, J. S., Crawford, T. D., Lee, T. J., 2012b, JChPh, 136, 234309  
 Fortenberry, R. C. Crawford, T. D., 2011a, J. Chem. Phys., 134, 154304  
 Fortenberry, R. C., Crawford, T. D., 2011b, Annu. Rep. Comput. Chem., 7, 195  
 Fortenberry, R. C., Crawford, T. D., 2011c, JPCA, 115, 8119  
 Frisch, M. J.; Trucks, G. W.; Schlegel, H. B., et al. 2009, Gaussian 09, Revision D.01, D. J. Gaussian, Inc.,  
     Wallingford CT

- Gerin, M., Combes, F., Encrenaz, P., Turner, B., Wootten, A., Bogey, M., Destombes, J.L., 1989, *A&A*, 224, L24-L26
- Gibb, E. L., et al. 2000, *ApJ*, 536, 347
- Goldsmith, P. F., Heyer, M., Narayanan, G., et al. 2008, *ApJ*, 680, 428
- Hasegawa, T., Herbst, E., Leung, C.M., 1992, *APJ*, 82, 167
- Hasegawa, T., Herbst, E., 1993, *MNRAS*, 261, 83
- Herbig, G. H. 1995, *Annu. Rev. Astrophys.*, 33, 19
- Herbst, E. 2001, *Chem. Soc. Rev.*, 30, 168
- Herbst, E., 1985, *ApJ*, 291, 226
- Herbst, E. 2006, in *Springer Handbook of Atomic, Molecular, and Optical Physics*, ed. G. W. F. Drake (New York: Springer), 561
- Smith, I.W.M., Herbst, E., Chang, Q., 2004, *MNRAS*, 350
- Huang, X., Lee, T. J. 2008, *JChPh*, 129, 044312
- Huang, X., Lee, T. J. 2009, *JChPh*, 131, 104301
- Huang, X., Lee, T. J. 2011, *ApJ*, 736, 33
- Hudson, R. L., Moore, M. H., Gerakines, P. A. 2001, *ApJ*, 550, 1140
- Inostroza, N., Huang, X., Lee, T. J. 2011, *JChPh*, 135, 244310
- Irvine, W. M., Friberg, P., Hjalmarson, A., et al. 1988, *ApJ*, 334, L107
- Lee, H., H., Herbst, E., Pineau des Forets, G., Roueff, E., Le Bourlot, J., 1996, *A&A*, 311, 690
- Lee C., Yang W., Parr R. G., 1988, *Phys. Rev. B*, 58, 785
- Leitch-Devlin, M., A., Williams, D., A., 213, 295, *MNRAS*, 1985
- Linsky, J.L., Diplas, A., Wood, B.E., Brown, A., Ayres, T.R., Savage, B.D., 1995. *ApJ*. 451, 335B351
- Lykke K. R., Neumark D. M., Andersen T., Trapa V. J., Lineberger W. C., 1987, *J. Chem. Phys.*, 87, 6842
- Person, W. B., Kubulat, K., *J. Mol. Struc.*, 1990, 224, 225
- Majumdar, L., Das, A., Chakrabarti, S.K., Chakrabarti, S., 2013, *New Astronomy*, 20, 15
- Majumdar, L., Das, A., Chakrabarti, S.K., Chakrabarti, S., 2012, *Research in Astronomy & Astrophysics*, 12, 1613
- McElroy, D., Walsh, C., Markwick, A. J., Cordiner, M. A., Smith, K., Millar, T. J., 2013 *A&A*, 550, A36
- Novozamsky, J. H., Schutte, W. A., Keane, J. V. 2001, *A&A*, 379, 588
- Nutter, D., Kirk, J. M., Stamatellos, D., Ward-Thompson, D. 2008, *MNRAS*, 384, 755
- Ohishi M., Irvine, W. M., Kaifu, N., 1992, *IAUS*, 150, 1710
- Ostriker, J. 1964, *ApJ*, 140, 1056
- Ozeki, H., Hirao, T., Saito, S., & Yamamoto, S. 2004, *ApJ*, 617, 680
- Park, J. Y. & Woon, D. E., 2006, *ApJ*, 648, 1285
- Palmeirim, P., Ph. Andre, Ph., Kirk, J. et al. 2013, *A&A*, 550, 38
- Pascual-Ahuir, J. L., Silla, E., Tun, I., *J. Comp. Chem.*, 1994, 15, 1127
- Pickett, H. M., *J. Mol. Spectrosc.*, 1991, 148, 371
- Pilbratt, G. L., Riedinger, J. R., Passvogel, T., et al. 2010, *A&A*, 518, L1+
- Roberts, H., Millar, T. J., 2000, *A&A*, 361, 388
- Prasad, S. S., Huntress Jr., W. T, 1980, *APJS*, 43, 1
- Sarre, P. J. 2006, *J. Mol. Spec.*, 238, 1
- Sarre, P. J. 2000, *MNRAS*, 313, L14

- Schutte, W. A., & Greenberg, J. M. 1997, A&A, 317, L43
- Schutte, W. A., Greenberg, J. M., van Dishoeck, E. F., Tielens, A. G. G. M., Boogert, A. C. A., Whittet, D. C. B. 1997, Ap&SS, 255, 61
- Schutte, W. A., et al. 1999, A&A, 343, 966
- Shalabiea, O. M., greenberg, J. M., 1994, A&A, 290, 266
- Stantcheva, T., Shematovich, V. I., Herbst, E., 2002, A&A, 391, 1069
- Soifer, B. T., Puetter, R. C., Russell, R. W., Willner, S. P., Harvey, P. M., Gillett, F. C. 1979, ApJ, 232, L53
- Schneider, S., Elmegreen, B. G. 1979, ApJS, 41, 87
- Su, T., & Chesnavich, W. J. 1982, J. Chem. Phys., 76, 5183
- Tielens A. G. G. M., Tokunaga A. T., Geballe T. R., Baas F., 1991, ApJ, 381, 181
- Tomasi, J., Cammi, R., Mennucci, B., Cappelli, C., and Corni, S., Phys. Chem. Chem. Phys., 2002, 4, 5697
- Tomasi, J., Mennucci, B., Cammi, R., Chem. Rev., 2005, 105, 2999
- Tomasi, J., Mennucci, B., Cancs, E., J. Mol. Struct. (Theochem), 1999, 464, 211
- Turner, B. E., 2001, APJS, 136, 579
- Woon, D. E., Herbst, E., 2009, APJS, 185, 273
- Woodall, J., Agndez, M., Markwick-Kemper, A.J., Millar, T.J., 2007, A&A, 466, 1197

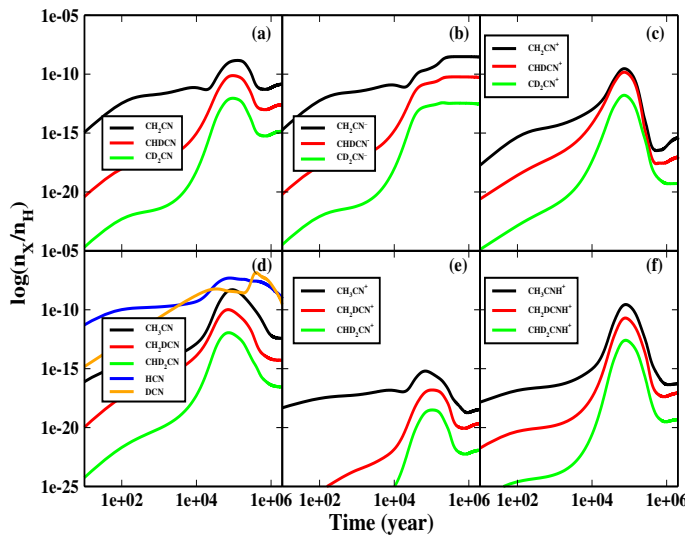


**Fig. A1. (a-f).** Chemical evolution of the cyanomethyl radical and its related species.

## Appendix A

### Chemical modeling:

In order to study various forms of the cyanomethyl radical in the interstellar medium (ISM), we develop a chemical model which includes the gas phase as well as the grain surface chemical network. Our gas phase chemical network consists of the network of Woodall et al. (2007) and the deuterated network used in Das et al. (2013b). Moreover, we include certain new reactions for the formation and destruction of various forms of cyanomethyl radical and its related species. Our surface network mainly adopted from Das et al. (2013b) and references therein. Our present gas phase chemical network consists of 6296 reactions and present surface chemical network consists of 285 reactions. Except molecular hydrogen (according to Leitch & Williams 1985, sticking coefficient of H<sub>2</sub> ~ 0) and Helium (Roberts & Millar 2000 assumed that Helium would not stick to the grain), depletion of all the gas phase neutral species onto the grain surface are considered with a sticking probability one.

In Table A1, we have presented only those reactions which are responsible for the formation and destruction of various deuterated isotopomers of cyanomethyl radical and its related species. Various types of reactions are considered in the network, namely, ion(cation)-neutral (IN), neutral-neutral (NN), charge exchange (CE), dissociative recombination (DR), photo-dissociation (PH), cosmic ray induced photo-dissociation (CRP), radiative association (RA), associative detachment (AD), radiative electron attachment (REA) and mutual neutralization (MN). The reaction network given in Table A1 is constructed mainly by assuming that reaction pathways are similar as those of hydrogenated reactions in Woodall et al. (2007). Following are

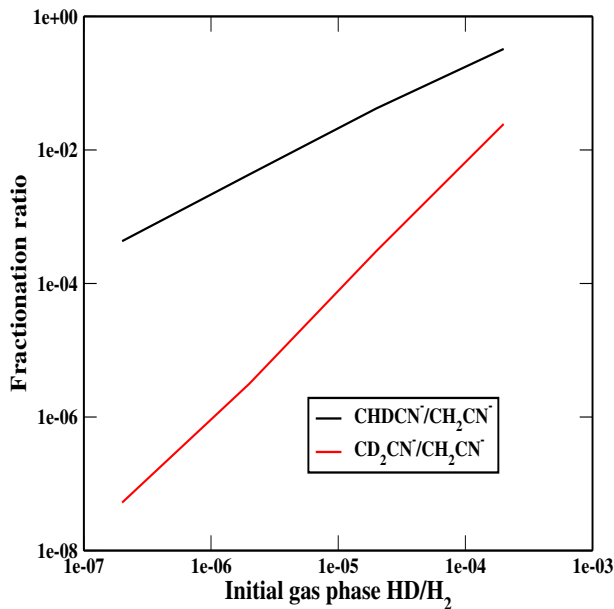


**Fig. A2.** Variation of fractionation ratio of  $\text{CH}_2\text{CN}^-$  with the initial gas phase fractionation ratio (abundance of HD/abundance of  $\text{H}_2$ ).

the adequate discussion regarding the adopted network for the various forms of cyanomethyl radical and its related species.

#### **Ion-neutral:**

Ion(cation)-neutral reactions ( $A^+ + B \rightarrow C^+ + D$ ) are the dominant means for the destruction of a neutral interstellar species. All the deuterated ion neutral reactions are assumed to be similar to the corresponding hydrogenated reactions given in the network of Woodall et al. (2007). The reaction numbers from R1 to R55 of Table A1 are of this kind. According to Herbst (2006), for a ion-molecular reaction, rate coefficient can be determined using the capture theory where the translational energy of the reactant must only surpass a long-range centrifugal barrier for the reaction to occur. The collision rate coefficient between an ion and non-polar neutral molecule can be determined using the so called Langevin collision rate

$$k_L = 2\pi e \sqrt{\frac{\alpha_d}{\mu}}, \quad (2)$$

where,  $e$  is the electronic charge,  $\alpha$  is the polarizability of the neutral non-polar molecule in  $\text{Å}^3$ ,  $\mu$  is the reduced mass of the reactants. But for polar neutral species, a complex situation arises due to the attraction between a charge and rotating permanent dipole moment. Su & Chesnavich, (1982) predicted the rate coefficients for this type of reactions. According to Woon & Herbst, (2009), the Su-Chesnavich formula can be written in two different ways and both of which uses

a parameter

$$x = \mu_D / \sqrt{2akT},$$

where k is the Boltzmann constant,  $\mu_D$  is the dipole moment of the polar neutral species in Debye & T is the temperature in Kelvin. Depending on the values of 'x', rate coefficients could be calculated by following two equations;

$$k_{IN} = (0.4767x + 0.6200) k_L \text{ for } x \geq 2, \quad (3)$$

$$k_{IN} = [(x + 0.5090)^2 / 10.526 + 0.9754] k_L \text{ for } x < 2. \quad (4)$$

Note that for  $x = 0$ , above equations reduces to the Langevin expression. Alternatively, Woon & Herbst (2009) expressed the equation for  $x \geq 2$  in powers of temperature T as following;

$$k_{IN} = c_1 + c_2 / \sqrt{T}, \quad (5)$$

where,  $c_1 = 0.62 k_L$  and  $c_2 = (0.4767\mu_D / \sqrt{2ak}) k_L$ .

For the computation of the rate coefficients, value of the polarizability and the dipole moment of the neutral molecules are taken from Woon & Herbst (2009). Here we have considered that polarizability and dipole moment will be invariant under the isotopic substitution. Theoretical computation of the polarizability and dipole moment depends on the derivatives of the electronic energy with respect to the external electric field. Since this electronic energy is not dependent on the mass of the nuclei (as the calculations are based on the Born-Oppenheimer approximation), isotopic substitution will not affect the results. But, since isotopic substitution changes the effective reduced mass of the reactants, the rate coefficients for the deuterated reactions could be different. Computed rate coefficients for the reaction numbers from R1 to R55 are also given in Table A1 for  $T = 10K$ . Polarizability of the neutral reactants in the unit of  $A^{\circ 3}$  and their respective dipole moments in the unit of Debye which are used for the computation of the rate coefficients are also given in Table A1.

### **Neutral-neutral:**

Reaction numbers R56 to R58 of Table A1 are the neutral-neutral ( $A + B \rightarrow C + D$ ) type reactions. From Woodall et al. (2007), we took those neutral-neutral reactions where neutral CH<sub>2</sub>CN is involved and assumed that similar reactions would be possible for its deuterated isotopomers. For the computation of rate coefficients for the neutral-neutral reactions, one needs to calculate the electronic energy barrier. But this electronic energy barrier is independent of the atomic mass. Due to this reason, we have assumed that the rate coefficients would be similar to those values for neutral CH<sub>2</sub>CN in Woodall et al. (2007). In Woodall et al. (2007), rate coefficients of this type of reactions were calculated by;

$$k_{NN} = \alpha \left( \frac{T}{300} \right)^\beta \exp \left( -\frac{\gamma}{T} \right), \quad (6)$$

where,  $\alpha, \beta$  and  $\gamma$  are the three constants. For reaction R56 & R57, we have assumed that  $\alpha = 1 \times 10^{-10}$ ,  $\beta = 0$  and  $\gamma = 0$  by following the reaction  $C + CH_2CN \rightarrow HC_3N + H$  in Woodall et al. (2007) (Smith, Herbst & Chang 2004) and for the reaction R58, we have assumed  $\alpha = 6.2 \times 10^{-11}$ ,  $\beta = 0$  and  $\gamma = 0$  by following the reaction  $N + C_2H_3 \rightarrow CH_2CN + H$  in Woodall et al. (2007). Woodall et al., (2007), used these rate coefficients by following Smith, Herbst & Chang (2004).

### **Charge Exchange:**

Charge Exchange ( $A^+ + B \rightarrow A + B^+$ ) type reactions are very common in the ISM. We have considered eight reactions (R59-R66) which are of this type. Rate constants ( $\alpha, \beta$  &  $\gamma$ ) of these reactions are also assumed to be similar to their hydrogenated counterpart as mentioned in Woodall et al. (2007) and the rate coefficients are calculated by using Eqn. 6. Woodall et al. (2007) used  $\alpha = 6.3 \times 10^{-9}$ ,  $\beta = 0$  and  $\gamma = 0$  for  $H^+ + CH_2CN \rightarrow CH_2CN^+ + H$ . We have assumed that these values are also applicable for the reactions containing deuterated isotopomers of  $CH_2CN$ .

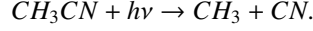
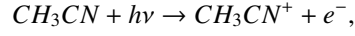
### **Dissociative Recombination:**

Interstellar cations are mainly destroyed by the dissociative recombination ( $A + e^- \rightarrow C + D$ ) processes. In our network, R67-R78 are of this kind. Dissociative recombination reaction pathways for the deuterated species are developed by following the pathways available for  $CH_3CN^+$ ,  $CH_3CNH^+$ ,  $CH_2CN^+$  from Woodall et al. (2007). Rate coefficients for the reaction numbers from R67 to R78 are computed by using eqn. 2. As before, here also, we have assumed that the isotopic substitution does not influence the computed rate coefficients very much. The rate constants ( $\alpha, \beta$  &  $\gamma$ ) of the deuterated reactants are assumed to be similar to the hydrogenated reactions in Woodall et al. (2007). For the reaction R67-R78,  $\alpha = 1.5 \times 10^{-7}$ ,  $\beta = -0.5$  and  $\gamma = 0$  are used by following the DR channel of  $CH_3CN^+$ ,  $CH_3CNH^+$ ,  $CH_2CN^+$  used in Woodall et al. (2007). Typical values of these kind of rate coefficients are of the order of  $\sim 10^{-7} \text{ cm}^3 \text{s}^{-1}$ .

### **Photo-dissociation:**

Reaction numbers R79 to R82 of Table A1 are the photo-dissociation type reactions ( $AB + h\nu \rightarrow A + B/AB + h\nu \rightarrow AB^+ + e^-$ ). These reactions are taken from Woodall et al. (2007) and are applied for the deuterated reactions as well. They have considered these dissociation reactions for  $CH_3CN$  and here, we assumed that these dissociation reactions are also possible for  $CH_2DCN$  and  $CHD_2CN$ . For the photo-dissociation reaction of  $CH_3CN$ , Woodall et al. (2007) assumed that

there would be two branching ratio;



For the first reaction,  $\alpha = 6.2 \times 10^{-10}$ ,  $\beta = 0$  and  $\gamma = 3.1$  were assumed and for the second reaction,  $\alpha = 3.4 \times 10^{-9}$ ,  $\beta = 0$  and  $\gamma = 2.0$  were assumed. Here, we have adopted similar values for the deuterated reactions. Following Woodall et al. (2007), the rate coefficient for these reactions could be adopted as following:

$$k_{PH} = \alpha \exp(\gamma A_V) \text{ s}^{-1}, \quad (7)$$

where,  $A_V$  is the visual extinction parameter. In Table A1, we presented the rate coefficients for all the reactions having  $T=10\text{K}$  and  $A_V=10$  (cold and dense cloud condition).

#### Cosmic ray induced photo-dissociation:

In Table A1, the reaction numbers from R83 to R86 are for cosmic ray induced photo dissociation ( $A + CRP \rightarrow A^+ + e^- / A + CRP \rightarrow C + D$ ). Rate coefficients for these kind of reactions could be adopted as follows:

$$k_{CR}(T) = \alpha \left( \frac{T}{300} \right)^\beta \frac{\gamma}{(1 - \omega)}, \quad (8)$$

where,  $\alpha$  is the cosmic-ray ionization rate,  $\gamma$  is the probability per cosmic-ray ionization that the appropriate photo reaction taking place, and  $\omega$  is the dust grain albedo in the far ultraviolet. Following Woodall et al. (2007), we use the cosmic ray ionization rate of  $\alpha = 1.3 \times 10^{-17}$  and  $\omega=0.6$ . These reactions (R83-R86) are taken from Woodall et al. (2007) and are applied for the deuterated reactions here. Woodall et al. (2007) assumed two photo-dissociation channel for  $CH_3CN$ . They used  $\gamma = 1122.5$  &  $2388.0$  and  $\beta = 0$  &  $0$  for these two channels respectively. We have used same values of  $\beta$  &  $\gamma$  for the dissociation channels of  $CH_2DCN$  and  $CHD_2CN$ .

#### Radiative association:

The reaction numbers from R87 to R90 of Table A1 are the radiative association type reactions ( $A + B \rightarrow C + h\nu$ ). These reactions along with the rate coefficients are taken from the hydrogenated reactions of Woodall et al. (2007) and applied here for the deuterated reactions. Rate coefficients of these reactions are calculated by using Eqn. 6. Following the reaction  $CH_3 + CN \rightarrow CH_3CN + h\nu$  in Woodall et al. (2007), we have assumed that reaction R87 and R89 would also possible with  $\alpha = 1 \times 10^{-16}$ ,  $\beta = 0$  and  $\gamma = 0$ . Woodall et. al., (2007) considered this rate coefficients by following Prasad & Huntress (1980). Similarly, by following the reaction  $CH_3^+ + HCN \rightarrow CH_3CNH^+ + h\nu$  in Woodall et al. (2007) (they adopted it from Herbst 1985), we have assumed that similar reaction would be possible for the deuterated species (reaction

R88 and R90) having  $\alpha = 9.0 \times 10^{-9}$ ,  $\beta = -0.5$  and  $\gamma = 0$ .

#### **Associative detachment:**

R91 & R92 of Table A1 are the associative detachment type ( $A + B^- \rightarrow C + e^-$ ) reactions. These are taken from Woodall et al. (2007) for the formation of CH<sub>3</sub>CN and are applied here for the deuterated reactions. Rate constants are assumed to be the same and are computed by using Eqn. 6.  $\alpha = 1 \times 10^{-9}$ ,  $\beta = 0$  and  $\gamma = 0$ , were adopted in Woodall et al. (2007) for the reaction  $CH_3 + CN^- \rightarrow CH_3CN + e^-$ , here we assumed similar values of  $\alpha$ ,  $\beta$  and  $\gamma$  for the reaction R91 and R92.

#### **Radiative electron attachment:**

The anions (CH<sub>2</sub>CN<sup>-</sup>, CHDCN<sup>-</sup> & CD<sub>2</sub>CN<sup>-</sup>) are formed primarily via radiative electron attachment ( $A + e^- \rightarrow A^- + h\nu$ ) reactions (the reaction numbers from R93 to R95 of Table A1). Following McElroy et al. (2009), we have adopted the following formula for the computation of the rate coefficient of this type:

$$k_{REA} = 1.25 \times 10^{-7} \left( \frac{T}{300} \right)^{-0.5} \text{ cm}^3 \text{ s}^{-1}. \quad (9)$$

#### **Mutual neutralization:**

Interstellar anions could efficiently be destroyed by the cations. These type of reactions are called mutual neutralization reaction ( $A^- + B^+ \rightarrow A + B$ ). Reaction number R96 to R116 of Table A1 are of this type. According to Das et al. (2013b), H<sub>3</sub><sup>+</sup>, C<sup>+</sup>, H<sub>3</sub>O<sup>+</sup>, HCO<sup>+</sup>, HN<sub>2</sub><sup>+</sup>, O<sup>+</sup> and H<sup>+</sup> are the major interstellar cations. For the mutual neutralization reactions, we have taken the reactions between these cations and different isotopomers of CH<sub>2</sub>CN<sup>-</sup>. Following Walsh et al. (2009), the rate coefficients of these reactions are computed by following relationship:

$$k_{MN} = 7.5 \times 10^{-8} \left( \frac{T}{300} \right)^{-0.5} \text{ cm}^3 \text{ s}^{-1}. \quad (10)$$

**Table A1.** Added Reaction network for cyanomethyl radical and its related species.

Reaction number	Reaction type	Reaction pathways for different isotopomers of Cyanomethyl radical	Rate coefficient at T=10K A <sub>v</sub> = 10
R1	IN	$H_3^+ + CD_2CN$ (4.382, 3.499 <sup>a</sup> ) → $CH_2DCN^+ + HD$	$4.60 \times 10^{-08} \text{ cm}^3 \text{s}^{-1}$
R2	IN	$He^+ + CD_2CN$ (4.382, 3.499 <sup>a</sup> ) → $CN + CD_2^+ + He$	$5.58 \times 10^{-08} \text{ cm}^3 \text{s}^{-1}$
R3	IN	$CHD_2CN^+ + CO$ (1.951, 0.101 <sup>a</sup> ) → $CD_2CN + HCO^+$	$1.04 \times 10^{-09} \text{ cm}^3 \text{s}^{-1}$
R4	IN	$H^+ + CHD_2CN$ (4.315, 3.932 <sup>a</sup> ) → $CD_2CN^+ + H_2$	$8.72 \times 10^{-08} \text{ cm}^3 \text{s}^{-1}$
R5	IN	$CD_2^+ + HCN$ (2.497, 3.007 <sup>a</sup> ) → $CD_2CN^+ + H$	$2.08 \times 10^{-08} \text{ cm}^3 \text{s}^{-1}$
R6	IN	$C_2HD^+ + ND$ (1.447, 1.522 <sup>a</sup> ) → $CD_2CN^+ + H$	$1.07 \times 10^{-08} \text{ cm}^3 \text{s}^{-1}$
R7	IN	$CHD_2^+ + CN$ (2.884, 1.390 <sup>a</sup> ) → $CD_2CN^+ + H$	$9.94 \times 10^{-09} \text{ cm}^3 \text{s}^{-1}$
R8	IN	$C_2D^+ + NHD$ (1.782, 1.768 <sup>a</sup> ) → $CD_2CN^+ + H$	$1.22 \times 10^{-08} \text{ cm}^3 \text{s}^{-1}$
R9	IN	$C_2D^+ + NH_2D$ (2.087, 1.519 <sup>a</sup> ) → $CD_2CN^+ + H_2$	$1.05 \times 10^{-08} \text{ cm}^3 \text{s}^{-1}$
R10	IN	$H^+ + CH_2DCN$ (4.315, 3.932 <sup>a</sup> ) → $CHDCN^+ + H_2$	$8.72 \times 10^{-08} \text{ cm}^3 \text{s}^{-1}$
R11	IN	$H^+ + CH_2DCN$ (4.315, 3.932 <sup>a</sup> ) → $CH_2D^+ + HCN$	$8.72 \times 10^{-08} \text{ cm}^3 \text{s}^{-1}$
R12	IN	$H^3 + +CH_2DCN$ (4.315, 3.932 <sup>a</sup> ) → $CH_2DCNH^+ + H_2$	$5.15 \times 10^{-08} \text{ cm}^3 \text{s}^{-1}$
R13	IN	$He^+ + CH_2DCN$ (4.315, 3.932 <sup>a</sup> ) → $CN + CH_2D^+ + He$	$6.24 \times 10^{-08} \text{ cm}^3 \text{s}^{-1}$
R14	IN	$H_3O^+ + CH_2DCN$ (4.315, 3.932 <sup>a</sup> ) → $CH_2DCNH^+ + H_2O$	$2.38 \times 10^{-08} \text{ cm}^3 \text{s}^{-1}$
R15	IN	$C_2H_2^+ + CH_2DCN$ (4.315, 3.932 <sup>a</sup> ) → $CH_2DCNH^+ + C_2H$	$2.15 \times 10^{-08} \text{ cm}^3 \text{s}^{-1}$
R16	IN	$HCNH^+ + CH_2DCN$ (4.315, 3.932 <sup>a</sup> ) → $CH_2DCNH^+ + HCN$	$2.10 \times 10^{-08} \text{ cm}^3 \text{s}^{-1}$
R17	IN	$HCNH^+ + CH_2DCN$ (4.315, 3.932 <sup>a</sup> ) → $CH_2DCNH^+ + HNC$	$2.10 \times 10^{-08} \text{ cm}^3 \text{s}^{-1}$
R18	IN	$HCO^+ + CH_2DCN$ (4.315, 3.932 <sup>a</sup> ) → $CH_2DCNH^+ + CO$	$2.08 \times 10^{-08} \text{ cm}^3 \text{s}^{-1}$
R19	IN	$HN_2^+ + CH_2DCN$ (4.315, 3.932 <sup>a</sup> ) → $CH_2DCNH^+ + N_2$	$2.08 \times 10^{-08} \text{ cm}^3 \text{s}^{-1}$
R20	IN	$C_2H_5^+ + CH_2DCN$ (4.315, 3.932 <sup>a</sup> ) → $CH_2DCNH^+ + C_2H_4$	$2.08 \times 10^{-08} \text{ cm}^3 \text{s}^{-1}$
R21	IN	$HCO_2^+ + CH_2DCN$ (4.315, 3.932 <sup>a</sup> ) → $CO_2 + CH_2DCNH^+$	$1.85 \times 10^{-08} \text{ cm}^3 \text{s}^{-1}$
R22	IN	$HCOOH_2^+ + CH_2DCN$ (4.315, 3.932 <sup>a</sup> ) → $CH_2DCNH^+ + HCOOH$	$1.83 \times 10^{-08} \text{ cm}^3 \text{s}^{-1}$
R23	IN	$HC_3NH^+ + CH_2DCN$ (4.315, 3.932 <sup>a</sup> ) → $CH_2DCNH^+ + HC_3N$	$1.79 \times 10^{-08} \text{ cm}^3 \text{s}^{-1}$
R24	IN	$H_3^+ + CHDCN$ (4.382, 3.499 <sup>a</sup> ) → $CH_2DCN^+ + H_2$	$4.61 \times 10^{-08} \text{ cm}^3 \text{s}^{-1}$
R25	IN	$C_2HD^+ + NH_2$ (1.782, 1.768 <sup>a</sup> ) → $CH_2DCN^+ + H$	$1.24 \times 10^{-08} \text{ cm}^3 \text{s}^{-1}$
R26	IN	$CH_2DCN^+ + CO$ (1.951, 0.101 <sup>a</sup> ) → $CHDCN + HCO^+$	$1.04 \times 10^{-09} \text{ cm}^3 \text{s}^{-1}$
R27	IN	$CH_2DCN^+ + H_2$ (0.773, 0 <sup>a</sup> ) → $CH_2DCNH^+ + H$	$1.48 \times 10^{-09} \text{ cm}^3 \text{s}^{-1}$
R28	IN	$C_2H_7^+ + DCN$ (2.497, 3.007 <sup>a</sup> ) → $CH_2DCNH^+ + CH_4$	$1.71 \times 10^{-08} \text{ cm}^3 \text{s}^{-1}$
R29	IN	$CH_3OH_2^+ + DCN$ (2.497, 3.007 <sup>a</sup> ) → $CH_2DCNH^+ + H_2O$	$1.69 \times 10^{-08} \text{ cm}^3 \text{s}^{-1}$
R30	IN	$HCOOH_2^+ + CH_2DCN$ (4.315, 3.932 <sup>a</sup> ) → $CH_2DCNH^+ + HCOOH$	$1.83 \times 10^{-08} \text{ cm}^3 \text{s}^{-1}$
R31	IN	$HC_3NH^+ + CH_2DCN$ (4.315, 3.932 <sup>a</sup> ) → $CH_2DCNH^+ + HC_3N$	$1.78 \times 10^{-08} \text{ cm}^3 \text{s}^{-1}$
R32	IN	$H^+ + CHD_2CN$ (4.315, 3.932 <sup>a</sup> ) → $CHD_2^+ + HCN$	$8.72 \times 10^{-08} \text{ cm}^3 \text{s}^{-1}$
R33	IN	$H^3 + +CHD_2CN$ (4.315, 3.932 <sup>a</sup> ) → $CHD_2CNH^+ + H_2$	$5.14 \times 10^{-08} \text{ cm}^3 \text{s}^{-1}$
R34	IN	$He^+ + CHD_2CN$ (4.315, 3.932 <sup>a</sup> ) → $CN + CHD_2^+ + He$	$6.23 \times 10^{-08} \text{ cm}^3 \text{s}^{-1}$
R35	IN	$H_3O^+ + CHD_2CN$ (4.315, 3.932 <sup>a</sup> ) → $CHD_2CNH^+ + H_2O$	$2.37 \times 10^{-08} \text{ cm}^3 \text{s}^{-1}$
R36	IN	$C_2H_2^+ + CHD_2CN$ (4.315, 3.932 <sup>a</sup> ) → $CHD_2CNH^+ + C_2H$	$2.14 \times 10^{-08} \text{ cm}^3 \text{s}^{-1}$
R37	IN	$HCNH^+ + CHD_2CN$ (4.315, 3.932 <sup>a</sup> ) → $CHD_2CNH^+ + HCN$	$2.09 \times 10^{-08} \text{ cm}^3 \text{s}^{-1}$
R38	IN	$HCNH^+ + CHD_2CN$ (4.315, 3.932 <sup>a</sup> ) → $CHD_2CNH^+ + HNC$	$2.09 \times 10^{-08} \text{ cm}^3 \text{s}^{-1}$
R39	IN	$HCO^+ + CHD_2CN$ (4.315, 3.932 <sup>a</sup> ) → $CHD_2CNH^+ + CO$	$2.07 \times 10^{-08} \text{ cm}^3 \text{s}^{-1}$
R40	IN	$HN_2^+ + CHD_2CN$ (4.315, 3.932 <sup>a</sup> ) → $CHD_2CNH^+ + N_2$	$2.07 \times 10^{-08} \text{ cm}^3 \text{s}^{-1}$
R41	IN	$C_2H_5^+ + CHD_2CN$ (4.315, 3.932 <sup>a</sup> ) → $CHD_2CNH^+ + C_2H_4$	$2.07 \times 10^{-08} \text{ cm}^3 \text{s}^{-1}$
R42	IN	$HCO_2^+ + CHD_2CN$ (4.315, 3.932 <sup>a</sup> ) → $CO_2 + CHD_2CNH^+$	$1.83 \times 10^{-08} \text{ cm}^3 \text{s}^{-1}$
R43	IN	$HCOOH_2 + +CHD_2CN$ (4.315, 3.932 <sup>a</sup> ) → $CHD_2CNH^+ + HCOOH$	$1.81 \times 10^{-08} \text{ cm}^3 \text{s}^{-1}$
R44	IN	$HC_3NH^+ + CHD_2CN$ (4.315, 3.932 <sup>a</sup> ) → $CHD_2CNH^+ + HC_3N$	$1.78 \times 10^{-08} \text{ cm}^3 \text{s}^{-1}$
R45	IN	$H_3^+ + CD_2CN$ (4.382, 3.499 <sup>a</sup> ) → $CHD_2CN^+ + H_2$	$4.60 \times 10^{-08} \text{ cm}^3 \text{s}^{-1}$
R46	IN	$C_2HD^+ + NHD$ (1.782, 1.768 <sup>a</sup> ) → $CHD_2CN^+ + H$	$1.21 \times 10^{-08} \text{ cm}^3 \text{s}^{-1}$
R47	IN	$CHD_2CN^+ + H_2$ (0.773, 0 <sup>a</sup> ) → $CHD_2CNH^+ + H$	$1.48 \times 10^{-09} \text{ cm}^3 \text{s}^{-1}$
R48	IN	$H_3^+ + CHD_2CN$ (4.315, 3.932 <sup>a</sup> ) → $CHD_2CNH^+ + H_2$	$5.14 \times 10^{-08} \text{ cm}^3 \text{s}^{-1}$
R49	IN	$CH_3OH^+ + DCN$ (2.497, 3.007 <sup>a</sup> ) → $CHD_2CNH^+ + H_2O$	$1.68 \times 10^{-08} \text{ cm}^3 \text{s}^{-1}$
R50	IN	$He^+ + CHDCN$ (4.382, 3.499 <sup>a</sup> ) → $CN + CHD^+ + He$	$5.58 \times 10^{-08} \text{ cm}^3 \text{s}^{-1}$
R51	IN	$CHD^+ + HCN$ (2.497, 3.007 <sup>a</sup> ) → $CHDCN^+ + H$	$2.12 \times 10^{-08} \text{ cm}^3 \text{s}^{-1}$
R52	IN	$C_2HD^+ + NH$ (1.447, 1.522 <sup>a</sup> ) → $CHDCN^+ + H$	$1.09 \times 10^{-08} \text{ cm}^3 \text{s}^{-1}$
R53	IN	$CH_2D^+ + CN$ (2.884, 1.390 <sup>a</sup> ) → $CHDCN^+ + H$	$1.01 \times 10^{-08} \text{ cm}^3 \text{s}^{-1}$
R54	IN	$C_2D^+ + NH_2$ (1.782, 1.768 <sup>a</sup> ) → $CHDCN^+ + H$	$1.25 \times 10^{-08} \text{ cm}^3 \text{s}^{-1}$
R55	IN	$C_2D + +NH_3$ (2.087, 1.519 <sup>a</sup> ) → $CHDCN^+ + H_2$	$1.06 \times 10^{-08} \text{ cm}^3 \text{s}^{-1}$

Reaction number	Reaction type	Reaction pathways for different isotopomers of Cyanomethyl radical	Rate coefficient at T=10K A <sub>V</sub> = 10
R56	NN	$C + CD_2CN \rightarrow DC_3N + D$	$1.00 \times 10^{-10} \text{ cm}^3 \text{ s}^{-1}$
R57	NN	$C + CHDCN \rightarrow HC_3N + D$	$1.00 \times 10^{-10} \text{ cm}^3 \text{ s}^{-1}$
R58	NN	$N + C_2H_2D \rightarrow CHDCN + H$	$6.20 \times 10^{-11} \text{ cm}^3 \text{ s}^{-1}$
R59	CE	$H^+ + CD_2CN \rightarrow CD_2CN^+ + H$	$6.30 \times 10^{-09} \text{ cm}^3 \text{ s}^{-1}$
R60	CE	$C^+ + CD_2CN \rightarrow CD_2CN^+ + C$	$2.00 \times 10^{-09} \text{ cm}^3 \text{ s}^{-1}$
R61	CE	$H^+ + CH_2DCN \rightarrow CH_2DCN^+ + H$	$8.40 \times 10^{-09} \text{ cm}^3 \text{ s}^{-1}$
R62	CE	$O^+ + CH_2DCN \rightarrow CH_2DCN^+ + O$	$2.94 \times 10^{-09} \text{ cm}^3 \text{ s}^{-1}$
R63	CE	$H^+ + CHD_2CN \rightarrow CHD_2CN^+ + H$	$8.40 \times 10^{-09} \text{ cm}^3 \text{ s}^{-1}$
R64	CE	$O^+ + CHD_2CN \rightarrow CHD_2CN^+ + O$	$2.94 \times 10^{-09} \text{ cm}^3 \text{ s}^{-1}$
R65	CE	$H^+ + CHDCN \rightarrow CHDCN^+ + H$	$6.30 \times 10^{-09} \text{ cm}^3 \text{ s}^{-1}$
R66	CE	$C^+ + CHDCN \rightarrow CHDCN^+ + C$	$2.00 \times 10^{-09} \text{ cm}^3 \text{ s}^{-1}$
R67	DR	$CHD_2CN^+ + e^- \rightarrow CD_2CN + H$	$8.22 \times 10^{-07} \text{ cm}^3 \text{ s}^{-1}$
R68	DR	$CHD_2CNH^+ + e^- \rightarrow CD_2CN + H_2$	$8.22 \times 10^{-07} \text{ cm}^3 \text{ s}^{-1}$
R69	DR	$CD_2CN^+ + e^- \rightarrow CN + CD_2$	$8.22 \times 10^{-07} \text{ cm}^3 \text{ s}^{-1}$
R70	DR	$CD_2CN^+ + e^- \rightarrow DCN + CD$	$8.22 \times 10^{-07} \text{ cm}^3 \text{ s}^{-1}$
R71	DR	$CH_2DCNH^+ + e^- \rightarrow CH_2DCN + H$	$8.22 \times 10^{-07} \text{ cm}^3 \text{ s}^{-1}$
R72	DR	$CH_2DCN^+ + e^- \rightarrow DCN + CH_2$	$8.22 \times 10^{-07} \text{ cm}^3 \text{ s}^{-1}$
R73	DR	$CH_2DCN^+ + e^- \rightarrow CHDCN + H$	$8.22 \times 10^{-07} \text{ cm}^3 \text{ s}^{-1}$
R74	DR	$CHD_2CNH^+ + e^- \rightarrow CHD_2CN + H$	$8.22 \times 10^{-07} \text{ cm}^3 \text{ s}^{-1}$
R75	DR	$CHD_2CN^+ + e^- \rightarrow DCN + CHD$	$8.22 \times 10^{-07} \text{ cm}^3 \text{ s}^{-1}$
R76	DR	$CH_2DCNH^+ + e^- \rightarrow CHDCN + H_2$	$8.22 \times 10^{-07} \text{ cm}^3 \text{ s}^{-1}$
R77	DR	$CHDCN^+ + e^- \rightarrow CN + CHD$	$8.22 \times 10^{-07} \text{ cm}^3 \text{ s}^{-1}$
R78	DR	$CHDCN^+ + e^- \rightarrow DCN + CH$	$8.22 \times 10^{-07} \text{ cm}^3 \text{ s}^{-1}$
R79	PH	$CH_2DCN + PHOTON \rightarrow CH_2DCN^+ + e^-$	$2.13 \times 10^{-23} \text{ s}^{-1}$
R80	PH	$CH_2DCN + PHOTON \rightarrow CN + CH_2D$	$7.01 \times 10^{-18} \text{ s}^{-1}$
R81	PH	$CHD_2CN + PHOTON \rightarrow CHD_2CN^+ + e^-$	$2.13 \times 10^{-23} \text{ s}^{-1}$
R82	PH	$CHD_2CN + PHOTON \rightarrow CN + CHD_2$	$7.01 \times 10^{-18} \text{ s}^{-1}$

Reaction number	Reaction type	Reaction pathways for different isotopomers of Cyanomethyl radical	Rate coefficient at T=10K A <sub>V</sub> = 10
R83	CRP	$CH_2DCN + CRPHOT \rightarrow CH_2DCN^+ + e^-$	$3.65 \times 10^{-14} \text{ s}^{-1}$
R84	CRP	$CH_2DCN + CRPHOT \rightarrow CN + CH_2D$	$7.76 \times 10^{-14} \text{ s}^{-1}$
R85	CRP	$CHD_2CN + CRPHOT \rightarrow CHD_2CN^+ + e^-$	$3.65 \times 10^{-17} \text{ s}^{-1}$
R86	CRP	$CHD_2CN + CRPHOT \rightarrow CN + CHD_2$	$7.76 \times 10^{-14} \text{ s}^{-1}$
R87	RA	$CH_2D + CN \rightarrow CH_2DCN + PHOTON$	$1.00 \times 10^{-16} \text{ cm}^3 \text{ s}^{-1}$
R88	RA	$CH_2D^+ + HCN \rightarrow CH_2DCNH + +PHOTON$	$4.93 \times 10^{-08} \text{ cm}^3 \text{ s}^{-1}$
R89	RA	$CHD_2 + CN \rightarrow CHD_2CN + PHOTON$	$1.00 \times 10^{-16} \text{ cm}^3 \text{ s}^{-1}$
R90	RA	$CHD_2^+ + HCN \rightarrow CHD_2CNH^+ + PHOTON$	$4.93 \times 10^{-08} \text{ cm}^3 \text{ s}^{-1}$
R91	AD	$CH_2D + CN^- \rightarrow CH_2DCN + e^-$	$1.00 \times 10^{-09} \text{ cm}^3 \text{ s}^{-1}$
R92	AD	$CHD_2 + CN^- \rightarrow CHD_2CN + e^-$	$1.00 \times 10^{-09} \text{ cm}^3 \text{ s}^{-1}$
R93	REA	$CH_2CN + e^- \rightarrow CH_2CN^- + PHOTON$	$6.85 \times 10^{-7} \text{ cm}^3 \text{ s}^{-1}$
R94	REA	$CD_2CN + e^- \rightarrow CD_2CN^- + PHOTON$	$6.85 \times 10^{-7} \text{ cm}^3 \text{ s}^{-1}$
R95	REA	$CHDCN + e^- \rightarrow CHDCN^- + PHOTON$	$6.85 \times 10^{-7} \text{ cm}^3 \text{ s}^{-1}$
R96	MN	$CH_2CN^- + H_3^+ \rightarrow CH_2CN + H_2 + H$	$4.11 \times 10^{-7} \text{ cm}^3 \text{ s}^{-1}$
R97	MN	$CH_2CN^- + C^+ \rightarrow CH_2CN + C$	$4.11 \times 10^{-7} \text{ cm}^3 \text{ s}^{-1}$
R98	MN	$CH_2CN^- + H_3O^+ \rightarrow CH_2CN + H + H_2O$	$4.11 \times 10^{-7} \text{ cm}^3 \text{ s}^{-1}$
R99	MN	$CH_2CN^- + HCO^+ \rightarrow CH_2CN + H + CO$	$4.11 \times 10^{-7} \text{ cm}^3 \text{ s}^{-1}$
R100	MN	$CH_2CN^- + HN_2^+ \rightarrow CH_2CN + H + N_2$	$4.11 \times 10^{-7} \text{ cm}^3 \text{ s}^{-1}$
R101	MN	$CH_2CN^- + O^+ \rightarrow CH_2CN + O$	$4.11 \times 10^{-7} \text{ cm}^3 \text{ s}^{-1}$
R102	MN	$CH_2CN^- + H^+ \rightarrow CH_2CN + H$	$4.11 \times 10^{-7} \text{ cm}^3 \text{ s}^{-1}$
R103	MN	$CHDCN^- + H_3^+ \rightarrow CHDCN + H_2 + H$	$4.11 \times 10^{-7} \text{ cm}^3 \text{ s}^{-1}$
R104	MN	$CHDCN^- + C^+ \rightarrow CHDCN + C$	$4.11 \times 10^{-7} \text{ cm}^3 \text{ s}^{-1}$
R105	MN	$CHDCN^- + H_3O^+ \rightarrow CHDCN + H + H_2O$	$4.11 \times 10^{-7} \text{ cm}^3 \text{ s}^{-1}$
R106	MN	$CHDCN^- + HCO^+ \rightarrow CHDCN + H + CO$	$4.11 \times 10^{-7} \text{ cm}^3 \text{ s}^{-1}$
R107	MN	$CHDCN^- + HN_2^+ \rightarrow CHDCN + H + N_2$	$4.11 \times 10^{-7} \text{ cm}^3 \text{ s}^{-1}$
R108	MN	$CHDCN^- + O^+ \rightarrow CHDCN + O$	$4.11 \times 10^{-7} \text{ cm}^3 \text{ s}^{-1}$
R109	MN	$CHDCN^- + H^+ \rightarrow CHDCN + H$	$4.11 \times 10^{-7} \text{ cm}^3 \text{ s}^{-1}$
R110	MN	$CD_2CN^- + H_3^+ \rightarrow CD_2CN + H_2 + H$	$4.11 \times 10^{-7} \text{ cm}^3 \text{ s}^{-1}$
R111	MN	$CD_2CN^- + C^+ \rightarrow CD_2CN + C$	$4.11 \times 10^{-7} \text{ cm}^3 \text{ s}^{-1}$
R112	MN	$CD_2CN^- + H_3O^+ \rightarrow CD_2CN + H + H_2O$	$4.11 \times 10^{-7} \text{ cm}^3 \text{ s}^{-1}$
R113	MN	$CD_2CN^- + HCO^+ \rightarrow CD_2CN + H + CO$	$4.11 \times 10^{-7} \text{ cm}^3 \text{ s}^{-1}$
R114	MN	$CD_2CN^- + HN_2^+ \rightarrow CD_2CN + H + N_2$	$4.11 \times 10^{-7} \text{ cm}^3 \text{ s}^{-1}$
R115	MN	$CD_2CN^- + O^+ \rightarrow CD_2CN + O$	$4.11 \times 10^{-7} \text{ cm}^3 \text{ s}^{-1}$
R116	MN	$CD_2CN^- + H^+ \rightarrow CD_2CN + H$	$4.11 \times 10^{-7} \text{ cm}^3 \text{ s}^{-1}$

<sup>a</sup> Polarizability of neutral reactants in units of  $A^{\circ 3}$  and dipole moment in Debye (Woon & Herbst 2009)

**Table A2.** Initial abundances relative to the total hydrogen nuclei

Species	Abundance
H <sub>2</sub>	5.00 × 10 <sup>-01</sup>
He	1.00 × 10 <sup>-01</sup>
N	2.14 × 10 <sup>-05</sup>
O	1.76 × 10 <sup>-04</sup>
H <sub>3</sub> <sup>+</sup>	1.00 × 10 <sup>-11</sup>
C <sup>+</sup>	7.30 × 10 <sup>-05</sup>
S <sup>+</sup>	8.00 × 10 <sup>-08</sup>
Si <sup>+</sup>	8.00 × 10 <sup>-09</sup>
Fe <sup>+</sup>	3.00 × 10 <sup>-09</sup>
Na <sup>+</sup>	2.00 × 10 <sup>-09</sup>
Mg <sup>+</sup>	7.00 × 10 <sup>-09</sup>
P <sup>+</sup>	3.00 × 10 <sup>-09</sup>
Cl <sup>+</sup>	4.00 × 10 <sup>-09</sup>
e <sup>-</sup>	7.31 × 10 <sup>-05</sup>
HD	1.6 × 10 <sup>-05</sup>

## Chemical evolution and Deuterium enrichment:

Depending on the concentration of the gas phase species, all the neutral species (except H<sub>2</sub> and He) are allowed to accrete on the grain surface. Surface species are allowed to populate the gas phase by the thermal evaporation or cosmic ray induced evaporation processes. Initial elemental abundances have been chosen to be same as in Das et al. (2013b) and these are the typical low metal abundances often adopted for TMC-1 cloud. Initial elemental abundances are given in Table A2. Unless otherwise stated, for all the cases, we assume the initial abundance of HD to be  $1.6 \times 10^{-5}$  with respect to total hydrogen nuclei. This implies to the initial fractionation ratio (HD/H<sub>2</sub>)  $3.2 \times 10^{-5}$ .

According to Palmeirim et al. (2013) and references therein, interstellar filaments could play a fundamental role in the star formation process. Taurus molecular cloud were known to exhibit large scale filamentary structure long before the Herschel (Schneider & Elmegreen 1979; Goldsmith et al. 2008). TMC-1 has recently been mapped with Herschel (Pilbratt et al. 2010) as a part of the Gould Belt Survey (Andre et al. 2010). Results obtained from the Herschel Gould Belt survey confirm the omnipresence of parsec scale filaments in nearby molecular clouds and suggest that the observed filamentary structure is directly related to the formation of prestellar cores. Herschel observations now demonstrate that filaments are truly ubiquitous in the cold interstellar medium (ISM). Palmeirim et al. (2013) made an attempt to prepare an analytical model for an idealized cylindrical filament. As per their model, filament will have dense, flat inner portion and have a power law behaviour at the larger radii. They assumed the Plummer-like function (Nutter et al., 2008; Arzoumanian et al., 2011) for the density profile;

$$\rho_p(r) = \rho_c / [1 + (r/R_{flat})^2]^{p/2} \rightarrow N(r) = A_p \frac{\rho_c R_{flat}}{[1 + (r/R_{flat})^2]^{(p-1)/2}},$$

where,  $\rho_c$  is the central density,  $R_{flat}$  is the size of the flat inner part, parameter  $p$  defines the steepness of the profile in the outer part,  $A_p$  is a finite factor which controls filament's inclination angle to the plane of sky. As per Ostriker (1964), the density structure of an isothermal gas cylinder in hydrostatic equilibrium could follow above equation with  $p = 4$ . In order to start with

a simple realistic physical condition for TMC-1 cloud, we have considered different regions of the cloud possessing different values of visual extinction parameter ( $A_V$ ). Lee et al., (1996) assumed a static, plane parallel, semi infinite cloud with a constant temperature 30K and a density profile to mimic the condition of a self gravitating isothermal sphere. Following relation was considered by them:

$$n_H = n_{H0}/(1 - cr/r_{max})^2,$$

where,  $n_H = n(H) + 2n(H_2)$  is the number density of the hydrogen nuclei in the units of  $\text{cm}^{-3}$ ,  $n_{H0}$  is the cloud density at the cloud surface,  $n_{Hmax}$  is the maximum number density,  $r_{max}$  is the maximum cloud depth,  $n_{H0}$  is the hydrogen density at the cloud surface ( $r=0$ ) and  $c$  is a constant. By evaluating the constant  $c$ , they derived the following relationship between the hydrogen number density and the visual extinction parameter:

$$n_H = n_{H0}[1 + [(\frac{n_{Hmax}}{n_{H0}})^{1/2} - 1]\frac{A_v}{A_{vmax}}]^2, \quad (11)$$

$A_{vmax}$  is the maximum visual extinction considered very deep inside the cloud. Lee et al. (1996) considered above relationship for  $T = 30\text{K}$ ,  $n_{H0} = 1 \times 10^2 \text{ cm}^{-3}$ ,  $n_{Hmax} = 1.042 \times 10^4 \text{ cm}^{-3}$ ,  $A_{vmax} = 10.86$ . As in Das & Chakrabarti (2011), in the present simulation, we assume that this relationship also holds for  $T=10\text{K}$ . Values of  $n_{H0}$ ,  $n_{Hmax}$  and  $A_{vmax}$  are assumed to be similar to the values assumed by Lee et al. (1996).

In Fig. A1.(a-f), we show chemical evolution of different forms of cyanomethyl radical and some of its related molecules. We have considered  $A_V = 10$ , which corresponds to a hydrogen number density of  $(n_H) = 8984.52 \text{ cm}^{-3}$ . Due to the huge abundances of hydrogenated species, abundances of any interstellar species are normally described with respect to the total number of hydrogen or with respect to the hydrogen molecule. In our case, we have presented the chemical abundances with respect to the total hydrogen nuclei in all forms. From the past observations, it is now known that water, Methanol and Carbon-di oxide are the major constituents of the interstellar grain mantle. According to Tielens et al. (1991), the abundance of water around the dense cloud region in the ice phase is  $\sim 10^{-4}$  and according to Das, Acharyya & Chakrabarti (2010) and references therein, abundances of  $\text{CO}_2$  and methanol in the ice phase could vary between 5-20% and 2-30% respectively with respect to the solid state water. These huge abundances could be manifested in the gas phase through some interstellar energetic events. Recent observational facility, such as the Atacama Large Millimeter/submillimeter Array (ALMA) could be very useful for the confirmed detection of the interstellar complex species having magnitudes  $\sim 10^{10}$  times lower than the Water molecules. Most of the molecules in Fig. A1 attain a peak value near  $\sim 10^5$  years. In Fig. A1.a, different forms of neutral  $\text{CH}_2\text{CN}$  are shown and it is evident that all the deuterated forms of  $\text{CH}_2\text{CN}$  are reasonably abundant (peak abundance  $> 10^{-14}$  with respect to  $n_H$ ). In Fig. A1.b, the chemical evolution of  $\text{CH}_2\text{CN}^-$  and its two deuterated isotopomers are shown. Different forms of these molecules are also reasonably abundant (peak abundances  $> 10^{-13}$  with respect to  $n_H$ ). Chemical evolution of  $\text{CH}_2\text{CN}^+$  and two of its deuterated isotopomers are shown in Fig. A1.c. Deuterated isotopomers of  $\text{CH}_2\text{CN}^+$  are not very

abundant (peak abundances  $> 10^{-15}$  with respect to  $n_H$ ). In Fig. A1.d, the chemical evolution of  $\text{CH}_3\text{CN}$  along with its two deuterated isotopomers and chemical evolution of HCN and DCN are shown. All of them are found to be abundant (peak abundances  $> 10^{-13}$  with respect to  $n_H$ ). Chemical evolution of  $\text{CH}_3\text{CN}^+$  along with its two deuterated isotopomers are shown in Fig. A1.e. Abundances of these species are several orders lower than the present observational limit. Figure 3f shows the chemical evolutions of  $\text{CH}_3\text{CNH}^+$  ion and its two deuterated isotopomers. Deuterated isotopomers of this ion are not very abundant. In brief, from Fig. A1, it is evident that various forms of  $\text{CH}_2\text{CN}^-$  are reasonably abundant and could be observed with the present observational facility. In order to justify our modeling results, in Table A3, we have compared our calculated abundances of some related species of the cyanomethyl anions with the existing theoretical/observational results.

In Table A4, we have presented peak column densities of all the species for  $A_V=1$  ( $n_H = 341.46 \text{ cm}^{-3}$ ), 5 ( $n_H = 2745.07 \text{ cm}^{-3}$ ) and 10 ( $n_H = 8984.52 \text{ cm}^{-3}$ ). Column densities of the species are computed by following the relationship developed by Shalabiea et al. (1994):

$$N(A) = n_H x_i R, \quad (12)$$

where,  $n_H$  is the total hydrogen number density,  $x_i$  is the abundance of the  $i^{th}$  species and  $R$  is the path length along the line of sight ( $= \frac{1.6 \times 10^{21} \times A_V}{n_H}$ ). From Table A4, it is evident that the column density of all the species are increasing linearly up to the intermediate region ( $A_V=5$  and  $n_H = 2745.07 \text{ cm}^{-3}$ ) of the cloud and beyond that the column density of all the species increases very slowly. From Table A4, it is evident that  $\text{CH}_2\text{CN}^-$  along with its deuterated isotopomers are the most abundant and require detail spectral studies to observe them in or around ISMs.

Despite the low elemental D/H ratio ( $\sim 10^{-5}$ , Linsky et al. 1995), several molecules in the interstellar medium are found to be heavily fractionated. In our simulation, we vary the initial fractionation ratio to check the fractionation of  $\text{CH}_2\text{CN}^-$ . To mimic the physical condition, we have considered  $A_V = 10$ ,  $n_H = 8984.52 \text{ cm}^{-3}$  and  $T=10\text{K}$  for this case. Fractionation ratio of the  $\text{CH}_2\text{CN}^-$  attaining a peak value near the intermediate time scale. In Fig. A2, only the peak values of the fractionation ratio is shown for different initial fractionation ratio. We have also checked the fractionation ratios for  $\text{CH}_2\text{CN}$  and  $\text{CH}_2\text{CN}^+$  and found that they behave in the same way as  $\text{CH}_2\text{CN}^-$  (fractionation values are also very similar). It is interesting to note that the fractionation ratio for the singly deuterated cyanomethyl anion often crosses the elemental D/H ratio. For the doubly deuterated isotopomer, the fractionation ratio crosses the elemental D/H ratio for an initial fractionation ratio  $> 10^{-5}$ .

**Table A3.** Comparison of fractional abundances with other observations/models.

Species	Fractional abundance by observations/other chemical models	Fractional abundance by our model <sup>C</sup>	
		Peak abundance	Abundance after $2 \times 10^6$ year
<b>CH<sub>2</sub>CN</b>	$2.5 \times 10^{-9}$ <sup>O</sup> , $4.59 \times 10^{-11}$ <sup>W</sup>	$1.46 \times 10^{-9}$	$1.43 \times 10^{-11}$
<b>CH<sub>3</sub>CN</b>	$5.00 \times 10^{-10}$ <sup>O</sup> , $6.95 \times 10^{-12}$ <sup>W</sup>	$5.01 \times 10^{-9}$	$3.74 \times 10^{-13}$
<b>HCN</b>	$1.00 \times 10^{-8}$ <sup>O</sup> , $2.95 \times 10^{-9}$ <sup>W</sup>	$4.93 \times 10^{-8}$	$9.01 \times 10^{-10}$
<b>CH<sub>3</sub>CN<sup>+</sup></b>	$1.02 \times 10^{-18}$ <sup>W</sup>	$6.24 \times 10^{-16}$	$3.49 \times 10^{-19}$
<b>CH<sub>3</sub>CNH<sup>+</sup></b>	$2.55 \times 10^{-14}$ <sup>W</sup>	$2.78 \times 10^{-10}$	$5.36 \times 10^{-17}$
<b>DCN</b>	$2.1 - 3.7 \times 10^{-10}$ <sup>T</sup>	$1.38 \times 10^{-7}$	$2.69 \times 10^{-10}$

<sup>O</sup> Observation by Ohishi, Irvine & Kaifu (1992) in TMC-1.  
<sup>W</sup> Chemical model by Woodall et al. (2007), by considering  $n_H = 2 \times 10^4 \text{ cm}^{-3}$ ,  $T = 10K$ ,  $A_V = 15$   
<sup>T</sup> Observation by Turner (2001) in TMC-1.  
<sup>C</sup> Our model by considering  $n_H = 8984.52 \text{ cm}^{-3}$ ,  $T = 10K$ ,  $A_V = 10$ .

**Table A4.** Column densities of various forms of CH<sub>2</sub>CN and its related molecules around different regions of the ISM.

Species	Isotopomers	AV <sub>1</sub> ( $n_H = 341.46 \text{ cm}^{-3}$ )	AV <sub>5</sub> ( $n_H = 2745.07 \text{ cm}^{-3}$ )	AV <sub>10</sub> ( $n_H = 8984.52 \text{ cm}^{-3}$ )
<b>CH<sub>2</sub>CN</b>	CH <sub>2</sub> CN	$2.11 \times 10^{07}$	$1.10 \times 10^{13}$	$2.33 \times 10^{13}$
	CHDCN	$8.76 \times 10^{02}$	$4.95 \times 10^{11}$	$1.21 \times 10^{12}$
	CD <sub>2</sub> CN	$4.69 \times 10^{-02}$	$3.89 \times 10^{09}$	$1.44 \times 10^{10}$
<b>CH<sub>2</sub>CN<sup>-</sup></b>	CH <sub>2</sub> CN <sup>-</sup>	$3.52 \times 10^{07}$	$4.35 \times 10^{13}$	$4.91 \times 10^{13}$
	CHDCN <sup>-</sup>	$1.46 \times 10^{03}$	$1.04 \times 10^{12}$	$9.43 \times 10^{11}$
	CD <sub>2</sub> CN <sup>-</sup>	$7.85 \times 10^{-02}$	$6.03 \times 10^{09}$	$5.99 \times 10^{09}$
<b>CH<sub>2</sub>CN<sup>+</sup></b>	CH <sub>2</sub> CN <sup>+</sup>	$2.76 \times 10^{04}$	$2.42 \times 10^{11}$	$4.67 \times 10^{12}$
	CHDCN <sup>+</sup>	$1.99 \times 10^{01}$	$1.09 \times 10^{11}$	$2.34 \times 10^{12}$
	CD <sub>2</sub> CN <sup>+</sup>	$1.05 \times 10^{-03}$	$9.88 \times 10^{08}$	$2.56 \times 10^{10}$
<b>CH<sub>3</sub>CN</b>	CH <sub>3</sub> CN	$1.38 \times 10^{05}$	$2.59 \times 10^{13}$	$8.02 \times 10^{13}$
	CH <sub>2</sub> DCN	$9.42 \times 10^{01}$	$6.81 \times 10^{11}$	$1.64 \times 10^{12}$
	CHD <sub>2</sub> CN	$5.05 \times 10^{-03}$	$5.12 \times 10^{09}$	$1.81 \times 10^{10}$
<b>CH<sub>3</sub>CN<sup>+</sup></b>	CH <sub>3</sub> CN <sup>+</sup>	$4.67 \times 10^{02}$	$4.08 \times 10^{06}$	$9.99 \times 10^{06}$
	CH <sub>2</sub> DCN <sup>+</sup>	$1.73 \times 10^{-02}$	$3.03 \times 10^{05}$	$2.49 \times 10^{05}$
	CHD <sub>2</sub> CN <sup>+</sup>	$9.58 \times 10^{-07}$	$2.43 \times 10^{03}$	$5.00 \times 10^{03}$
<b>CH<sub>3</sub>CNH<sup>+</sup></b>	CH <sub>3</sub> CNH <sup>+</sup>	$4.28 \times 10^{03}$	$3.31 \times 10^{11}$	$4.44 \times 10^{12}$
	CHDCNH <sup>+</sup>	$2.31 \times 10^{00}$	$2.27 \times 10^{10}$	$3.18 \times 10^{11}$
	CD <sub>3</sub> CNH <sup>+</sup>	$1.24 \times 10^{-04}$	$2.24 \times 10^{08}$	$4.10 \times 10^{09}$
<b>HCN</b>	HCN	$5.66 \times 10^{10}$	$6.09 \times 10^{14}$	$7.88 \times 10^{14}$
	DCN	$2.23 \times 10^{12}$	$2.61 \times 10^{15}$	$2.20 \times 10^{15}$

## Appendix B

**Table B1.** Vibrational frequencies of different forms of CH<sub>2</sub>CN in gas phase and water ice at B3LYP/6-311G++ level

Species name	Charge	Spin state	Peak positions (Gas phase) (Wavenumber in cm <sup>-1</sup> )	Absorbance	Peak positions (H <sub>2</sub> O ice) (Wavenumber in cm <sup>-1</sup> )	Absorbance
<chem>CH2CN</chem>	Neutral	<b>Doublet</b>	380.17	0.01	385.95	0.05
			422.18	0.14	428.20	0.0002
			741.27	71.00	751.76	93.08
			1056.15	6.08	1053.51	8.59
			1063.44	0.006	1058.47	0.14
			1466.41	6.00	1449.31	12.60
			2053.44	0.2927	2059.24	10.1890
			3146.77	0.079	3151.71	1.10
			3253.38	0.01	3261.55	1.29
		<b>Quartet</b>	401.64	3.42	406.18	7.018
			556.11	8.80	548.63	12.04
			875.41	8.60	881.00	14.6476
			879.36	65.39	887.16	86.94
			1104.57	12.98	1116.92	15.47
			1296.70	11.87	1295.95	30.54
			1456.34	20.54	1441.09	37.11
			3052.49	1.00	3054.17	5.09
			3186.69	1.70	3185.07	4.62
		<b>Sextet</b>	346.18	10.91	345.31	18.83
			428.48	1.42	433.95	1.88
			608.07	23.39	605.39	24.95
			705.71	53.97	699.05	103.80
			958.65	2.94	958.74	5.04
			1080.66	35.15	1082.93	58.80
			1448.14	3.18	1435.41	5.81
			3046.08	8.38	3051.37	5.48
			3144.26	10.31	3152.23	8.39
	<b>Cation</b>	<b>Singlet</b>	332.70	1.80	333.41	1.11
			361.52	3.38	347.41	2.37
			1065.83	0.007	1055.97	0.12
			1098.41	59.90	1088.41	130.90
			1190.97	11.68	1206.97	10.25
			1472.11	12.54	1444.50	10.20
			2166.72	337.15	2188.75	429.60
			3072.41	45.84	3111.38	54.35
			3182.95	62.98	3225.45	77.92
		<b>Triplet</b>	297.90	3.08	288.14	0.54
			367.58	1.02	370.92	0.93
			769.81	76.01	748.11	103.45
			795.38	97.74	767.54	113.28
			1071.82	0.72	1085.46	0.01
			1258.22	190.80	1202.05	301.70
			1633.10	0.56	1671.14	2.36
			2966.42	359.92	2985.29	533.60
			3018.48	212.29	3042.26	258.24

Species name	Charge	Spin state	Peak positions	Absorbance	Peak positions	Absorbance
			(Gas phase) (Wavenumber in cm <sup>-1</sup> )		(H <sub>2</sub> O ice) (Wavenumber in cm <sup>-1</sup> )	
		<b>Quintet</b>	346.84	5.33	349.97	7.44
			462.66	1.00	483.27	2.29
			753.89	11.34	774.18	16.94
			949.30	57.41	966.14	65.41
			1028.76	1.00	1039.23	5.06
			1317.33	16.46	1345.83	14.82
			1444.11	72.83	1439.88	112.56
			3050.21	92.34	3087.88	106.8981
			3174.04	55.18	3209.66	57.81
			359.32 (343.2 <sup>f</sup> )	327.78	352.23	557.70
		<b>Singlet</b>	414.56 (434.5 <sup>f</sup> )	2.55	415.95	3.02
			533.07 (585.5 <sup>f</sup> )	10.77	532.56	12.91
			1048.07 (1045.5 <sup>f</sup> )	0.26	1044.80	0.83
			1075.67 (991.5 <sup>f</sup> )	16.93	1088.82	26.07
			1444.91 (1298.2 <sup>f</sup> )	11.31	1436.32	34.49
			2056.73 (2115.7 <sup>f</sup> )	673.64	2016.35	1451.74
			3112.82 (3122.3 <sup>f</sup> )	15.15	3124.48	3.64
			3190.46 (3191.3 <sup>f</sup> )	51.00	3208.80	25.05
			267.97	97.84	230.03	270.80
			380.97	120.36	327.49	44100.90
	<b>Anion</b>	<b>Triplet</b>	724.28	648.90	710.95	470.37
			998.59	686.60	983.77	10158.64
			1029.93	22.97	1008.78	149.60
			1414.96	880.97	1345.70	3023.70
			2047.42	12.02	2041.51	509.41
			3004.22	8.9511	2854.88	1248.3729
			3075.31	426.77	3344.74	430118.36
			380.69	55.85	377.65	52.17
			528.98	254.03	470.96	36.07
			848.23	248.93	530.66	95.05
		<b>Quintet</b>	866.53	1075.23	780.28	43.80
			1093.33	264.32	923.99	1.48
			1300.64	242.77	1139.37	89.16
			1413.46	487.14	1429.66	5.21
			2943.40	21.20	2958.33	161.83
			3053.47	115.4081	3006.99	128.18

Species name	Charge	Spin state	Peak positions (Gas phase) (Wavenumber in cm <sup>-1</sup> )	Absorbance	Peak positions (H <sub>2</sub> O ice) (Wavenumber in cm <sup>-1</sup> )	Absorbance
CHDCN	Neutral	<b>Doublet</b>	360.12	0.0305	364.81	0.3103
			414.01	0.3487	420.29	0.0622
			674.97	53.6634	683.66	70.3703
			894.49	1.8954	892.34	2.8317
			1055.05	4.7613	1052.14	6.7508
			1337.89	3.2483	1322.47	7.1377
			2052.21	0.2364	2058.10	10.4464
			2349.18	0.2326	2353.90	0.4898
			3204.29	0.0384	3211.04	1.2018
		<b>Quartet</b>	367.00	3.26	371.42	6.71
			508.89	3.61	503.27	5.62
			796.55	62.02	803.16	81.68
			805.91	4.28	807.13	8.06
			1046.16	11.57	1060.44	12.96
			1240.95	21.08	1240.38	43.42
			1375.51	13.01	1364.19	23.7859
			2250.01	0.33	2252.38	1.90
			3171.93	2.37	3169.75	7.63
		<b>Sextet</b>	316.41	8.3996	317.46	14.4958
			380.63	3.5056	383.53	5.4820
			584.05	27.9405	586.27	34.1346
			679.35	33.6185	670.45	70.1195
			808.06	3.2080	807.46	4.9155
			1072.42	33.7646	1075.20	56.6412
			1307.13	3.5049	1296.24	6.9014
			2266.78	4.3870	2271.75	3.0207
			3098.56	9.4154	3105.36	7.0616
	<b>Cation</b>	<b>Singlet</b>	327.28	1.0415	328.67	0.5740
			342.81	1.4710	330.06	0.6979
			896.55	8.7921	891.23	15.5052
			1080.99	5.3437	1080.71	109.5207
			1090.64	50.2969	1095.07	4.1450
			1347.18	2.6195	1321.79	0.9668
			2156.55	336.6641	2181.29	427.8153
			2308.93	9.8690	2335.43	11.3447
			3132.20	55.7510	3173.15	67.9790
		<b>Triplet</b>	279.82	3.4254	268.24	0.9614
			362.00	0.9464	364.66	0.9042
			676.34	53.8833	671.54	74.4633
			720.96	68.9088	696.44	80.0691
			1042.19	15.2728	1034.36	91.3915
			1143.64	136.3938	1112.61	146.0176
			1624.63	0.2071	1662.24	0.6087
			2198.34	159.8451	2213.71	227.5224
			2992.93	287.4476	3014.33	396.0676
		<b>Quintet</b>	336.09	5.50	340.23	7.70
			377.56	1.71	394.24	3.08
			691.98	8.97	707.33	14.13
			882.81	46.11	894.99	53.63
			945.72	0.48	957.60	2.50
			1245.25	0.46	1252.44	5.20
			1360.00	72.87	1380.17	102.28
			2302.28	47.10	2323.43	53.74
			3092.36	64.05	3136.19	73.83



Species name	Charge	Spin state	Peak positions (Gas phase) (Wavenumber in cm <sup>-1</sup> )	Absorbance	Peak positions (H <sub>2</sub> O ice) (Wavenumber in cm <sup>-1</sup> )	Absorbance
<b>Anion</b>	<b>Singlet</b>		320.38	265.9975	315.18	445.8616
			390.54	2.0832	391.19	2.7553
			532.73	14.1738	531.43	22.1992
			890.57	0.7390	890.03	1.0047
			1068.77	14.2137	1079.21	20.9991
			1320.07	13.3165	1314.13	35.9126
			2053.96	671.4335	2013.34	1438.5730
			2314.43	10.3086	2326.47	15.7194
	<b>Triplet</b>		3153.96	34.8815	3169.35	15.4877
			256.03	73.2647	224.97	257.8315
			373.69	126.5104	315.27	40032.8173
			659.32	447.5905	649.24	314.4611
			838.42	533.0538	815.96	13084.5480
			1022.75	106.1802	1002.20	1273.5056
			1286.26	690.3204	1229.75	2932.2540
<b>CD<sub>2</sub>CN</b>	<b>Neutral</b>	<b>Quintet</b>	2045.45	8.9107	2038.72	1030.7865
			2239.84	41.39	2228.67	43853.1197
			3042.11	231.0028	3157.93	283695.8348
			362.33	66.32	324.83	48.00
			429.86	212.83	425.17	23.09
			739.90	194.13	516.60	74.48
			810.32	587.01	772.71	23.19
			1082.59	127.96	791.52	20.15
			1199.89	567.59	1124.15	79.07
			1351.70	91.59	1295.14	11.46
	<b>Quartet</b>		2193.92	37.333	2184.96	84.31
			3012.36	52.63	2983.33	143.03
			344.40	0.13	348.54	0.63
			397.78	0.80	404.60	0.34
			606.56	36.40	613.17	48.00
	<b>Sextet</b>		870.49	0.24	869.34	0.02
			937.96	7.22	934.57	11.69
			1168.69	0.03	1156.60	0.27
			2050.54	0.18	2056.49	10.54
			2283.18	0.16	2286.56	0.88
			2424.21	0.30	2430.64	0.09
			356.14	3.08	360.18	6.23
			436.96	5.69	431.70	7.60
			705.79	32.37	712.16	41.85
			745.87	4.23	746.78	8.19
			1000.62	3.80	995.42	9.63
			1080.21	25.93	1097.22	37.52
			1335.61	7.67	1329.22	17.85
			2221.86	1.00	2222.68	4.01
			2362.52	1.00	2361.63	1.27



Species name	Charge	Spin state	Peak positions (Gas phase) (Wavenumber in cm <sup>-1</sup> )	Absorbance	Peak positions (H <sub>2</sub> O ice) (Wavenumber in cm <sup>-1</sup> )	Absorbance
Cation	Singlet		318.34	0.2651	316.60	0.0929
			328.26	0.5487	320.36	0.0361
			869.40	1.8879	866.28	1.1613
			950.70	39.7773	940.72	75.7327
			959.62	0.9499	970.72	0.3826
			1201.42	9.0447	1180.60	33.1407
			2137.45	307.90	2166.38	394.2006
			2261.07	28.5996	2282.02	30.7198
	Triplet		2374.60	20.7168	2405.56	26.2027
			265.88	3.7658	316.60	0.0929
			351.80	0.7345	320.36	0.0361
			640.54	41.4409	866.28	1.1613
			643.21	49.7048	940.72	75.7327
			881.69	52.4016	970.72	0.3826
			1086.73	41.6529	1180.60	33.1407
			1615.46	0.9962	2166.38	394.2006
Anion	Singlet		2164.45	206.2750	2282.02	30.7198
			2234.00	114.3264	2405.56	26.2027
			315.20	4.46	318.61	6.56
			362.42	1.21	377.86	2.41
			680.50	8.55	695.04	12.83
			759.64	24.26	772.30	27.80
			900.04	2.38	908.44	6.94
			1037.39	3.00	1036.94	4.41
	Triplet		1330.49	54.80	1359.99	78.72
			2214.89	60.13	2241.36	70.72
			2363.00	21.62	2390.47	23.87
			277.57	204.9094	272.73	334.5490
			372.18	1.7243	372.41	2.5120
			532.47	16.9905	530.58	30.9795
			866.57	0.8907	866.50	1.3089
			942.63	1.5371	942.87	0.7288
Quintet	Singlet		1167.74	25.6880	1173.99	53.0751
			2050.23	663.9194	2009.48	1413.2486
			2261.10	6.7069	2271.46	34.4696
			2373.80	22.5826	2388.17	10.7051
			246.64	56.9436	216.52	235.1422
			360.02	130.5705	305.25	36839.6098
			591.20	250.5390	581.93	169.2967
			802.93	597.9890	784.05	18556.8130
	Triplet		915.87	187.5826	881.66	901.8334
			1122.78	269.6364	1084.62	675.4565
			2042.43	6.3038	2025.21	1008.1370
			2188.64	1.7398	2095.03	220.3006
			2296.73	111.0626	2488.81	224264.5837
			334.90	65.68	311.27	56.61
			416.91	189.14	354.95	15.50
			698.46	468.08	487.92	35.46

<sup>f</sup> Computed vibrational (harmonic) frequencies by Fortenberry, Crawford & Lee (2013)

**Table B2.** Rotational transitions for gas phase  $\text{CH}_2\text{CN}^-$  by considering the experimental values of the spectroscopic constants. Errors on the computed line frequencies are related to the errors on the constants given in Table 2 and from there, the error ( $d\nu/\nu$ ) on any line frequency for  $\text{CH}_2\text{CN}^-$  is found to be  $= 6.16 \times 10^{-5}$ .

Frequency (in MHz)	I <sup>c</sup>	D <sup>d</sup>	E <sub>lower</sub> <sup>e</sup> (in cm <sup>-1</sup> )	g <sub>up</sub> <sup>f</sup>	QnF <sup>h</sup>	Upper state (Qn <sub>up</sub> <sup>i</sup> )	Lower state (Qn <sub>lower</sub> <sup>j</sup> )
19950.2455	-6.1365	3	-0.0000	3	304	1 0 1 1	0 0 0 1
19950.9319	-5.9147	3	-0.0000	5	304	1 0 1 2	0 0 0 1
19951.9617	-6.6136	3	-0.0000	1	304	1 0 1 0	0 0 0 1
39900.8618	-5.8376	3	0.6655	5	304	2 0 2 2	1 0 1 2
39900.9762	-5.7126	3	0.6655	3	304	2 0 2 1	1 0 1 0
39901.5483	-5.3605	3	0.6655	5	304	2 0 2 2	1 0 1 1
39901.5973	-5.0894	3	0.6655	7	304	2 0 2 3	1 0 1 2
39902.6924	-5.8376	3	0.6655	3	304	2 0 2 1	1 0 1 1
59851.3698	-5.6650	3	1.9965	7	304	3 0 3 3	2 0 2 3
59851.9909	-4.9326	3	1.9965	5	304	3 0 3 2	2 0 2 1
59852.1053	-4.7619	3	1.9964	7	304	3 0 3 3	2 0 2 2
59852.1326	-4.6016	3	1.9965	9	304	3 0 3 4	2 0 2 3
59853.1351	-5.6649	3	1.9964	5	304	3 0 3 2	2 0 2 2
79801.6393	-5.5449	3	3.9929	9	304	4 0 4 4	3 0 3 4
79802.3530	-4.4869	3	3.9929	7	304	4 0 4 3	3 0 3 2
79802.4020	-4.3688	3	3.9929	9	304	4 0 4 4	3 0 3 3
79802.4193	-4.2536	3	3.9929	11	304	4 0 4 5	3 0 3 4
79803.3827	-5.5449	3	3.9929	7	304	4 0 4 3	3 0 3 3
99751.5713	-5.4542	3	6.6548	11	304	5 0 5 5	4 0 4 5
99752.3242	-4.1654	3	6.6548	9	304	5 0 5 4	4 0 4 3
99752.3514	-4.0740	3	6.6548	11	304	5 0 5 5	4 0 4 4
99752.3634	-3.9837	3	6.6548	13	304	5 0 5 6	4 0 4 5
99753.3049	-5.4542	3	6.6548	9	304	5 0 5 4	4 0 4 4
119701.0747	-5.3826	3	9.9822	13	304	6 0 6 6	5 0 5 6
119701.8494	-3.9135	3	9.9822	11	304	6 0 6 5	5 0 5 4
119701.8668	-3.8386	3	9.9822	13	304	6 0 6 6	5 0 5 5
119701.8756	-3.7642	3	9.9822	15	304	6 0 6 7	5 0 5 6
119702.8029	-5.3826	3	9.9822	11	304	6 0 6 5	5 0 5 5
139650.0604	-5.3247	3	13.9750	15	304	7 0 7 7	6 0 6 7
139650.8493	-3.7071	3	13.9750	13	304	7 0 7 6	6 0 6 5
139650.8613	-3.6435	3	13.9750	15	304	7 0 7 7	6 0 6 6
139650.8680	-3.5802	3	13.9750	17	304	7 0 7 8	6 0 6 7
139651.7854	-5.3247	3	13.9750	13	304	7 0 7 6	6 0 6 6
159598.4405	-5.2771	3	18.6333	17	304	8 0 8 8	7 0 7 8
159599.2393	-3.5331	3	18.6333	15	304	8 0 8 7	7 0 7 6
159599.2481	-3.4778	3	18.6333	17	304	8 0 8 8	7 0 7 7
159599.2534	-3.4226	3	18.6333	19	304	8 0 8 9	7 0 7 8
159600.1634	-5.2771	3	18.6333	15	304	8 0 8 7	7 0 7 7
179546.1275	-5.2378	3	23.9570	19	304	9 0 9 9	8 0 8 9
179546.9337	-3.3836	3	23.9570	17	304	9 0 9 8	8 0 8 7
179546.9404	-3.3347	3	23.9569	19	304	9 0 9 9	8 0 8 8
179546.9447	-3.2858	3	23.9570	21	304	9 0 9 10	8 0 8 9
179547.8490	-5.2378	3	23.9569	17	304	9 0 9 8	8 0 8 8
199493.0342	-5.2052	3	29.9460	21	304	10 0 10 10	9 0 9 10
199493.8461	-3.2535	3	29.9460	19	304	10 0 10 9	9 0 9 8
199493.8514	-3.2095	3	29.9460	21	304	10 0 10 10	9 0 9 9
199493.8550	-3.1657	3	29.9460	23	304	10 0 10 11	9 0 9 10
199494.7547	-5.2052	3	29.9460	19	304	10 0 10 9	9 0 9 9
219439.0735	-5.1783	3	36.6004	23	304	11 0 11 11	10 0 10 11
219439.8900	-3.1390	3	36.6004	21	304	11 0 11 10	10 0 10 9
219439.8943	-3.0992	3	36.6004	23	304	11 0 11 11	10 0 10 10

219439.8973	-3.0593	3	36.6004	25	304	11 01112	10 01011
219440.7933	-5.1783	3	36.6004	21	304	11 01110	10 01010
239384.1585	-5.1565	3	43.9201	25	304	12 01212	11 01112
239384.9787	-3.0377	3	43.9201	23	304	12 01211	11 01110
239384.9823	-3.0012	3	43.9201	25	304	12 01212	11 01111
239384.9848	-2.9647	3	43.9201	27	304	12 01213	11 01112
239385.8777	-5.1565	3	43.9201	23	304	12 01211	11 01111
259328.2022	-5.1391	3	51.9051	27	304	13 01313	12 01213
259329.0255	-2.9474	3	51.9051	25	304	13 01312	12 01211
259329.0285	-2.9138	3	51.9051	27	304	13 01313	12 01212
259329.0307	-2.8802	3	51.9051	29	304	13 01314	12 01213
259329.9209	-5.1391	3	51.9051	25	304	13 01312	12 01212
279271.1177	-5.1256	3	60.5554	29	304	14 01414	13 01314
279271.9437	-2.8668	3	60.5554	27	304	14 01413	13 01312
279271.9462	-2.8356	3	60.5554	29	304	14 01414	13 01313
279271.9481	-2.8044	3	60.5554	31	304	14 01415	13 01314
279272.8361	-5.1256	3	60.5554	27	304	14 01413	13 01313
299212.8181	-5.1158	3	69.8709	31	304	15 01515	14 01415
299213.6463	-2.7946	3	69.8709	29	304	15 01514	14 01413
299213.6485	-2.7655	3	69.8709	31	304	15 01515	14 01414
299214.5362	-5.1158	3	69.8709	29	304	15 01514	14 01414
319154.0468	-2.7300	3	79.8516	31	304	16 01615	15 01514
319154.9344	-5.1092	3	79.8516	31	304	16 01615	15 01515

<sup>1</sup> <sup>c</sup> Base 10 logarithm of the integrated intensity at 300K in nm<sup>2</sup> MHz

<sup>d</sup> Degrees of freedom in the rotational partition function (0 for atoms, 2 for linear molecules, 3 for non linear molecules)

<sup>e</sup> Lower state energy in cm<sup>-1</sup> relative to the lowest energy level in the ground vibrionic state.

<sup>f</sup> Upper state degeneracy :  $g_{up} = g_I \times g_N$ , where  $g_I$  is the spin statistical weight and  $g_N = 2N + 1$  the rotational degeneracy.

<sup>g</sup> Molecule Tag

<sup>h</sup> Coding for the format of quantum numbers. QnF=100 ×  $Q + 10 \times H + N_{Qn}$ ;  $N_{Qn}$  is the number of quantum numbers for each state; H indicates the number of half integer quantum numbers; Qmod5, the residual when Q is divided by 5, gives the number of principal quantum numbers (without the spin designating ones).

<sup>i</sup> Quantum numbers for the upper state

<sup>j</sup> Quantum numbers for the lower state

**Table B3.** Computed rotational transitions for gas phase CHDCN<sup>-</sup> by considering our calculated values of spectroscopic constants. Since there are no experimentally fitted rotational and distortional constants available, we are only providing the line frequencies based on our theoretically calculated spectroscopic constants which are given in Table 2.

Frequency (in MHz)	I <sup>c</sup>	D <sup>d</sup>	E <sub>lower</sub> <sup>e</sup>	g <sub>up</sub> <sup>f</sup>	QnF <sup>h</sup>	Upper state (Qn <sub>up</sub> <sup>i</sup> )	Lower state (Qn <sub>lower</sub> <sup>j</sup> )
18477.4689	-6.2141	3	-0.0000	5	305	1 0 1 1 2	0 0 0 1 2
18478.1537	-5.9430	3	-0.0000	7	305	1 0 1 2 3	0 0 0 1 2
36955.3164	-5.9169	3	0.6164	7	305	2 0 2 2 3	1 0 1 2 3
36955.4305	-5.6651	3	0.6164	5	305	2 0 2 1 2	1 0 1 0 1
36956.0012	-5.3887	3	0.6163	7	305	2 0 2 2 3	1 0 1 1 2
36956.0501	-5.1546	3	0.6164	9	305	2 0 2 3 4	1 0 1 2 3
36957.1425	-5.9150	3	0.6163	5	305	2 0 2 1 2	1 0 1 1 2
55433.0730	-5.7579	3	1.8491	9	305	3 0 3 3 4	2 0 2 3 4
55433.6926	-4.9605	3	1.8491	7	305	3 0 3 2 3	2 0 2 1 2
55433.8067	-4.8268	3	1.8491	9	305	3 0 3 3 4	2 0 2 2 3
55433.8339	-4.6885	3	1.8491	11	305	3 0 3 4 5	2 0 2 3 4
55434.8339	-5.7440	3	1.8491	7	305	3 0 3 2 3	2 0 2 2 3
73910.6172	-5.6492	3	3.6982	11	305	4 0 4 4 5	3 0 3 4 5
73911.3292	-4.5514	3	3.6982	9	305	4 0 4 3 4	3 0 3 2 3
73911.3781	-4.4553	3	3.6981	11	305	4 0 4 4 5	3 0 3 3 4
73911.3954	-4.3548	3	3.6982	13	305	4 0 4 5 6	3 0 3 4 5
73912.3565	-5.6375	3	3.6981	9	305	4 0 4 3 4	3 0 3 3 4
92387.8593	-5.5671	3	6.1636	13	305	5 0 5 5 6	4 0 4 5 6
92388.6103	-4.2515	3	6.1636	11	305	5 0 5 4 5	4 0 4 3 4
92388.6375	-4.1747	3	6.1636	13	305	5 0 5 5 6	4 0 4 4 5
92388.6495	-4.0948	3	6.1636	15	305	5 0 5 6 7	4 0 4 5 6
92389.5886	-5.5580	3	6.1636	11	305	5 0 5 4 5	4 0 4 4 5
110864.7166	-5.5021	3	9.2453	15	305	6 0 6 6 7	5 0 5 6 7
110865.4895	-4.0136	3	9.2453	13	305	6 0 6 5 6	5 0 5 4 5
110865.5067	-3.9491	3	9.2453	15	305	6 0 6 6 7	5 0 5 5 6
110865.5155	-3.8825	3	9.2453	17	305	6 0 6 7 8	5 0 5 6 7
110866.4406	-5.4950	3	9.2453	13	305	6 0 6 5 6	5 0 5 5 6
129341.1089	-5.4492	3	12.9434	17	305	7 0 7 7 8	6 0 6 7 8
129341.8959	-3.8169	3	12.9434	15	305	7 0 7 6 7	6 0 6 5 6
129341.9078	-3.7611	3	12.9434	17	305	7 0 7 7 8	6 0 6 6 7
129341.9146	-3.7039	3	12.9434	19	305	7 0 7 8 9	6 0 6 7 8
129342.8297	-5.4435	3	12.9434	15	305	7 0 7 6 7	6 0 6 6 7
147816.9571	-5.4055	3	17.2578	19	305	8 0 8 8 9	7 0 7 8 9
147817.7540	-3.6500	3	17.2578	17	305	8 0 8 7 8	7 0 7 6 7
147817.7628	-3.6007	3	17.2578	19	305	8 0 8 8 9	7 0 7 7 8
147817.7681	-3.5504	3	17.2578	21	305	8 0 8 9 10	7 0 7 8 9
147818.6759	-5.4009	3	17.2578	17	305	8 0 8 7 8	7 0 7 7 8
166292.1826	-5.3691	3	22.1885	21	305	9 0 9 9 10	8 0 8 9 10
166292.9868	-3.5057	3	22.1885	19	305	9 0 9 8 9	8 0 8 7 8
166292.9935	-3.4616	3	22.1884	21	305	9 0 9 9 10	8 0 8 8 9
166292.9978	-3.4167	3	22.1885	23	305	9 0 9 10 11	8 0 8 9 10
166293.8999	-5.3652	3	22.1884	19	305	9 0 9 8 9	8 0 8 8 9
184766.7068	-5.3387	3	27.7354	23	305	10 0 1 0 1 0 1 1	9 0 9 10 1
184767.5168	-3.3794	3	27.7354	21	305	10 0 1 0 9 1 0	9 0 9 8 9
184767.5221	-3.3395	3	27.7354	23	305	10 0 1 0 1 0 1 1	9 0 9 9 1 0
184767.5256	-3.2989	3	27.7354	25	305	10 0 1 0 1 1 1 2	9 0 9 10 1 1
184768.4231	-5.3355	3	27.7354	21	305	10 0 1 0 9 1 0	9 0 9 9 1 0
203240.4516	-5.3135	3	33.8986	25	305	11 0 1 1 1 1 1 2	10 0 1 0 1 1 1 2
203241.2661	-3.2679	3	33.8986	23	305	11 0 1 1 1 0 1 1	10 0 1 0 9 1 0
203241.2704	-3.2313	3	33.8986	25	305	11 0 1 1 1 1 1 2	10 0 1 0 1 0 1 1
203241.2733	-3.1943	3	33.8986	27	305	11 0 1 1 1 2 1 3	10 0 1 0 1 1 1 2
203242.1671	-5.3108	3	33.8986	23	305	11 0 1 1 1 0 1 1	10 0 1 0 1 0 1 1

221713.3386	-5.2928	3	40.6780	27	305	12 0121213	11 0111213
221714.1568	-3.1686	3	40.6780	25	305	12 0121112	11 0111011
221714.1604	-3.1349	3	40.6779	27	305	12 0121213	11 0111112
221714.1629	-3.1009	3	40.6780	29	305	12 0121314	11 0111213
221715.0536	-5.2905	3	40.6779	25	305	12 0121112	11 0111112
240185.2898	-5.2762	3	48.0736	29	305	13 0131314	12 0121314
240186.1112	-3.0799	3	48.0736	27	305	13 0131213	12 0121112
240186.1141	-3.0486	3	48.0735	29	305	13 0131314	12 0121213
240186.1163	-3.0171	3	48.0736	31	305	13 0131415	12 0121314
240187.0044	-5.2741	3	48.0735	27	305	13 0131213	12 0121213
258656.2271	-5.2631	3	56.0853	31	305	14 0141415	13 0131415
258657.0511	-3.0003	3	56.0853	29	305	14 0141314	13 0131213
258657.0536	-2.9711	3	56.0853	31	305	14 0141415	13 0131314
258657.0555	-2.9708	3	56.0853	31	305	14 0141515	13 0131414
258657.9413	-5.2613	3	56.0853	29	305	14 0141314	13 0131314
277126.0723	-5.2824	3	64.7132	31	305	15 0151515	14 0141515
277126.8985	-2.9287	3	64.7132	31	305	15 0151415	14 0141314
277126.9007	-2.9305	3	64.7132	31	305	15 0151515	14 0141414
277126.9024	-2.9284	3	64.7132	31	305	15 0151615	14 0141514
277127.7862	-5.2518	3	64.7132	31	305	15 0151415	14 0141415
295594.7474	-5.2995	3	73.9571	31	305	16 0161615	15 0151615
295595.5756	-2.8933	3	73.9571	31	305	16 0161515	15 0151414
295595.5775	-2.8931	3	73.9571	31	305	16 0161615	15 0151514
295596.4611	-5.2743	3	73.9571	31	305	16 0161515	15 0151515
314063.0042	-2.8608	3	83.8172	31	305	17 0171615	16 0161514
314063.8878	-5.2944	3	83.8171	31	305	17 0171615	16 0161615

**Table B4.** Computed rotational transitions for gas phase CD<sub>2</sub>CN<sup>-</sup> by considering the experimental values of spectroscopic constants. Errors on the computed line frequencies are related to the errors on the constants given in Table 2 and from there, the error ( $\delta\nu/\nu$ ) on any line frequency for CD<sub>2</sub>CN<sup>-</sup> is found to be =  $3.77 \times 10^{-5}$ .

Frequency (in MHz)	I <sup>c</sup>	D <sup>d</sup>	E <sub>lower</sub> <sup>e</sup>	g <sub>up</sub> <sup>f</sup>	QnF <sup>h</sup>	Upper state (Qn <sub>up</sub> <sup>i</sup> )	Lower state (Qn <sub>lower</sub> <sup>j</sup> )
17491.5240	-6.7467	3	-0.0000	3	306	1 0 1 1 2	0 0 0 1 2
17491.5263	-6.8375	3	-0.0000	3	306	1 0 1 1 1	0 0 0 1 1
17491.5272	-6.2622	3	-0.0000	7	306	1 0 1 2 3	0 0 0 1 2
17491.5280	-6.3625	3	-0.0000	5	306	1 0 1 2 2	0 0 0 1 1
17491.5294	-6.7629	3	-0.0000	3	306	1 0 1 2 1	0 0 0 1 2
17491.5297	-6.5680	3	-0.0000	5	306	1 0 1 1 2	0 0 0 1 2
17491.5306	-6.9370	3	-0.0000	1	306	1 0 1 1 1	0 0 0 1 1
17492.2107	-6.4360	3	-0.0000	5	306	1 0 1 1 1	0 0 0 1 0
17492.2119	-6.2616	3	-0.0000	7	306	1 0 1 1 2	0 0 0 1 2
17492.2122	-6.7089	3	-0.0000	3	306	1 0 1 1 0	0 0 0 1 1
17492.2136	-6.0898	3	-0.0000	7	306	1 0 1 2 2	0 0 0 1 1
17492.2153	-5.9791	3	-0.0000	9	306	1 0 1 2 3	0 0 0 1 2
17492.2162	-6.3622	3	-0.0000	5	306	1 0 1 2 1	0 0 0 1 1
17492.2163	-6.7543	3	-0.0000	3	306	1 0 1 0 1	0 0 0 1 2
17492.2169	-6.4956	3	-0.0000	5	306	1 0 1 0 1	0 0 0 1 2
17493.2439	-6.5643	3	-0.0000	5	306	1 0 1 2 3	0 0 0 1 2
34983.4413	-6.8689	3	0.5835	5	306	2 0 2 2 2	1 0 1 0 1
34983.4415	-6.9289	3	0.5835	7	306	2 0 2 2 3	1 0 1 0 1
34983.4424	-6.9847	3	0.5835	3	306	2 0 2 2 1	1 0 1 2 1
34983.4430	-6.6835	3	0.5835	7	306	2 0 2 2 3	1 0 1 2 3
34983.4433	-6.8516	3	0.5835	3	306	2 0 2 1 1	1 0 1 0 1
34983.4434	-6.9706	3	0.5835	7	306	2 0 2 3 3	1 0 1 2 1
34983.4446	-6.9738	3	0.5835	3	306	2 0 2 1 1	1 0 1 0 1
34983.4450	-6.3605	3	0.5835	5	306	2 0 2 1 2	1 0 1 0 1
34983.4452	-6.3107	3	0.5835	5	306	2 0 2 3 2	1 0 1 2 1
34983.4455	-5.9790	3	0.5835	9	306	2 0 2 3 4	1 0 1 2 3
34983.4456	-6.8107	3	0.5835	5	306	2 0 2 2 2	1 0 1 1 2
34983.4460	-6.0650	3	0.5835	7	306	2 0 2 3 3	1 0 1 2 2
34983.4464	-6.5117	3	0.5835	3	306	2 0 2 2 1	1 0 1 1 0
34983.4465	-6.3150	3	0.5835	7	306	2 0 2 2 3	1 0 1 1 2
34983.4466	-6.8500	3	0.5835	1	306	2 0 2 1 1	1 0 1 0 1
34983.4468	-6.4550	3	0.5835	5	306	2 0 2 2 2	1 0 1 1 1
34983.4476	-6.8082	3	0.5835	7	306	2 0 2 2 3	1 0 1 1 1
34983.4478	-6.9684	3	0.5835	5	306	2 0 2 3 2	1 0 1 2 2
34983.4489	-6.6807	3	0.5835	9	306	2 0 2 3 4	1 0 1 1 2
34983.4492	-6.9814	3	0.5835	5	306	2 0 2 3 2	1 0 1 1 0
34983.4500	-6.9227	3	0.5835	5	306	2 0 2 1 2	1 0 1 1 2
34983.4507	-6.8627	3	0.5835	3	306	2 0 2 1 1	1 0 1 1 1
34983.5574	-6.5097	3	0.5835	1	306	2 0 2 2 1	1 0 1 2 2
34983.5582	-5.8121	3	0.5835	5	306	2 0 2 2 3	1 0 1 2 3
34983.5585	-6.2001	3	0.5835	3	306	2 0 2 2 2	1 0 1 2 1
34983.5600	-5.8118	3	0.5835	5	306	2 0 2 3 3	1 0 1 2 2
34983.5608	-5.6640	3	0.5835	7	306	2 0 2 3 4	1 0 1 2 3
34983.5617	-6.0355	3	0.5835	3	306	2 0 2 3 2	1 0 1 2 2
34983.5640	-6.1993	3	0.5835	3	306	2 0 2 1 2	1 0 1 2 3
34984.1278	-6.1593	3	0.5835	5	306	2 0 2 2 2	1 0 1 1 2
34984.1280	-6.1597	3	0.5835	3	306	2 0 2 2 1	1 0 1 1 1
34984.1281	-5.8786	3	0.5835	5	306	2 0 2 2 2	1 0 1 2 1
34984.1286	-5.7089	3	0.5835	7	306	2 0 2 2 3	1 0 1 1 2
34984.1312	-6.0114	3	0.5835	7	306	2 0 2 2 3	1 0 1 2 3
34984.1316	-5.5349	3	0.5835	7	306	2 0 2 3 3	1 0 1 2 2
34984.1317	-6.5110	3	0.5835	3	306	2 0 2 1 1	1 0 1 1 2

34984.1320	-6.5334	3	0.5835	3	306	2 0 2 1 1	1 0 1 2 1
34984.1322	-6.2869	3	0.5835	5	306	2 0 2 1 2	1 0 1 1 2
34984.1323	-6.2797	3	0.5835	3	306	2 0 2 2 1	1 0 1 1 1
34984.1325	-6.4787	3	0.5835	5	306	2 0 2 1 2	1 0 1 2 1
34984.1334	-6.2907	3	0.5835	5	306	2 0 2 3 2	1 0 1 2 2
34984.1337	-5.4253	3	0.5835	9	306	2 0 2 3 4	1 0 1 2 3
34984.1351	-5.8074	3	0.5835	5	306	2 0 2 3 2	1 0 1 1 1
34984.1375	-6.1897	3	0.5835	3	306	2 0 2 1 1	1 0 1 1 2
34984.1379	-5.9350	3	0.5835	5	306	2 0 2 1 2	1 0 1 1 2
34984.1389	-6.5467	3	0.5835	1	306	2 0 2 1 1	1 0 1 1 2
34984.1773	-6.3693	3	0.5835	5	306	2 0 2 2 1	1 0 1 2 1
34984.1777	-6.0879	3	0.5835	9	306	2 0 2 2 3	1 0 1 2 3
34984.1790	-6.1437	3	0.5835	7	306	2 0 2 2 2	1 0 1 1 2
34984.1797	-6.3216	3	0.5835	5	306	2 0 2 1 1	1 0 1 0 1
34984.1802	-5.5038	3	0.5835	7	306	2 0 2 2 2	1 0 1 1 1
34984.1803	-5.8073	3	0.5835	5	306	2 0 2 1 1	1 0 1 0 1
34984.1811	-5.3012	3	0.5835	9	306	2 0 2 3 3	1 0 1 2 2
34984.1813	-5.6317	3	0.5835	5	306	2 0 2 2 1	1 0 1 1 0
34984.1815	-5.4747	3	0.5835	7	306	2 0 2 1 2	1 0 1 0 1
34984.1818	-5.2125	3	0.5835	11	306	2 0 2 3 4	1 0 1 2 3
34984.1832	-6.1088	3	0.5835	3	306	2 0 2 1 0	1 0 1 0 1
34984.1843	-6.3696	3	0.5835	7	306	2 0 2 3 2	1 0 1 2 2
34984.1846	-6.9554	3	0.5835	5	306	2 0 2 1 1	1 0 1 1 2
34984.1858	-6.1983	3	0.5835	5	306	2 0 2 1 1	1 0 1 1 1
34984.1864	-6.3547	3	0.5835	7	306	2 0 2 1 2	1 0 1 1 2
34985.2727	-6.7772	3	0.5835	3	306	2 0 2 2 2	1 0 1 1 2
34985.2759	-6.0613	3	0.5835	5	306	2 0 2 3 3	1 0 1 2 2
34985.2776	-5.9668	3	0.5835	7	306	2 0 2 3 4	1 0 1 2 3
34985.2782	-6.4488	3	0.5835	3	306	2 0 2 1 2	1 0 1 1 2
34985.2784	-6.4764	3	0.5835	3	306	2 0 2 2 2	1 0 1 1 2
34985.2785	-6.4731	3	0.5835	3	306	2 0 2 1 2	1 0 1 2 1
34985.2793	-6.7612	3	0.5835	3	306	2 0 2 3 2	1 0 1 1 1
52475.2897	-6.8740	3	1.7504	7	306	3 0 3 3 3	2 0 2 1 1
52475.2909	-6.7947	3	1.7504	9	306	3 0 3 3 4	2 0 2 3 4
52475.2917	-6.8334	3	1.7504	5	306	3 0 3 2 2	2 0 2 1 0
52475.2932	-6.8544	3	1.7504	7	306	3 0 3 3 3	2 0 2 2 3
52475.2942	-6.5225	3	1.7504	3	306	3 0 3 2 1	2 0 2 1 0
52475.2943	-6.0668	3	1.7504	7	306	3 0 3 2 3	2 0 2 1 2
52475.2944	-6.0565	3	1.7504	7	306	3 0 3 4 3	2 0 2 3 2
52475.2945	-5.8318	3	1.7504	11	306	3 0 3 4 5	2 0 2 3 4
52475.2946	-6.4255	3	1.7504	5	306	3 0 3 2 2	2 0 2 1 1
52475.2948	-5.9056	3	1.7504	9	306	3 0 3 4 4	2 0 2 3 3
52475.2949	-6.1861	3	1.7504	5	306	3 0 3 3 2	2 0 2 2 1
52475.2950	-6.0282	3	1.7504	9	306	3 0 3 3 4	2 0 2 2 3
52475.2953	-6.1358	3	1.7504	7	306	3 0 3 3 3	2 0 2 2 2
52475.2971	-6.8305	3	1.7504	3	306	3 0 3 2 1	2 0 2 1 1
52475.2986	-6.7906	3	1.7504	11	306	3 0 3 4 5	2 0 2 2 3
52475.3002	-6.8678	3	1.7504	5	306	3 0 3 2 2	2 0 2 2 2
52475.9112	-6.6728	3	1.7504	5	306	3 0 3 3 3	2 0 2 3 4
52475.9121	-5.8568	3	1.7504	3	306	3 0 3 3 2	2 0 2 3 2
52475.9126	-5.5875	3	1.7504	7	306	3 0 3 3 4	2 0 2 3 4
52475.9135	-5.4538	3	1.7504	5	306	3 0 3 3 3	2 0 2 2 2
52475.9138	-5.7326	3	1.7504	5	306	3 0 3 3 3	2 0 2 2 3
52475.9143	-5.7640	3	1.7504	3	306	3 0 3 2 2	2 0 2 1 2
52475.9150	-5.5078	3	1.7504	5	306	3 0 3 2 3	2 0 2 1 2
52475.9152	-5.2813	3	1.7504	7	306	3 0 3 3 4	2 0 2 2 3
52475.9154	-5.1071	3	1.7504	7	306	3 0 3 4 4	2 0 2 3 3
52475.9163	-5.7303	3	1.7504	3	306	3 0 3 3 2	2 0 2 2 1

52475.9165	-4.9960	3	1.7504	9	306	3 0 3 4 5	2 0 2 3 4
52475.9166	-5.3780	3	1.7504	5	306	3 0 3 4 3	2 0 2 3 2
52475.9182	-6.8033	3	1.7504	5	306	3 0 3 2 3	2 0 2 3 4
52475.9183	-5.8589	3	1.7504	5	306	3 0 3 4 3	2 0 2 3 3
52475.9198	-6.0984	3	1.7504	3	306	3 0 3 2 2	2 0 2 2 2
52475.9201	-6.0766	3	1.7504	3	306	3 0 3 2 2	2 0 2 2 3
52475.9205	-6.0423	3	1.7504	5	306	3 0 3 2 3	2 0 2 2 2
52475.9208	-5.8523	3	1.7504	5	306	3 0 3 2 3	2 0 2 2 3
52475.9221	-6.4449	3	1.7504	1	306	3 0 3 2 1	2 0 2 2 2
52476.0270	-6.0354	3	1.7504	5	306	3 0 3 3 2	2 0 2 3 2
52476.0272	-5.7547	3	1.7504	9	306	3 0 3 3 4	2 0 2 3 4
52476.0278	-5.8141	3	1.7504	7	306	3 0 3 3 3	2 0 2 2 3
52476.0287	-5.1755	3	1.7504	7	306	3 0 3 3 3	2 0 2 2 2
52476.0292	-5.9885	3	1.7504	5	306	3 0 3 2 2	2 0 2 1 2
52476.0297	-5.0505	3	1.7504	9	306	3 0 3 3 4	2 0 2 2 3
52476.0299	-4.9731	3	1.7504	9	306	3 0 3 4 4	2 0 2 3 3
52476.0308	-4.8848	3	1.7504	11	306	3 0 3 4 5	2 0 2 3 4
52476.0309	-5.1337	3	1.7504	7	306	3 0 3 4 3	2 0 2 3 2
52476.0317	-6.9995	3	1.7504	3	306	3 0 3 2 1	2 0 2 1 2
52476.0322	-5.7826	3	1.7504	3	306	3 0 3 2 1	2 0 2 1 1
52476.0327	-6.0458	3	1.7504	7	306	3 0 3 4 3	2 0 2 3 3
52476.0331	-7.8450	3	1.7504	7	306	3 0 3 2 3	2 0 2 3 3
52476.0336	-5.8790	3	1.7504	5	306	3 0 3 2 2	2 0 2 2 2
52476.0343	-6.0331	3	1.7504	7	306	3 0 3 2 3	2 0 2 2 3
52476.0352	-6.8521	3	1.7504	7	306	3 0 3 2 3	2 0 2 2 2
52476.0361	-6.8754	3	1.7504	3	306	3 0 3 2 1	2 0 2 2 2
52476.0531	-6.1318	3	1.7504	7	306	3 0 3 3 2	2 0 2 3 2
52476.0534	-5.8470	3	1.7504	11	306	3 0 3 3 4	2 0 2 3 4
52476.0549	-5.8759	3	1.7504	9	306	3 0 3 3 3	2 0 2 2 3
52476.0551	-6.1056	3	1.7504	7	306	3 0 3 2 2	2 0 2 1 2
52476.0568	-5.1456	3	1.7504	7	306	3 0 3 2 2	2 0 2 1 1
52476.0570	-4.9745	3	1.7504	9	306	3 0 3 3 3	2 0 2 2 2
52476.0573	-4.8348	3	1.7504	11	306	3 0 3 4 4	2 0 2 3 3
52476.0575	-4.8784	3	1.7504	11	306	3 0 3 3 4	2 0 2 2 3
52476.0576	-4.9499	3	1.7504	9	306	3 0 3 4 3	2 0 2 3 2
52476.0577	-4.7609	3	1.7504	13	306	3 0 3 4 5	2 0 2 3 4
52476.0602	-5.8480	3	1.7504	5	306	3 0 3 2 1	2 0 2 1 1
52476.0603	-6.9782	3	1.7504	7	306	3 0 3 2 2	2 0 2 2 3
52476.0608	-6.1342	3	1.7504	9	306	3 0 3 4 3	2 0 2 3 3
52476.0625	-5.8938	3	1.7504	7	306	3 0 3 2 2	2 0 2 2 2
52476.0628	-6.1217	3	1.7504	9	306	3 0 3 2 3	2 0 2 2 3
52477.0545	-6.6825	3	1.7504	5	306	3 0 3 3 3	2 0 2 1 1
52477.0554	-6.7445	3	1.7504	7	306	3 0 3 3 4	2 0 2 1 2
52477.0562	-6.8136	3	1.7504	3	306	3 0 3 3 2	2 0 2 3 2
52477.0565	-6.5100	3	1.7504	7	306	3 0 3 3 4	2 0 2 3 4
52477.0576	-6.6271	3	1.7504	5	306	3 0 3 3 3	2 0 2 2 3
52477.0579	-6.7952	3	1.7504	7	306	3 0 3 4 4	2 0 2 3 2
52477.0584	-6.2707	3	1.7504	5	306	3 0 3 3 3	2 0 2 2 2
52477.0589	-6.1326	3	1.7504	7	306	3 0 3 3 4	2 0 2 2 3
52477.0591	-6.3296	3	1.7504	3	306	3 0 3 3 2	2 0 2 2 1
52477.0594	-6.6884	3	1.7504	3	306	3 0 3 2 2	2 0 2 1 1
52477.0597	-5.8903	3	1.7504	7	306	3 0 3 4 4	2 0 2 3 3
52477.0598	-6.6287	3	1.7504	7	306	3 0 3 3 4	2 0 2 2 2
52477.0603	-6.8110	3	1.7504	3	306	3 0 3 2 2	2 0 2 1 2
52477.0604	-5.8094	3	1.7504	9	306	3 0 3 4 5	2 0 2 3 4
52477.0608	-6.1447	3	1.7504	5	306	3 0 3 4 3	2 0 2 3 2
52477.0611	-6.1988	3	1.7504	5	306	3 0 3 2 3	2 0 2 1 2
52477.0615	-6.8125	3	1.7504	5	306	3 0 3 2 3	2 0 2 1 1

52477.0626	-6.7966	3	1.7504	5	306	3 0 3 4 3	2 0 2 3 3
52477.0629	-6.5118	3	1.7504	9	306	3 0 3 4 5	2 0 2 2 3
52477.0631	-6.6895	3	1.7504	1	306	3 0 3 2 1	2 0 2 1 1
52477.0636	-6.8158	3	1.7504	5	306	3 0 3 4 3	2 0 2 2 1
52477.0646	-6.7484	3	1.7504	5	306	3 0 3 2 3	2 0 2 2 3
52477.0647	-6.6863	3	1.7504	3	306	3 0 3 2 2	2 0 2 2 2
69966.9584	-6.9358	3	3.5008	9	306	4 0 4 4 4	3 0 3 2 2
69966.9594	-6.8910	3	3.5008	11	306	4 0 4 4 5	3 0 3 4 5
69966.9601	-6.9064	3	3.5008	7	306	4 0 4 3 3	3 0 3 2 1
69966.9613	-6.9265	3	3.5008	9	306	4 0 4 4 4	3 0 3 3 4
69966.9632	-6.1942	3	3.5008	5	306	4 0 4 3 2	3 0 3 2 1
69966.9633	-5.9056	3	3.5008	9	306	4 0 4 5 4	3 0 3 4 3
69966.9634	-5.7321	3	3.5008	13	306	4 0 4 5 6	3 0 3 4 5
69966.9635	-6.1214	3	3.5008	7	306	4 0 4 3 3	3 0 3 2 2
69966.9636	-5.7965	3	3.5008	11	306	4 0 4 5 5	3 0 3 4 4
69966.9637	-5.8696	3	3.5008	11	306	4 0 4 4 5	3 0 3 3 4
69966.9639	-5.9550	3	3.5008	9	306	4 0 4 4 4	3 0 3 3 3
69966.9663	-6.9234	3	3.5008	11	306	4 0 4 4 5	3 0 3 3 3
69966.9666	-6.9029	3	3.5008	5	306	4 0 4 3 2	3 0 3 2 2
69966.9677	-6.8866	3	3.5008	13	306	4 0 4 5 6	3 0 3 3 4
69966.9689	-6.9298	3	3.5008	7	306	4 0 4 3 3	3 0 3 3 3
69967.6711	-6.8581	3	3.5008	7	306	4 0 4 4 4	3 0 3 4 5
69967.6729	-5.7640	3	3.5008	5	306	4 0 4 4 3	3 0 3 4 3
69967.6733	-5.4827	3	3.5008	9	306	4 0 4 4 5	3 0 3 4 5
69967.6751	-5.5401	3	3.5008	7	306	4 0 4 4 4	3 0 3 3 4
69967.6753	-5.7159	3	3.5008	5	306	4 0 4 3 3	3 0 3 2 3
69967.6760	-5.2029	3	3.5008	5	306	4 0 4 3 3	3 0 3 2 2
69967.6764	-4.9008	3	3.5008	7	306	4 0 4 4 4	3 0 3 3 3
69967.6767	-5.5042	3	3.5008	3	306	4 0 4 3 2	3 0 3 2 1
69967.6770	-4.6977	3	3.5008	9	306	4 0 4 5 5	3 0 3 4 4
69967.6771	-4.8706	3	3.5008	7	306	4 0 4 3 4	3 0 3 2 3
69967.6773	-4.7748	3	3.5008	9	306	4 0 4 4 5	3 0 3 3 4
69967.6775	-4.8578	3	3.5008	7	306	4 0 4 5 4	3 0 3 4 3
69967.6776	-4.6089	3	3.5008	11	306	4 0 4 5 6	3 0 3 4 5
69967.6783	-6.7246	3	3.5008	3	306	4 0 4 3 2	3 0 3 2 3
69967.6790	-5.5053	3	3.5008	3	306	4 0 4 3 2	3 0 3 2 2
69967.6804	-5.7673	3	3.5008	7	306	4 0 4 5 4	3 0 3 4 4
69967.6809	-6.3543	3	3.5008	5	306	4 0 4 3 3	3 0 3 3 4
69967.6822	-5.5977	3	3.5008	5	306	4 0 4 3 3	3 0 3 3 3
69967.6828	-5.7529	3	3.5008	7	306	4 0 4 3 4	3 0 3 3 4
69967.6841	-6.5733	3	3.5008	7	306	4 0 4 3 4	3 0 3 3 3
69967.6853	-6.5911	3	3.5008	3	306	4 0 4 3 2	3 0 3 3 3
69967.7224	-5.8942	3	3.5008	7	306	4 0 4 4 3	3 0 3 4 3
69967.7226	-5.6097	3	3.5008	11	306	4 0 4 4 5	3 0 3 4 5
69967.7238	-5.6407	3	3.5008	9	306	4 0 4 4 4	3 0 3 3 4
69967.7242	-5.8687	3	3.5008	7	306	4 0 4 3 3	3 0 3 2 3
69967.7256	-4.7411	3	3.5008	9	306	4 0 4 4 4	3 0 3 3 3
69967.7258	-4.9116	3	3.5008	7	306	4 0 4 3 3	3 0 3 2 2
69967.7261	-4.6014	3	3.5008	11	306	4 0 4 5 5	3 0 3 4 4
69967.7262	-4.6453	3	3.5008	11	306	4 0 4 4 5	3 0 3 3 4
69967.7263	-5.0550	3	3.5008	5	306	4 0 4 3 2	3 0 3 2 1
69967.7264	-4.7198	3	3.5008	9	306	4 0 4 3 4	3 0 3 2 3
69967.7265	-4.7165	3	3.5008	9	306	4 0 4 5 4	3 0 3 4 3
69967.7266	-4.5276	3	3.5008	13	306	4 0 4 5 6	3 0 3 4 5
69967.7288	-6.7481	3	3.5008	7	306	4 0 4 3 3	3 0 3 3 4
69967.7289	-5.6171	3	3.5008	5	306	4 0 4 3 2	3 0 3 2 2
69967.7294	-5.9040	3	3.5008	9	306	4 0 4 5 4	3 0 3 4 4
69967.7307	-5.6661	3	3.5008	7	306	4 0 4 3 3	3 0 3 3 3

69967.7311	-5.8927	3	3.5008	9	306	4 0 4 3 4	3 0 3 3 4
69967.7337	-6.9988	3	3.5008	5	306	4 0 4 3 2	3 0 3 3 3
69967.7391	-5.9785	3	3.5008	9	306	4 0 4 4 3	3 0 3 4 3
69967.7394	-5.6936	3	3.5008	13	306	4 0 4 4 5	3 0 3 4 5
69967.7407	-5.7101	3	3.5008	11	306	4 0 4 4 4	3 0 3 3 4
69967.7408	-5.9612	3	3.5008	9	306	4 0 4 3 3	3 0 3 2 3
69967.7432	-4.7265	3	3.5008	9	306	4 0 4 3 3	3 0 3 2 2
69967.7434	-4.6066	3	3.5008	11	306	4 0 4 4 4	3 0 3 3 3
69967.7435	-4.5008	3	3.5008	13	306	4 0 4 5 5	3 0 3 4 4
69967.7436	-4.5920	3	3.5008	11	306	4 0 4 3 4	3 0 3 2 3
69967.7437	-4.5288	3	3.5008	13	306	4 0 4 4 5	3 0 3 3 4
69967.7438	-4.4373	3	3.5008	15	306	4 0 4 5 6	3 0 3 4 5
69967.7468	-5.6879	3	3.5008	7	306	4 0 4 3 2	3 0 3 2 2
69967.7472	-5.9818	3	3.5008	11	306	4 0 4 5 4	3 0 3 4 4
69967.7487	-5.7179	3	3.5008	9	306	4 0 4 3 3	3 0 3 3 3
69967.7489	-5.9715	3	3.5008	11	306	4 0 4 3 4	3 0 3 3 4
69968.7013	-6.7383	3	3.5008	7	306	4 0 4 4 4	3 0 3 2 2
69968.7019	-6.9334	3	3.5008	9	306	4 0 4 4 5	3 0 3 2 3
69968.7027	-6.9720	3	3.5008	5	306	4 0 4 4 3	3 0 3 4 3
69968.7029	-6.6739	3	3.5008	9	306	4 0 4 4 5	3 0 3 4 5
69968.7040	-6.9621	3	3.5008	9	306	4 0 4 5 5	3 0 3 4 3
69968.7043	-6.7265	3	3.5008	7	306	4 0 4 4 4	3 0 3 3 4
69968.7046	-6.7130	3	3.5008	5	306	4 0 4 3 3	3 0 3 2 1
69968.7055	-6.9595	3	3.5008	5	306	4 0 4 3 3	3 0 3 2 3
69968.7062	-6.0061	3	3.5008	7	306	4 0 4 4 4	3 0 3 3 3
69968.7065	-5.9018	3	3.5008	9	306	4 0 4 4 5	3 0 3 3 4
69968.7066	-6.0607	3	3.5008	5	306	4 0 4 4 3	3 0 3 3 2
69968.7068	-5.7835	3	3.5008	9	306	4 0 4 5 5	3 0 3 4 4
69968.7071	-6.3093	3	3.5008	5	306	4 0 4 3 3	3 0 3 2 2
69968.7072	-5.7140	3	3.5008	11	306	4 0 4 5 6	3 0 3 4 5
69968.7073	-5.9408	3	3.5008	7	306	4 0 4 5 4	3 0 3 4 3
69968.7074	-5.9524	3	3.5008	7	306	4 0 4 3 4	3 0 3 2 3
69968.7076	-6.4112	3	3.5008	3	306	4 0 4 3 2	3 0 3 2 1
69968.7084	-6.7286	3	3.5008	9	306	4 0 4 4 5	3 0 3 3 3
69968.7090	-6.9616	3	3.5008	7	306	4 0 4 3 4	3 0 3 2 2
69968.7101	-6.7152	3	3.5008	3	306	4 0 4 3 2	3 0 3 2 2
69968.7102	-6.9645	3	3.5008	7	306	4 0 4 5 4	3 0 3 4 4
69968.7108	-6.6769	3	3.5008	11	306	4 0 4 5 6	3 0 3 3 4
69968.7112	-6.9753	3	3.5008	7	306	4 0 4 5 4	3 0 3 3 2
69968.7120	-6.7429	3	3.5008	5	306	4 0 4 3 3	3 0 3 3 3
87458.3688	-6.9756	3	5.8347	13	306	5 0 5 5 6	4 0 4 5 6
87458.3695	-6.9829	3	5.8347	9	306	5 0 5 4 4	4 0 4 3 2
87458.3704	-6.9996	3	5.8347	11	306	5 0 5 5 5	4 0 4 4 5
87458.3729	-5.7995	3	5.8347	11	306	5 0 5 6 5	4 0 4 5 4
87458.3730	-5.6571	3	5.8347	15	306	5 0 5 6 7	4 0 4 5 6
87458.3731	-5.7140	3	5.8347	13	306	5 0 5 6 6	4 0 4 5 5
87458.3732	-5.7623	3	5.8347	13	306	5 0 5 5 6	4 0 4 4 5
87458.3733	-5.8335	3	5.8347	11	306	5 0 5 5 5	4 0 4 4 4
87458.3761	-6.9962	3	5.8347	13	306	5 0 5 5 6	4 0 4 4 4
87458.3765	-6.9791	3	5.8347	7	306	5 0 5 4 3	4 0 4 3 3
87458.3774	-6.9711	3	5.8347	15	306	5 0 5 6 7	4 0 4 4 5
87458.3784	-6.9988	3	5.8347	9	306	5 0 5 4 4	4 0 4 4 4
87459.1214	-5.6933	3	5.8347	7	306	5 0 5 5 4	4 0 4 5 4
87459.1217	-5.4085	3	5.8347	11	306	5 0 5 5 6	4 0 4 5 6
87459.1233	-6.9650	3	5.8347	11	306	5 0 5 6 6	4 0 4 5 6
87459.1234	-5.4381	3	5.8347	9	306	5 0 5 5 5	4 0 4 4 5
87459.1253	-4.7079	3	5.8347	7	306	5 0 5 4 4	4 0 4 3 3
87459.1256	-4.5372	3	5.8347	9	306	5 0 5 5 5	4 0 4 4 4

87459.1258	-4.3973	3	5.8347	11	306	5 0 5 6 6	4 0 4 5 5
87459.1259	-4.5156	3	5.8347	9	306	5 0 5 4 5	4 0 4 3 4
87459.1260	-4.4411	3	5.8347	11	306	5 0 5 5 6	4 0 4 4 5
87459.1262	-4.3233	3	5.8347	13	306	5 0 5 6 7	4 0 4 5 6
87459.1287	-5.4109	3	5.8347	5	306	5 0 5 4 3	4 0 4 3 3
87459.1289	-6.5420	3	5.8347	7	306	5 0 5 4 4	4 0 4 4 5
87459.1294	-5.6974	3	5.8347	9	306	5 0 5 6 5	4 0 4 5 5
87459.1311	-5.4577	3	5.8347	7	306	5 0 5 4 4	4 0 4 4 4
87459.1314	-5.6851	3	5.8347	9	306	5 0 5 4 5	4 0 4 4 5
87459.1336	-6.8842	3	5.8347	9	306	5 0 5 4 5	4 0 4 4 4
87459.1345	-6.7880	3	5.8347	5	306	5 0 5 4 3	4 0 4 4 4
87459.1490	-5.7949	3	5.8347	9	306	5 0 5 5 4	4 0 4 5 4
87459.1492	-5.5101	3	5.8347	13	306	5 0 5 5 6	4 0 4 5 6
87459.1504	-5.5280	3	5.8347	11	306	5 0 5 5 5	4 0 4 4 5
87459.1505	-6.9159	3	5.8347	13	306	5 0 5 6 6	4 0 4 5 6
87459.1506	-5.7781	3	5.8347	9	306	5 0 5 4 4	4 0 4 3 4
87459.1528	-4.4262	3	5.8347	11	306	5 0 5 5 5	4 0 4 4 4
87459.1531	-4.3204	3	5.8347	13	306	5 0 5 6 6	4 0 4 5 5
87459.1532	-4.3485	3	5.8347	13	306	5 0 5 5 6	4 0 4 4 5
87459.1533	-4.4103	3	5.8347	11	306	5 0 5 6 5	4 0 4 5 4
87459.1534	-4.2570	3	5.8347	15	306	5 0 5 6 7	4 0 4 5 6
87459.1555	-6.8478	3	5.8347	9	306	5 0 5 4 4	4 0 4 4 5
87459.1562	-5.5097	3	5.8347	7	306	5 0 5 4 3	4 0 4 3 3
87459.1566	-5.8040	3	5.8347	11	306	5 0 5 6 5	4 0 4 5 5
87459.1579	-5.5416	3	5.8347	9	306	5 0 5 4 4	4 0 4 4 4
87459.1581	-5.7944	3	5.8347	11	306	5 0 5 4 5	4 0 4 4 5
87459.1607	-5.8677	3	5.8347	11	306	5 0 5 5 4	4 0 4 5 4
87459.1608	-5.5847	3	5.8347	15	306	5 0 5 5 6	4 0 4 5 6
87459.1620	-6.8626	3	5.8347	15	306	5 0 5 6 6	4 0 4 5 6
87459.1621	-5.5944	3	5.8347	13	306	5 0 5 5 5	4 0 4 4 5
87459.1649	-4.4179	3	5.8347	11	306	5 0 5 4 4	4 0 4 3 3
87459.1650	-4.3254	3	5.8347	13	306	5 0 5 5 5	4 0 4 4 4
87459.1651	-4.2405	3	5.8347	15	306	5 0 5 6 6	4 0 4 5 5
87459.1652	-4.2598	3	5.8347	15	306	5 0 5 5 6	4 0 4 4 5
87459.1653	-4.1848	3	5.8347	17	306	5 0 5 6 7	4 0 4 5 6
87459.1686	-5.5757	3	5.8347	9	306	5 0 5 4 3	4 0 4 3 3
87459.1689	-5.8712	3	5.8347	13	306	5 0 5 6 5	4 0 4 5 5
87459.1702	-5.5982	3	5.8347	11	306	5 0 5 4 4	4 0 4 4 4
87459.1704	-5.8625	3	5.8347	13	306	5 0 5 4 5	4 0 4 4 5
87460.1011	-6.8299	3	5.8347	9	306	5 0 5 5 5	4 0 4 3 3
87460.1024	-6.7996	3	5.8347	11	306	5 0 5 5 6	4 0 4 5 6
87460.1036	-6.8118	3	5.8347	7	306	5 0 5 4 4	4 0 4 3 2
87460.1037	-6.8295	3	5.8347	9	306	5 0 5 5 5	4 0 4 4 5
87460.1061	-5.8563	3	5.8347	9	306	5 0 5 5 5	4 0 4 4 4
87460.1064	-5.7741	3	5.8347	11	306	5 0 5 5 6	4 0 4 4 5
87460.1065	-5.7038	3	5.8347	11	306	5 0 5 6 6	4 0 4 5 5
87460.1066	-6.0316	3	5.8347	7	306	5 0 5 4 4	4 0 4 3 3
87460.1068	-5.6432	3	5.8347	13	306	5 0 5 6 7	4 0 4 5 6
87460.1069	-5.8221	3	5.8347	9	306	5 0 5 4 5	4 0 4 3 4
87460.1088	-6.8320	3	5.8347	11	306	5 0 5 5 6	4 0 4 4 4
87460.1100	-6.8146	3	5.8347	5	306	5 0 5 4 3	4 0 4 3 3
87460.1108	-6.8031	3	5.8347	13	306	5 0 5 6 7	4 0 4 4 5
87460.1117	-6.8346	3	5.8347	7	306	5 0 5 4 4	4 0 4 4 4
104949.4514	-5.7188	3	8.7520	13	306	6 0 6 7 6	5 0 5 6 5
104949.4515	-5.5976	3	8.7520	17	306	6 0 6 7 8	5 0 5 6 7
104949.4516	-5.6485	3	8.7520	15	306	6 0 6 7 7	5 0 5 6 6
104949.4517	-5.7437	3	8.7520	13	306	6 0 6 6 6	5 0 5 5 5
104950.2218	-5.6361	3	8.7520	9	306	6 0 6 6 5	5 0 5 6 5

104950.2219	-6.8899	3	8.7520	11	306	6 0 6 6 6	5 0 5 6 6
104950.2220	-5.3512	3	8.7520	13	306	6 0 6 6 7	5 0 5 6 7
104950.2233	-6.7545	3	8.7520	13	306	6 0 6 7 7	5 0 5 6 7
104950.2234	-5.3681	3	8.7520	11	306	6 0 6 6 6	5 0 5 5 6
104950.2259	-4.3846	3	8.7520	9	306	6 0 6 5 5	5 0 5 4 4
104950.2261	-4.2649	3	8.7520	11	306	6 0 6 6 6	5 0 5 5 5
104950.2262	-4.1590	3	8.7520	13	306	6 0 6 7 7	5 0 5 6 6
104950.2263	-4.2488	3	8.7520	11	306	6 0 6 7 6	5 0 5 6 5
104950.2264	-4.0954	3	8.7520	15	306	6 0 6 7 8	5 0 5 6 7
104950.2265	-6.8870	3	8.7520	11	306	6 0 6 5 6	5 0 5 6 5
104950.2288	-6.6851	3	8.7520	9	306	6 0 6 5 5	5 0 5 5 6
104950.2295	-5.3464	3	8.7520	7	306	6 0 6 5 4	5 0 5 4 4
104950.2299	-5.6404	3	8.7520	11	306	6 0 6 7 6	5 0 5 6 6
104950.2315	-5.3769	3	8.7520	9	306	6 0 6 5 5	5 0 5 5 5
104950.2316	-5.6302	3	8.7520	11	306	6 0 6 5 6	5 0 5 5 6
104950.2350	-6.9407	3	8.7520	7	306	6 0 6 5 4	5 0 5 5 5
104950.2393	-5.7190	3	8.7520	11	306	6 0 6 6 5	5 0 5 6 5
104950.2393	-6.8264	3	8.7520	13	306	6 0 6 6 6	5 0 5 6 6
104950.2395	-5.4361	3	8.7520	15	306	6 0 6 6 7	5 0 5 6 7
104950.2406	-5.4467	3	8.7520	13	306	6 0 6 6 6	5 0 5 5 6
104950.2407	-5.7066	3	8.7520	11	306	6 0 6 5 5	5 0 5 4 5
104950.2434	-4.1793	3	8.7520	13	306	6 0 6 6 6	5 0 5 5 5
104950.2435	-6.9313	3	8.7520	13	306	6 0 6 7 6	5 0 5 4 5
104950.2436	-4.0944	3	8.7520	15	306	6 0 6 7 7	5 0 5 6 6
104950.2437	-4.1138	3	8.7520	15	306	6 0 6 6 7	5 0 5 5 6
104950.2438	-4.0388	3	8.7520	17	306	6 0 6 7 8	5 0 5 6 7
104950.2457	-6.9357	3	8.7520	11	306	6 0 6 5 5	5 0 5 5 6
104950.2469	-5.4316	3	8.7520	9	306	6 0 6 5 4	5 0 5 4 4
104950.2469	-6.8276	3	8.7520	11	306	6 0 6 6 5	5 0 5 5 5
104950.2472	-5.7273	3	8.7520	13	306	6 0 6 7 6	5 0 5 6 6
104950.2479	-5.7824	3	8.7520	13	306	6 0 6 6 5	5 0 5 6 5
104950.2480	-5.5027	3	8.7520	17	306	6 0 6 6 7	5 0 5 6 7
104950.2484	-5.4554	3	8.7520	11	306	6 0 6 5 5	5 0 5 5 5
104950.2486	-5.7191	3	8.7520	13	306	6 0 6 5 6	5 0 5 5 6
104950.2488	-6.9878	3	8.7520	9	306	6 0 6 5 4	5 0 5 5 4
104950.2491	-6.6759	3	8.7520	17	306	6 0 6 7 7	5 0 5 6 7
104950.2492	-5.5082	3	8.7520	15	306	6 0 6 6 6	5 0 5 5 6
104950.2522	-4.1741	3	8.7520	13	306	6 0 6 5 5	5 0 5 4 4
104950.2523	-4.0986	3	8.7520	15	306	6 0 6 6 6	5 0 5 5 5
104950.2524	-4.0277	3	8.7520	17	306	6 0 6 7 7	5 0 5 6 6
104950.2525	-3.9782	3	8.7520	19	306	6 0 6 7 8	5 0 5 6 7
104950.2526	-6.9742	3	8.7520	15	306	6 0 6 5 6	5 0 5 6 5
104950.2560	-5.4918	3	8.7520	11	306	6 0 6 5 4	5 0 5 4 4
104950.2562	-5.7858	3	8.7520	15	306	6 0 6 7 6	5 0 5 6 6
104950.2575	-5.5102	3	8.7520	13	306	6 0 6 5 5	5 0 5 5 5
104950.2576	-6.8964	3	8.7520	11	306	6 0 6 5 4	5 0 5 5 4
104951.1744	-6.9182	3	8.7520	11	306	6 0 6 6 6	5 0 5 4 4
104951.1754	-6.9033	3	8.7520	13	306	6 0 6 6 7	5 0 5 6 7
104951.1763	-6.9057	3	8.7520	9	306	6 0 6 5 5	5 0 5 4 3
104951.1766	-6.9226	3	8.7520	11	306	6 0 6 6 6	5 0 5 5 6
104951.1794	-5.7549	3	8.7520	11	306	6 0 6 6 6	5 0 5 5 5
104951.1796	-5.6868	3	8.7520	13	306	6 0 6 6 7	5 0 5 5 6
104951.1797	-5.6404	3	8.7520	13	306	6 0 6 7 7	5 0 5 6 6
104951.1798	-5.5869	3	8.7520	15	306	6 0 6 7 8	5 0 5 6 7
104951.1799	-5.7301	3	8.7520	11	306	6 0 6 7 6	5 0 5 6 5
104951.1824	-6.9254	3	8.7520	13	306	6 0 6 6 7	5 0 5 5 5
104951.1833	-6.9088	3	8.7520	7	306	6 0 6 5 4	5 0 5 4 4
104951.1840	-6.9071	3	8.7520	15	306	6 0 6 7 8	5 0 5 5 6

104951.1848	-6.9230	3	8.7520	9	306	6 0 6 5 5	5 0 5 5 5
122440.1294	-5.5489	3	12.2528	19	306	7 0 7 8 9	6 0 6 7 8
122440.1295	-5.5950	3	12.2528	17	306	7 0 7 8 8	6 0 6 7 7
122440.1296	-5.6739	3	12.2528	15	306	7 0 7 7 7	6 0 6 6 6
122440.9138	-5.5886	3	12.2528	11	306	7 0 7 7 6	6 0 6 7 6
122440.9139	-6.6942	3	12.2528	13	306	7 0 7 7 7	6 0 6 7 7
122440.9140	-5.3056	3	12.2528	15	306	7 0 7 7 8	6 0 6 7 8
122440.9152	-6.5838	3	12.2528	15	306	7 0 7 8 8	6 0 6 7 8
122440.9153	-5.3155	3	12.2528	13	306	7 0 7 7 7	6 0 6 6 7
122440.9171	-6.8974	3	12.2528	15	306	7 0 7 7 8	6 0 6 7 7
122440.9181	-4.1392	3	12.2528	11	306	7 0 7 6 6	6 0 6 5 5
122440.9182	-4.0468	3	12.2528	13	306	7 0 7 7 7	6 0 6 6 6
122440.9183	-3.9618	3	12.2528	15	306	7 0 7 8 8	6 0 6 7 7
122440.9184	-3.9811	3	12.2528	15	306	7 0 7 7 8	6 0 6 6 7
122440.9185	-3.9061	3	12.2528	17	306	7 0 7 8 9	6 0 6 7 8
122440.9200	-6.9837	3	12.2528	11	306	7 0 7 6 6	6 0 6 6 5
122440.9205	-6.8022	3	12.2528	11	306	7 0 7 6 6	6 0 6 6 7
122440.9218	-5.2973	3	12.2528	9	306	7 0 7 6 5	6 0 6 5 5
122440.9221	-5.5929	3	12.2528	13	306	7 0 7 8 7	6 0 6 7 7
122440.9235	-5.3200	3	12.2528	11	306	7 0 7 6 6	6 0 6 6 6
122440.9236	-5.5842	3	12.2528	13	306	7 0 7 6 7	6 0 6 6 7
122440.9237	-6.8550	3	12.2528	9	306	7 0 7 6 5	6 0 6 6 5
122440.9260	-5.6583	3	12.2528	13	306	7 0 7 7 6	6 0 6 7 6
122440.9261	-5.3787	3	12.2528	17	306	7 0 7 7 8	6 0 6 7 8
122440.9272	-5.3849	3	12.2528	15	306	7 0 7 7 7	6 0 6 6 7
122440.9292	-6.9030	3	12.2528	17	306	7 0 7 7 8	6 0 6 7 7
122440.9302	-3.9768	3	12.2528	15	306	7 0 7 7 7	6 0 6 6 6
122440.9303	-3.9059	3	12.2528	17	306	7 0 7 8 8	6 0 6 7 7
122440.9304	-3.8564	3	12.2528	19	306	7 0 7 8 9	6 0 6 7 8
122440.9305	-6.8526	3	12.2528	15	306	7 0 7 6 7	6 0 6 7 6
122440.9317	-6.9691	3	12.2528	13	306	7 0 7 6 6	6 0 6 6 5
122440.9326	-5.4388	3	12.2528	19	306	7 0 7 7 8	6 0 6 7 8
122440.9337	-5.4416	3	12.2528	17	306	7 0 7 7 7	6 0 6 6 7
122440.9338	-6.6463	3	12.2528	13	306	7 0 7 7 6	6 0 6 6 6
122440.9339	-5.3717	3	12.2528	11	306	7 0 7 6 5	6 0 6 5 5
122440.9340	-5.6658	3	12.2528	15	306	7 0 7 8 7	6 0 6 7 7
122440.9352	-5.3910	3	12.2528	13	306	7 0 7 6 6	6 0 6 6 6
122440.9353	-5.6586	3	12.2528	15	306	7 0 7 6 7	6 0 6 6 7
122440.9354	-6.7748	3	12.2528	11	306	7 0 7 6 5	6 0 6 6 5
122440.9360	-6.9090	3	12.2528	19	306	7 0 7 7 8	6 0 6 7 7
122440.9369	-3.9731	3	12.2528	15	306	7 0 7 6 6	6 0 6 5 5
122440.9370	-3.8486	3	12.2528	19	306	7 0 7 8 8	6 0 6 7 7
122440.9371	-3.8040	3	12.2528	21	306	7 0 7 8 9 1	6 0 6 7 8
122440.9372	-6.9103	3	12.2528	17	306	7 0 7 6 7	6 0 6 7 6
122440.9384	-6.9562	3	12.2528	15	306	7 0 7 6 6	6 0 6 6 5
122440.9408	-5.4267	3	12.2528	13	306	7 0 7 6 5	6 0 6 5 5
122440.9409	-5.7173	3	12.2528	17	306	7 0 7 8 7	6 0 6 7 7
122440.9421	-5.4426	3	12.2528	15	306	7 0 7 6 6	6 0 6 6 6
122440.9422	-6.7060	3	12.2528	13	306	7 0 7 6 5	6 0 6 6 5
122441.8501	-6.9930	3	12.2528	15	306	7 0 7 7 8	6 0 6 7 8
122441.8509	-6.9906	3	12.2528	11	306	7 0 7 6 6	6 0 6 5 4
122441.8542	-5.6795	3	12.2528	13	306	7 0 7 7 7	6 0 6 6 6
122441.8544	-5.5885	3	12.2528	15	306	7 0 7 8 8	6 0 6 7 7
122441.8545	-5.5405	3	12.2528	17	306	7 0 7 8 9	6 0 6 7 8
122441.8546	-5.6624	3	12.2528	13	306	7 0 7 8 7	6 0 6 7 6
122441.8581	-6.9939	3	12.2528	9	306	7 0 7 6 5	6 0 6 5 5
122441.8588	-6.9969	3	12.2528	17	306	7 0 7 8 9	6 0 6 6 7
139930.3385	-5.5506	3	16.3370	19	306	8 0 8 9 9	7 0 7 8 8

139931.1327	-5.5486	3	16.3370	13	306	8 0 8 8 7	7 0 7 8 7
139931.1328	-5.2689	3	16.3370	17	306	8 0 8 8 9	7 0 7 8 9
139931.1340	-5.2745	3	16.3370	15	306	8 0 8 8 8	7 0 7 7 8
139931.1361	-6.7920	3	16.3370	17	306	8 0 8 8 9	7 0 7 8 8
139931.1371	-3.9406	3	16.3370	13	306	8 0 8 7 7	7 0 7 6 6
139931.1372	-3.7943	3	16.3370	17	306	8 0 8 9 9	7 0 7 8 8
139931.1373	-3.7447	3	16.3370	19	306	8 0 8 9 0	7 0 7 8 9
139931.1374	-6.7407	3	16.3370	15	306	8 0 8 7 8	7 0 7 8 7
139931.1387	-6.8565	3	16.3370	13	306	8 0 8 7 7	7 0 7 7 6
139931.1392	-6.9027	3	16.3370	13	306	8 0 8 7 7	7 0 7 7 8
139931.1409	-5.2585	3	16.3370	11	306	8 0 8 7 6	7 0 7 6 6
139931.1411	-5.5525	3	16.3370	15	306	8 0 8 9 8	7 0 7 8 8
139931.1416	-5.6085	3	16.3370	15	306	8 0 8 8 7	7 0 7 8 7
139931.1417	-5.3332	3	16.3370	19	306	8 0 8 8 9	7 0 7 8 9
139931.1423	-5.2770	3	16.3370	13	306	8 0 8 7 7	7 0 7 7 7
139931.1424	-5.5450	3	16.3370	15	306	8 0 8 7 8	7 0 7 7 8
139931.1425	-6.6629	3	16.3370	11	306	8 0 8 7 6	7 0 7 7 6
139931.1427	-6.4189	3	16.3370	19	306	8 0 8 9 9	7 0 7 8 9
139931.1428	-5.3366	3	16.3370	17	306	8 0 8 8 8	7 0 7 7 8
139931.1450	-6.8044	3	16.3370	19	306	8 0 8 8 9	7 0 7 8 8
139931.1459	-3.8694	3	16.3370	15	306	8 0 8 7 7	7 0 7 6 6
139931.1460	-3.7449	3	16.3370	19	306	8 0 8 9 9	7 0 7 8 8
139931.1461	-3.7003	3	16.3370	21	306	8 0 8 9 0 1	7 0 7 8 9
139931.1462	-6.8069	3	16.3370	17	306	8 0 8 7 8	7 0 7 8 7
139931.1468	-5.6582	3	16.3370	17	306	8 0 8 8 7	7 0 7 8 7
139931.1469	-5.3881	3	16.3370	21	306	8 0 8 8 9 1	7 0 7 8 9 1
139931.1473	-6.8537	3	16.3370	15	306	8 0 8 7 7	7 0 7 7 6
139931.1479	-5.3889	3	16.3370	19	306	8 0 8 8 8	7 0 7 7 8
139931.1497	-5.3247	3	16.3370	13	306	8 0 8 7 6	7 0 7 6 6
139931.1498	-5.6152	3	16.3370	17	306	8 0 8 9 8	7 0 7 8 8
139931.1504	-6.8180	3	16.3370	21	306	8 0 8 8 9 1	7 0 7 8 8
139931.1509	-5.3412	3	16.3370	15	306	8 0 8 7 7	7 0 7 7 7
139931.1510	-5.6088	3	16.3370	17	306	8 0 8 7 8	7 0 7 7 8
139931.1511	-6.6027	3	16.3370	13	306	8 0 8 7 6	7 0 7 7 6
139931.1513	-3.7476	3	16.3370	19	306	8 0 8 8 8	7 0 7 7 7
139931.1513	-3.6945	3	16.3370	21	306	8 0 8 9 9 1	7 0 7 8 8
139931.1514	-3.6540	3	16.3370	23	306	8 0 8 9 0 1	7 0 7 8 9 1
139931.1515	-6.8715	3	16.3370	19	306	8 0 8 7 8	7 0 7 8 7
139931.1526	-6.8519	3	16.3370	17	306	8 0 8 7 7	7 0 7 7 6
139931.1551	-5.3752	3	16.3370	15	306	8 0 8 7 6	7 0 7 6 6
139931.1552	-6.4610	3	16.3370	17	306	8 0 8 8 7	7 0 7 7 7
139931.1553	-5.6610	3	16.3370	19	306	8 0 8 9 8	7 0 7 8 8
139931.1563	-5.3894	3	16.3370	17	306	8 0 8 7 7	7 0 7 7 7
139931.1564	-5.6549	3	16.3370	19	306	8 0 8 7 8	7 0 7 7 8
139932.0612	-5.6204	3	16.3370	15	306	8 0 8 8 8	7 0 7 7 7
139932.0613	-5.5452	3	16.3370	17	306	8 0 8 9 9	7 0 7 8 8
139932.0614	-5.6081	3	16.3370	15	306	8 0 8 9 8	7 0 7 8 7
139932.0614	-5.5018	3	16.3370	19	306	8 0 8 9 0	7 0 7 8 9
139932.0615	-5.7487	3	16.3370	11	306	8 0 8 7 6	7 0 7 6 5
157420.0105	-5.4748	3	21.0046	23	306	9 0 9 1 0 1 1	8 0 8 9 1 0 1
157420.0106	-5.5284	3	21.0046	21	306	9 0 9 9 1 0 1	8 0 8 8 9 1
157420.8122	-5.5146	3	21.0046	15	306	9 0 9 9 8	8 0 8 9 8
157420.8123	-5.2393	3	21.0046	19	306	9 0 9 9 1 0	8 0 8 9 1 0
157420.8133	-6.3235	3	21.0046	19	306	9 0 9 1 0 1 0	8 0 8 9 1 0
157420.8134	-5.2422	3	21.0046	17	306	9 0 9 9 9	8 0 8 8 9
157420.8157	-6.7095	3	21.0046	19	306	9 0 9 9 1 0	8 0 8 9 9
157420.8166	-3.7739	3	21.0046	15	306	9 0 9 8 8	8 0 8 7 7
157420.8167	-3.6493	3	21.0046	19	306	9 0 9 1 0 1 0	8 0 8 9 9

157420.8168	-3.6047	3	21.0046	21	306	9 0 9 1 0 1 1 1	8 0 8 9 1 0
157420.8178	-6.9489	3	21.0046	19	306	9 0 9 1 0 1 0	8 0 8 8 9
157420.8180	-6.7572	3	21.0046	15	306	9 0 9 8 8	8 0 8 8 7
157420.8184	-6.9920	3	21.0046	15	306	9 0 9 8 8	8 0 8 8 9
157420.8190	-5.5670	3	21.0046	17	306	9 0 9 9 8	8 0 8 9 8
157420.8191	-5.2969	3	21.0046	21	306	9 0 9 9 1 0 1	8 0 8 9 1 0 1
157420.8200	-6.3052	3	21.0046	21	306	9 0 9 1 0 1 0 1	8 0 8 9 1 0 1
157420.8201	-5.2983	3	21.0046	19	306	9 0 9 9 9	8 0 8 8 9
157420.8204	-5.2276	3	21.0046	13	306	9 0 9 8 7	8 0 8 7 7
157420.8205	-6.4011	3	21.0046	15	306	9 0 9 9 8	8 0 8 8 8
157420.8206	-5.5182	3	21.0046	17	306	9 0 9 1 0 9	8 0 8 9 9
157420.8207	-6.9916	3	21.0046	17	306	9 0 9 8 9	8 0 8 9 9
157420.8217	-5.2436	3	21.0046	15	306	9 0 9 8 8	8 0 8 8 8
157420.8218	-5.5115	3	21.0046	17	306	9 0 9 8 9	8 0 8 8 9
157420.8219	-6.5068	3	21.0046	13	306	9 0 9 8 7	8 0 8 8 7
157420.8225	-6.7276	3	21.0046	21	306	9 0 9 9 1 0 1	8 0 8 9 9
157420.8232	-5.6117	3	21.0046	19	306	9 0 9 9 8	8 0 8 9 8
157420.8233	-5.3473	3	21.0046	23	306	9 0 9 9 1 0 1	8 0 8 9 1 0 1
157420.8234	-3.6051	3	21.0046	21	306	9 0 9 1 0 1 0 1	8 0 8 9 9
157420.8235	-3.5646	3	21.0046	23	306	9 0 9 1 0 1 1 1	8 0 8 9 1 0 1
157420.8236	-6.7823	3	21.0046	19	306	9 0 9 8 9	8 0 8 9 8
157420.8242	-5.6052	3	21.0046	19	306	9 0 9 8 8	8 0 8 7 8
157420.8243	-5.3469	3	21.0046	21	306	9 0 9 9 9 1	8 0 8 8 9 1
157420.8244	-6.9486	3	21.0046	21	306	9 0 9 1 0 1 0 1	8 0 8 8 9
157420.8246	-6.7637	3	21.0046	17	306	9 0 9 8 8	8 0 8 8 7
157420.8268	-6.7472	3	21.0046	23	306	9 0 9 9 1 0 1	8 0 8 9 9 1
157420.8272	-5.2873	3	21.0046	15	306	9 0 9 8 7	8 0 8 7 7
157420.8273	-5.5730	3	21.0046	19	306	9 0 9 1 0 9	8 0 8 9 9
157420.8277	-3.5601	3	21.0046	23	306	9 0 9 1 0 1 0 1	8 0 8 9 9 1
157420.8278	-3.5229	3	21.0046	25	306	9 0 9 1 0 1 1 1	8 0 8 9 1 0 1
157420.8283	-5.3020	3	21.0046	17	306	9 0 9 8 8	8 0 8 8 8
157420.8284	-5.5673	3	21.0046	19	306	9 0 9 8 9	8 0 8 8 9
157420.8287	-6.9533	3	21.0046	23	306	9 0 9 1 0 1 0 1	8 0 8 8 9 1
157420.8288	-6.7706	3	21.0046	19	306	9 0 9 8 8	8 0 8 8 7
157420.8316	-5.3340	3	21.0046	17	306	9 0 9 8 7	8 0 8 7 7
157420.8327	-5.3470	3	21.0046	19	306	9 0 9 8 8	8 0 8 8 8
157420.8328	-6.4190	3	21.0046	17	306	9 0 9 8 7	8 0 8 8 7
157421.7319	-5.5729	3	21.0046	17	306	9 0 9 9 9	8 0 8 8 8
157421.7320	-5.5090	3	21.0046	19	306	9 0 9 1 0 1 0	8 0 8 9 9
157421.7321	-5.4694	3	21.0046	21	306	9 0 9 1 0 1 1 1	8 0 8 9 1 0 1
174909.0780	-5.4466	3	26.2556	25	306	10 0 1 0 1 1 1 2 1	9 0 9 1 0 1 1 1
174909.0781	-5.4943	3	26.2556	23	306	10 0 1 0 1 0 1 1 1	9 0 9 1 0 1 0 1
174909.8854	-5.4858	3	26.2556	17	306	10 0 1 0 1 0 1 0 9	9 0 9 1 0 1 0 9
174909.8855	-5.2156	3	26.2556	21	306	10 0 1 0 1 0 1 1 1	9 0 9 1 0 1 1 1
174909.8865	-5.2166	3	26.2556	19	306	10 0 1 0 1 0 1 0	9 0 9 9 1 0
174909.8887	-6.9196	3	26.2556	17	306	10 0 1 0 1 0 1 0	9 0 9 8 8
174909.8889	-6.6455	3	26.2556	21	306	10 0 1 0 1 0 1 1 1	9 0 9 1 0 1 0
174909.8898	-3.6308	3	26.2556	17	306	10 0 1 0 1 0 9 9	9 0 9 8 8
174909.8899	-3.5223	3	26.2556	21	306	10 0 1 0 1 1 1 1 1	9 0 9 1 0 1 0
174909.8900	-3.4817	3	26.2556	23	306	10 0 1 0 1 1 1 2 1	9 0 9 1 0 1 1 1
174909.8908	-5.5323	3	26.2556	19	306	10 0 1 0 1 0 9	9 0 9 1 0 9
174909.8909	-5.2679	3	26.2556	23	306	10 0 1 0 1 0 1 1 1	9 0 9 1 0 1 1 1
174909.8910	-6.8662	3	26.2556	21	306	10 0 1 0 1 1 1 1 1	9 0 9 9 1 0
174909.8911	-6.6800	3	26.2556	17	306	10 0 1 0 1 0 9 9	9 0 9 9 8
174909.8918	-5.2678	3	26.2556	21	306	10 0 1 0 1 0 1 0 1	9 0 9 9 1 0 1
174909.8937	-5.2031	3	26.2556	15	306	10 0 1 0 1 0 9 8	9 0 9 8 8
174909.8938	-5.4889	3	26.2556	19	306	10 0 1 0 1 1 1 0	9 0 9 1 0 1 0
174909.8939	-6.9566	3	26.2556	19	306	10 0 1 0 9 1 0	9 0 9 1 0 1 0

174909.8941	-6.9145	3	26.2556	19	306	10 01010 9	9 09 8 8
174909.8943	-5.3145	3	26.2556	25	306	10 01010111	9 0910111
174909.8949	-5.2174	3	26.2556	17	306	10 010 9 9	9 09 9 9
174909.8950	-5.4829	3	26.2556	19	306	10 010 910	9 09 910
174909.8952	-3.4822	3	26.2556	23	306	10 01011111	9 0910101
174909.8953	-3.4451	3	26.2556	25	306	10 01011121	9 0910111
174909.8962	-6.8747	3	26.2556	23	306	10 01011111	9 09 9101
174909.8963	-6.6939	3	26.2556	19	306	10 010 9 9	9 09 9 8
174909.8977	-6.9138	3	26.2556	21	306	10 01010 91	9 09 8 8
174909.8979	-6.6926	3	26.2556	25	306	10 01010111	9 0910101
174909.8987	-6.8427	3	26.2556	23	306	10 01011101	9 09 8 91
174909.8988	-3.4073	3	26.2556	27	306	10 01011121	9 0910111
174909.8989	-6.8421	3	26.2556	23	306	10 010 9101	9 0910 91
174909.8990	-5.2575	3	26.2556	17	306	10 010 9 8	9 09 8 8
174909.8991	-5.5375	3	26.2556	21	306	10 01011101	9 0910101
174909.8997	-6.8872	3	26.2556	25	306	10 01011111	9 09 9101
174909.8998	-6.7075	3	26.2556	21	306	10 010 9 91	9 09 9 8
174909.9001	-5.2709	3	26.2556	19	306	10 010 9 9	9 09 9 9
174909.9002	-6.3415	3	26.2556	17	306	10 010 9 8	9 09 9 8
174909.9027	-5.3010	3	26.2556	19	306	10 010 9 8	9 09 8 8
174909.9037	-5.3131	3	26.2556	21	306	10 010 9 91	9 09 9 91
174909.9038	-6.3087	3	26.2556	19	306	10 010 9 8	9 09 9 8
174910.7984	-5.5340	3	26.2556	19	306	10 0101010	9 09 9 9
174910.7986	-5.4421	3	26.2556	23	306	10 01011121	9 0910111
192397.4734	-5.4231	3	32.0899	27	306	11 01112131	10 01011121
192397.4735	-5.5025	3	32.0899	23	306	11 01111111	10 01010101
192398.2853	-5.4613	3	32.0900	19	306	11 01111110	10 01011110
192398.2854	-5.1969	3	32.0900	23	306	11 01111121	10 01011121
192398.2863	-6.1365	3	32.0900	23	306	11 01112121	10 01011121
192398.2864	-5.1966	3	32.0900	21	306	11 01111111	10 01010111
192398.2887	-6.8415	3	32.0900	19	306	11 01111110	10 010 9 9
192398.2889	-6.5968	3	32.0900	23	306	11 01111121	10 01011111
192398.2897	-5.5030	3	32.0899	21	306	11 011111101	10 010111101
192398.2898	-3.4571	3	32.0900	21	306	11 01111111	10 0101010
192398.2899	-3.3727	3	32.0900	25	306	11 01112131	10 01011121
192398.2900	-6.7002	3	32.0900	21	306	11 01110111	10 01011110
192398.2906	-5.2437	3	32.0899	23	306	11 01111111	10 01010111
192398.2908	-6.8029	3	32.0900	23	306	11 01112121	10 01010111
192398.2910	-6.6206	3	32.0900	19	306	11 0111010	10 01010 9
192398.2926	-5.5400	3	32.0899	23	306	11 011111101	10 010111101
192398.2927	-5.2881	3	32.0899	27	306	11 01111121	10 01011121
192398.2931	-6.8465	3	32.0899	21	306	11 011111101	10 010 9 9
192398.2933	-6.6233	3	32.0899	25	306	11 01111121	10 01011111
192398.2935	-5.5348	3	32.0899	23	306	11 011110101	10 010 9101
192398.2936	-5.2861	3	32.0899	25	306	11 01111111	10 01010111
192398.2937	-5.1840	3	32.0900	17	306	11 01110 9	10 010 9 9
192398.2938	-5.4641	3	32.0900	21	306	11 01112111	10 01011111
192398.2939	-6.9349	3	32.0900	21	306	11 011110111	10 01011111
192398.2941	-3.4158	3	32.0899	23	306	11 01111111	10 01010101
192398.2942	-3.3390	3	32.0899	27	306	11 01112131	10 01011121
192398.2948	-5.1970	3	32.0900	19	306	11 0111010	10 0101010
192398.2949	-6.2688	3	32.0900	17	306	11 01110 9	10 01010 9
192398.2951	-6.8181	3	32.0899	25	306	11 01112121	10 01010111
192398.2952	-6.6404	3	32.0899	21	306	11 01110101	10 01010 9
192398.2962	-6.8540	3	32.0899	23	306	11 011111101	10 010 9 91
192398.2963	-6.6514	3	32.0899	27	306	11 01111121	10 01011111
192398.2971	-3.3748	3	32.0899	25	306	11 011111111	10 01010101
192398.2972	-3.3043	3	32.0899	29	306	11 01112131	10 01011121

192398.2980	-5.2339	3	32.0899	19	306	11 01110 9	10 010 9 9
192398.2981	-5.5077	3	32.0899	23	306	11 01112111	10 01011111
192398.2990	-5.2464	3	32.0899	21	306	11 01110101	10 01010101
192398.2991	-6.2408	3	32.0899	19	306	11 01110 9	10 01010 9
192398.3011	-5.2746	3	32.0899	21	306	11 01110 91	10 010 9 91
192398.3020	-5.2859	3	32.0899	23	306	11 01110101	10 01010101
192398.3021	-5.5372	3	32.0899	25	306	11 01110111	10 01010111
192399.1930	-5.5020	3	32.0899	21	306	11 01111111	10 01010101
192399.1931	-5.4531	3	32.0899	23	306	11 01112121	10 01011111
192399.1932	-5.4193	3	32.0899	25	306	11 01112131	10 01011121
209885.1291	-5.4037	3	38.5077	29	306	12 01213141	11 01112131
209885.1292	-5.4348	3	38.5077	27	306	12 01213131	11 01112121
209885.9448	-5.4408	3	38.5077	21	306	12 01212111	11 01112111
209885.9449	-5.1826	3	38.5077	25	306	12 01212131	11 01112131
209885.9458	-5.1812	3	38.5077	23	306	12 01212121	11 01111121
209885.9483	-6.7822	3	38.5077	21	306	12 01212111	11 0111010
209885.9484	-5.4786	3	38.5076	23	306	12 01212111	11 01112111
209885.9485	-5.2267	3	38.5076	27	306	12 01212131	11 01112131
209885.9488	-7.9490	3	38.5077	21	306	12 01212111	11 01112121
209885.9493	-3.3523	3	38.5077	23	306	12 01212121	11 01111111
209885.9494	-3.2755	3	38.5077	27	306	12 01213141	11 01112131
209885.9503	-6.7552	3	38.5077	25	306	12 01213131	11 01111121
209885.9504	-6.5760	3	38.5077	21	306	12 01211111	11 0111110
209885.9509	-5.5127	3	38.5077	25	306	12 01212111	11 01112111
209885.9510	-5.2672	3	38.5077	29	306	12 01212131	11 01112131
209885.9518	-5.2648	3	38.5077	27	306	12 01212121	11 01111121
209885.9519	-6.7949	3	38.5076	23	306	12 01212111	11 01110101
209885.9521	-6.5903	3	38.5076	27	306	12 01212131	11 01112121
209885.9529	-3.2761	3	38.5076	27	306	12 01213131	11 01112121
209885.9530	-3.2442	3	38.5076	29	306	12 01213141	11 01112131
209885.9532	-5.1693	3	38.5077	19	306	12 01211110	11 0111010
209885.9533	-5.4432	3	38.5077	23	306	12 01213121	11 01112121
209885.9534	-6.9239	3	38.5077	23	306	12 01211121	11 01112121
209885.9538	-6.7756	3	38.5076	27	306	12 01213131	11 01111121
209885.9539	-6.6004	3	38.5076	23	306	12 01211111	11 01111101
209885.9542	-6.9377	3	38.5077	23	306	12 01213121	11 01111121
209885.9543	-5.1814	3	38.5077	21	306	12 01211111	11 01111111
209885.9545	-6.8089	3	38.5077	25	306	12 01212111	11 01110101
209885.9546	-6.6212	3	38.5077	29	306	12 01212131	11 01112121
209885.9554	-3.3135	3	38.5077	25	306	12 01211111	11 01110101
209885.9555	-3.2122	3	38.5077	31	306	12 01213141	11 01112131
209885.9563	-6.7987	3	38.5077	29	306	12 01213131	11 01111121
209885.9564	-6.6236	3	38.5077	25	306	12 01211111	11 01111101
209885.9568	-5.2156	3	38.5076	21	306	12 01211101	11 01110101
209885.9569	-6.9769	3	38.5076	25	306	12 01211121	11 01112121
209885.9577	-5.2273	3	38.5076	23	306	12 01211111	11 01111111
209885.9578	-5.4783	3	38.5076	25	306	12 01211121	11 01111121
209885.9594	-5.2538	3	38.5077	23	306	12 01211101	11 01110101
209885.9603	-5.2645	3	38.5077	25	306	12 01211111	11 01111111
209886.8483	-5.4319	3	38.5076	25	306	12 01213131	11 01112121
209886.8484	-5.4005	3	38.5076	27	306	12 01213141	11 01112131
227371.9779	-5.3880	3	45.5087	31	306	13 01314151	12 01213141
227372.7976	-5.1700	3	45.5087	25	306	13 01313131	12 01212131
227372.7997	-5.4584	3	45.5087	25	306	13 01313121	12 01213121
227372.7998	-5.2130	3	45.5087	29	306	13 01313141	12 01213141
227372.8002	-6.7382	3	45.5087	23	306	13 01313121	12 01211111
227372.8004	-6.5352	3	45.5087	27	306	13 01313141	12 01213131
227372.8006	-5.2107	3	45.5087	27	306	13 01313131	12 01212131

227372.8012	-3.2202	3	45.5087	27	306	13 01314141	12 01213131
227372.8013	-3.1883	3	45.5087	29	306	13 01314151	12 01213141
227372.8019	-5.2510	3	45.5087	31	306	13 01313141	12 01213141
227372.8021	-6.7203	3	45.5087	27	306	13 01314141	12 01212131
227372.8022	-6.5435	3	45.5087	23	306	13 01312121	12 01212111
227372.8027	-5.2482	3	45.5087	29	306	13 01313131	12 01212131
227372.8033	-6.7567	3	45.5087	25	306	13 01313121	12 01211111
227372.8034	-6.5672	3	45.5087	29	306	13 01313141	12 01213131
227372.8042	-3.1591	3	45.5087	31	306	13 01314151	12 01213141
227372.8043	-6.7987	3	45.5087	27	306	13 01312131	12 01213121
227372.8050	-6.7447	3	45.5087	29	306	13 01314141	12 01212131
227372.8051	-5.1587	3	45.5087	21	306	13 01312111	12 01211111
227372.8052	-5.4259	3	45.5087	25	306	13 01314131	12 01213131
227372.8055	-6.7757	3	45.5087	27	306	13 01313121	12 01211111
227372.8056	-6.6003	3	45.5087	31	306	13 01313141	12 01213131
227372.8061	-5.1700	3	45.5087	23	306	13 01312121	12 01212121
227372.8064	-3.1573	3	45.5087	31	306	13 01314141	12 01213131
227372.8072	-6.7713	3	45.5087	31	306	13 01314141	12 01212131
227372.8073	-6.5982	3	45.5087	27	306	13 01312121	12 01212111
227372.8081	-5.2018	3	45.5087	23	306	13 01312111	12 01211111
227372.8082	-6.9747	3	45.5087	27	306	13 01312131	12 01213131
227372.8090	-5.2128	3	45.5087	25	306	13 01312121	12 01212121
227372.8103	-5.2378	3	45.5087	25	306	13 01312111	12 01211111
227372.8104	-5.4912	3	45.5087	29	306	13 01314131	12 01213131
227372.8112	-5.2479	3	45.5087	27	306	13 01312121	12 01212121
227372.8113	-6.0657	3	45.5087	25	306	13 01312111	12 01212111
227373.6966	-5.3853	3	45.5087	29	306	13 01314151	12 01213141
227373.6967	-5.4506	3	45.5087	25	306	13 01314131	12 01213121
244857.9522	-5.4031	3	53.0930	31	306	14 01415151	13 01314141
244857.9523	-5.4086	3	53.0930	31	306	14 01414151	13 01313141
244858.7737	-5.1648	3	53.0930	29	306	14 01414151	13 01314151
244858.7745	-5.1623	3	53.0930	27	306	14 01414141	13 01313141
244858.7763	-5.2030	3	53.0930	31	306	14 01414151	13 01314151
244858.7771	-5.2004	3	53.0930	29	306	14 01414141	13 01313141
244858.7772	-6.7066	3	53.0930	25	306	14 01414131	13 01312121
244858.7774	-6.5187	3	53.0930	29	306	14 01414151	13 01314141
244858.7781	-5.4714	3	53.0930	29	306	14 01414131	13 01314131
244858.7782	-3.1098	3	53.0930	31	306	14 01415161	13 01314151
244858.7783	-6.7494	3	53.0930	27	306	14 01413141	13 01314131
244858.7789	-5.2358	3	53.0930	31	306	14 01414141	13 01313141
244858.7790	-6.6961	3	53.0930	29	306	14 01415151	13 01313141
244858.7791	-6.5214	3	53.0930	25	306	14 01413131	13 01313121
244858.7798	-6.7299	3	53.0930	27	306	14 01414131	13 01312121
244858.7799	-6.5524	3	53.0930	31	306	14 01414151	13 01314141
244858.7807	-3.1104	3	53.0930	31	306	14 01415151	13 01314141
244858.7808	-3.1133	3	53.0930	31	306	14 01414151	13 01313141
244858.7815	-6.7236	3	53.0930	31	306	14 01415151	13 01313141
244858.7816	-6.5524	3	53.0930	27	306	14 01413131	13 01313121
244858.7818	-6.7524	3	53.0930	29	306	14 01414131	13 01312121
244858.7821	-5.1515	3	53.0930	23	306	14 01413121	13 01312121
244858.7822	-5.4119	3	53.0930	27	306	14 01415141	13 01314141
244858.7826	-3.1113	3	53.0930	31	306	14 01414141	13 01313131
244858.7827	-3.1094	3	53.0930	31	306	14 01415141	13 01314131
244858.7830	-5.1622	3	53.0930	25	306	14 01413131	13 01313131
244858.7831	-5.4076	3	53.0930	27	306	14 01413141	13 01313141
244858.7835	-6.5814	3	53.0930	29	306	14 01413131	13 01313121
244858.7847	-5.1919	3	53.0930	25	306	14 01413121	13 01312121
244858.7855	-5.2023	3	53.0930	27	306	14 01413131	13 01313131

244858.7856	-6.0192	3	53.0930	25	306	14 01413121	13 01313121
244858.7866	-5.2259	3	53.0930	27	306	14 01413121	13 01312121
244858.7875	-5.2355	3	53.0930	29	306	14 01413131	13 01313131
244859.6706	-5.3733	3	53.0930	31	306	14 01415161	13 01314151
262342.9848	-5.4194	3	61.2607	31	306	15 01516151	14 01415141
262342.9849	-5.4247	3	61.2607	31	306	15 01515151	14 01414141
262343.8085	-5.3995	3	61.2607	27	306	15 01515141	14 01415141
262343.8086	-5.1606	3	61.2607	31	306	15 01515161	14 01415161
262343.8093	-5.8985	3	61.2607	31	306	15 01516161	14 01415161
262343.8094	-5.1578	3	61.2607	29	306	15 01515151	14 01414151
262343.8107	-5.4290	3	61.2606	29	306	15 01515141	14 01415141
262343.8108	-5.9266	3	61.2606	31	306	15 01515151	14 01415151
262343.8115	-5.4250	3	61.2606	29	306	15 01514141	14 01413141
262343.8116	-5.1936	3	61.2606	31	306	15 01515151	14 01414151
262343.8121	-6.6855	3	61.2607	27	306	15 01515141	14 01413131
262343.8122	-6.5098	3	61.2607	31	306	15 01515161	14 01415151
262343.8124	-5.4565	3	61.2607	31	306	15 01515141	14 01415141
262343.8130	-3.0669	3	61.2607	31	306	15 01516161	14 01415151
262343.8131	-3.0699	3	61.2607	31	306	15 01515161	14 01414151
262343.8132	-5.4526	3	61.2607	31	306	15 01514141	14 01413141
262343.8139	-6.5080	3	61.2607	27	306	15 01514141	14 01414131
262343.8144	-6.7120	3	61.2606	29	306	15 01515141	14 01413131
262343.8152	-3.0681	3	61.2606	31	306	15 01516151	14 01415141
262343.8153	-6.8424	3	61.2606	31	306	15 01514151	14 01415141
262343.8161	-6.5410	3	61.2606	29	306	15 01514141	14 01414131
262343.8169	-3.0666	3	61.2607	31	306	15 01515141	14 01414131
262343.8170	-5.1475	3	61.2607	25	306	15 01514131	14 01413131
262343.8171	-6.9357	3	61.2607	29	306	15 01514151	14 01415151
262343.8177	-6.5721	3	61.2607	31	306	15 01514141	14 01414131
262343.8178	-6.9458	3	61.2607	29	306	15 01516151	14 01414151
262343.8179	-5.1577	3	61.2607	27	306	15 01514141	14 01414141
262343.8192	-5.1855	3	61.2606	27	306	15 01514131	14 01413131
262343.8200	-5.1953	3	61.2606	29	306	15 01514141	14 01414141
262343.8209	-5.2177	3	61.2607	29	306	15 01514131	14 01413131
262343.8217	-5.2268	3	61.2607	31	306	15 01514141	14 01414141
262344.7029	-5.3902	3	61.2606	31	306	15 01516161	14 01415151
279827.0083	-5.4374	3	70.0115	31	306	16 01616151	15 01515141
279827.8340	-5.3917	3	70.0115	29	306	16 01616151	15 01516151
279827.8348	-5.1562	3	70.0115	31	306	16 01616161	15 01515161
279827.8359	-5.4192	3	70.0115	31	306	16 01616151	15 01516151
279827.8367	-5.4154	3	70.0115	31	306	16 01615151	15 01514151
279827.8376	-6.6730	3	70.0115	29	306	16 01616151	15 01514141
279827.8385	-3.0299	3	70.0115	31	306	16 01615161	15 01514151
279827.8385	-3.0299	3	70.0115	31	306	16 01617161	15 01516151
279827.8394	-6.5020	3	70.0115	29	306	16 01615151	15 01515141
279827.8396	-6.7026	3	70.0115	31	306	16 01616151	15 01514141
279827.8404	-3.0302	3	70.0115	31	306	16 01616151	15 01515141
279827.8412	-6.5369	3	70.0115	31	306	16 01615151	15 01515141
279827.8419	-3.0294	3	70.0115	31	306	16 01615141	15 01514131
279827.8425	-5.1464	3	70.0115	27	306	16 01615141	15 01514141
279827.8433	-5.1560	3	70.0115	29	306	16 01615151	15 01515151
279827.8452	-5.1915	3	70.0115	31	306	16 01615151	15 01515151
279827.8459	-5.2128	3	70.0115	31	306	16 01615141	15 01514141
279827.8467	-5.9128	3	70.0115	31	306	16 01615141	15 01515141
279828.7261	-5.4133	3	70.0115	31	306	16 01616161	15 01515151
279828.7262	-5.4113	3	70.0115	31	306	16 01617161	15 01516151
297309.9554	-5.4562	3	79.3456	31	306	17 01716151	16 01615141
297310.7828	-5.3866	3	79.3456	31	306	17 01717161	16 01617161

297310.7835	-5.3827	3	79.3456	31	306	17 01716161	16 01615161	
297310.7864	-6.6681	3	79.3456	31	306	17 01717161	16 01615151	
297310.7873	-2.9968	3	79.3456	31	306	17 01717161	16 01616151	
297310.7881	-6.5024	3	79.3456	31	306	17 01716161	16 01616151	
297310.7889	-2.9976	3	79.3455	31	306	17 01716151	16 01615141	
297310.7912	-5.1479	3	79.3456	29	306	17 01716151	16 01615151	
297310.7921	-5.1570	3	79.3456	31	306	17 01716161	16 01616161	
297310.7929	-5.1817	3	79.3455	31	306	17 01716151	16 01615151	
297310.7937	-5.8814	3	79.3455	31	306	17 01716151	16 01616151	
297311.6730	-5.4305	3	79.3455	31	306	17 01717161	16 01616151	
297311.6731	-5.4353	3	79.3455	31	306	17 01716161	16 01615151	
314792.5921	-2.9684	3	89.2628	31	306	18 01817161	17 01716151	
314792.5961	-5.1518	3	89.2628	31	306	18 01817161	17 01716161	
314792.5969	-5.8518	3	89.2628	31	306	18 01817161	17 01717161	
314793.4762	-5.4538	3	89.2627	31	306	18 01817161	17 01716151	